



Graduate School of
Systemic Neurosciences

LMU Munich

**Analysis of adhesive and repulsive
functions of FLRT proteins in
central nervous system development**

Daniel Matthias Nagel

München 2014



**Analysis of adhesive and repulsive
functions of FLRT proteins in
central nervous system development**

Dissertation of the Graduate School

of Systemic Neurosciences

Ludwig-Maximilians Universität, München

Daniel Matthias Nagel

Supervisor

Prof. Rüdiger Klein

Second reviewer

Prof. Stephan Kröger

Third reviewer

Prof. Victor Tarabykin

Date of oral defense:

14.01.2015

Für Christine und Matilda

Table of Contents

| | |
|---|-----------|
| 1. Introduction | 1 |
| 1.1. Structure and development of the cerebral cortex | 3 |
| 1.2. Generation and migration of cortical projection neurons | 8 |
| 1.3. Molecular regulation of neuronal migration | 11 |
| 1.4. Cell adhesion in synapse formation | 15 |
| 1.5. Leucine-rich repeat proteins in nervous system development | 19 |
| 1.6. The fibronectin-leucine-rich-repeat-transmembrane (FLRT) family of proteins | 21 |
| 1.7. Aims of the study | 27 |
| 2. Results | 29 |
| 2.1. Involvement of FLRT family members in synapse formation | 29 |
| 2.1.1. FLRTs are enriched in synaptic fractions <i>in vivo</i> | 29 |
| 2.1.2. FLRTs do not induce pre- or postsynaptic differentiation in a mixed culture assay | 31 |
| 2.1.3. FLRT1 and FLRT3 do not regulate excitatory synapse number in primary hippocampal neurons | 37 |
| 2.1.3.1. Genetic knock-out of FLRT1 or FLRT3 does not change excitatory synapse number <i>in vitro</i> | 37 |
| 2.1.3.2. Sparse knock-out of FLRT3 does not change excitatory synapse number <i>in vitro</i> | 43 |
| 2.1.3.3. Overexpression of FLRT3 does not change excitatory synapse number <i>in vitro</i> | 46 |
| 2.1.4. Knock-out of FLRT1 and FLRT3 does not change expression of synaptic proteins in hippocampus <i>in vivo</i> | 48 |
| 2.1.5. Knock-out of FLRT3 does not change synapse density in the hippocampus <i>in vivo</i> | 51 |
| 2.2. Involvement of FLRT family members in neuronal migration during cortex development | 53 |

| | | |
|-----------|--|-----------|
| 2.2.1. | Generation of a variety of FLRT and Unc5 binding mutants based on crystal structures | 53 |
| 2.2.2. | Unc5D-induced inhibition of migration is partially dependent on FLRTs | 63 |
| 2.2.3. | Loss of FLRT3 does not affect radial migration of neurons | 67 |
| 2.2.4. | Ectopic expression of FLRT2 or FLRT3 interferes with radial migration independently of Unc5s | 70 |
| 2.2.5. | Homophilic binding of FLRTs is involved in inhibiting radial migration | 72 |
| 2.2.6. | FLRT3 signaling is involved in the inhibition of migration | 74 |
| 2.2.7. | Overexpression of FLRT3 does not change cell fate | 76 |
| 3. | Discussion | 78 |
| 3.1. | <i>FLRTs in synapse development</i> | 78 |
| 3.2. | <i>FLRT-FLRT and FLRT-Unc5 interactions occur via distinct surface domains and can be uncoupled</i> | 83 |
| 3.3. | <i>FLRTs in cortical development</i> | 85 |
| 3.3.1. | FLRT2 inhibits radial migration via Unc5D | 86 |
| 3.3.2. | Loss of FLRT3 does not influence radial migration | 88 |
| 3.3.3. | Overexpression of FLRTs inhibits radial migration by homophilic adhesion and via the intracellular domain | 90 |
| 3.3.4. | FLRT3 does not change cell fate of developing pyramidal neurons | 95 |
| 3.4. | <i>Conclusions and outlook</i> | 97 |
| 4. | Materials and Methods | 99 |
| 4.1. | <i>Materials</i> | 99 |
| 4.1.1. | Chemicals, reagents and kits | 99 |
| 4.1.2. | Buffers for biochemistry and stainings | 99 |
| 4.1.3. | Media for tissue culture | 102 |
| 4.1.4. | Oligonucleotides for genotyping | 104 |
| 4.1.5. | Plasmids | 105 |

| | | |
|----------|--|-----|
| 4.1.5.1. | Constructs used for coculture and synapse assays | 105 |
| 4.1.5.2. | Mutant FLRT and Unc5 constructs | 105 |
| 4.1.6. | Primary antibodies | 107 |
| 4.1.7. | Secondary antibodies | 108 |
| 4.1.8. | Mouse lines | 108 |
| 4.2. | <i>Methods</i> | 109 |
| 4.2.1. | Mouse genotyping | 109 |
| 4.2.2. | Preparation of glass coverslips | 109 |
| 4.2.3. | Tissue culture | 110 |
| 4.2.3.1. | Cell lines | 110 |
| 4.2.3.2. | Primary neurons and astrocytes | 110 |
| 4.2.3.3. | Transfections | 112 |
| 4.2.4. | Biochemistry | 113 |
| 4.2.4.1. | Western blots from cell lysates | 113 |
| 4.2.4.2. | Western blots from tissue lysates | 114 |
| 4.2.4.3. | Synaptic fractionation | 114 |
| 4.2.4.4. | Hippocampus microdissection | 115 |
| 4.2.5. | X-Gal staining | 116 |
| 4.2.6. | Immunostainings | 116 |
| 4.2.6.1. | Cell lines | 116 |
| 4.2.6.2. | Primary neurons | 117 |
| 4.2.6.3. | Tissue sections | 117 |
| 4.2.7. | HEK Neuron coculture assay | 118 |
| 4.2.8. | Synapse quantification on primary neurons | 119 |
| 4.2.9. | Electron microscopic analysis of synapses | 120 |
| 4.2.10. | Cell surface binding assay | 120 |
| 4.2.11. | HEK293 cell aggregation assay | 121 |
| 4.2.12. | <i>In utero</i> electroporation | 122 |

| | |
|------------------------------|------------|
| 4.2.13. Statistical analyses | 123 |
| 5. References | 124 |
| 6. Appendix | I |

Abstract

Fibronectin-leucine-rich-repeat-transmembrane proteins (FLRTs) are a family of three single pass transmembrane proteins with extracellular leucine rich repeats and a short intracellular domain of largely unknown function. They are broadly expressed in the developing and adult nervous system as well as in other tissues. FLRTs have been implicated in a variety of different developmental processes mainly via two functions: as homophilic cell adhesion molecules, and as repulsive ligands for Unc5-positive cells. Furthermore, they can regulate cell adhesion via control of surface expression of C-Cadherin and are involved in FGF signaling.

Previously we found that all FLRTs are localized to synapses in the mouse brain and thus investigated a potential involvement of FLRTs in synapse formation. However, using different *in vitro* and *in vivo* approaches ranging from HEK293 cell-neuron coculture assays to ultrastructural analysis of synapse density in FLRT3 knock-out mouse brains, I did not find any evidence for an involvement of FLRTs in synapse development. This is in contrast to published results but can be explained by differences in the experimental approaches and timing of the experiments.

In collaboration with structural biologists we solved the crystal structure of the FLRT and Unc5 extracellular domains and a complex of both, to gain insight into the structural basis of the adhesive and repulsive functions of FLRTs. We found that homophilic FLRT-FLRT and heterophilic FLRT-Unc5 interactions both occur via the FLRT LRR domain but at distinct structural surfaces. Thus, the interactions can be uncoupled. Based on the structural results we developed FLRT and Unc5 glycosylation mutants that specifically inhibit FLRT-FLRT or FLRT-Unc5 interaction and validated them *in vitro*. I then used these

mutants in *in utero* electroporation experiments to prove that the repulsive effect of Unc5D overexpression in radially migrating neurons that was discovered previously is indeed, at least partially, mediated by FLRT2. Furthermore I found that overexpression of FLRTs inhibits radial migration of cortical pyramidal neurons and this effect is dependent on FLRT-FLRT homophilic interaction and the FLRT intracellular domain but independent of FLRT-Unc5 binding.

In summary, the work presented here provides new insights into adhesive and repulsive functions of the FLRT family of proteins in the regulation of cell migration during cortical development.

1. Introduction

The mammalian brain is one of the most complicated biological structures. It constantly receives information about the status of the organism from different sensory organs, processes and integrates this information and computes the correct behavioral response. This output is then transmitted via the motor centers to the required muscle groups to perform the behavioral response. Furthermore, the brain can store information and retrieve and integrate this information with sensory inputs to create the required output. To achieve these functions, brain development requires millions of neurons migrating to exactly the right position after their generation in the different germinal zones, form projections to the right area and establish the appropriate number of synaptic connections with the proper partners. All these steps are regulated in part by intrinsic programs of the neurons and in part by extrinsic cues. These extrinsic cues interact with receptors expressed on the surface of the developing neurons and convey directional or spatial information. Extrinsic cues include soluble factors, membrane-bound proteins on surrounding cells and extracellular matrix (ECM). The main responses of binding to these cues are adhesion or repulsion.

The rodent brain is structurally less complex than brains of primates as it is not gyrified, however the general structure of the cerebral cortex is conserved, and the basic developmental programs guiding the assembly of this structure appear also to be conserved (Ayala et al., 2007). The main structural feature of the cerebral cortex in all species is the organization into horizontal layers and intersecting vertical (radial) columns (Rakic, 2007). The main difference between the brain and all other organs is that cells in the brain are generated far away from their final destination and then have

to migrate to the exact location to perform their function. In all other organs, cells are either generated locally or have to migrate after their generation, but without such high position-specificity, e.g. in gonads (Rakic, 2007).

A huge variety of cell surface receptors and ligands guiding the different steps of brain development have been discovered in the last decades and some of them have been characterized in great detail, for example Eph receptors and their ephrin ligands (Klein and Kania, 2014) or Plexin receptors and their Semaphorin ligands (Pasterkamp, 2012). But new pairs of receptors and ligands are still being discovered on a regular basis. One group of relatively recently described transmembrane proteins are the fibronectin leucine-rich repeat transmembrane proteins (FLRT proteins) (Lacy et al., 1999). The FLRT family of proteins consists of three members, FLRT1-3, with high sequence similarity (see section 1.6 for details). They are found exclusively in vertebrates, but here are conserved between species, in line with the expansion of genes during the evolution of complex organisms (Zipursky et al., 2006). All three members of the FLRT family are expressed in the developing nervous system and have been shown to be involved in different developmental processes, acting either as homo- or heterophilic adhesion molecules or repulsive ligands (Egea et al., 2008; Yamagishi et al., 2011; O'Sullivan et al., 2012, 2014; Karaulanov et al., 2009). The scope of this thesis was to dissect the adhesive and repulsive properties of FLRT family members in synapse formation and cortical neuron migration.

1.1. Structure and development of the cerebral cortex

The mammalian cerebral cortex is a highly complex assembly of different cell types. To achieve its sophisticated functions, a stereotyped program needs to be followed during development to ensure every cell migrates to and settles at the right location, sends projections to the proper places and establishes synaptic connections with the appropriate partners.

The developing cortex comprises the ventricular/subventricular zone (VZ/SVZ) where neurons are born and radial glia cell bodies are located. This is followed by the intermediate zone, and the cortical plate on top. The cortical plate is subdivided into six layers that can be distinguished molecularly by expression of several markers, or physiologically by their major function and projection targets (Molyneaux et al., 2007). The layers are numbered I-VI with layer I (also known as molecular layer (ML)) being the most superficial. This layer contains only a few neuronal cell bodies. However, it is densely packed with the apical dendrites of cortical pyramidal neurons and axons from cortical as well as thalamic neurons (Rubio-Garrido et al., 2009). Layers II/III contain pyramidal neurons with predominantly callosal projections. These efferent connections project to the contralateral hemisphere via the anterior commissure and the corpus callosum (Molyneaux et al., 2007). Layer IV mainly receives input to the cortical circuitry from subcortical regions, especially the thalamus (López-Bendito and Molnár, 2003). Deep-layer neurons of layers V and VI project mostly to subcortical regions. While neurons of layer V extend their efferents subcerebrally to the brainstem and the spinal cord, layer VI neurons provide thalamic nuclei with input from the cortex (Molyneaux et al., 2007). The above described projection neurons are excitatory

glutamatergic neurons with long projections to other brain regions. The other major cell type in the cortex is inhibitory γ -aminobutyric acid containing (GABAergic) interneurons. These neurons are interspersed between the projection neurons and have been shown to form local circuits modulating the activity of projection neurons (Gelman and Marín, 2010). Interneurons account for 15-30% of all neurons in the cortex (Anderson et al., 2001).

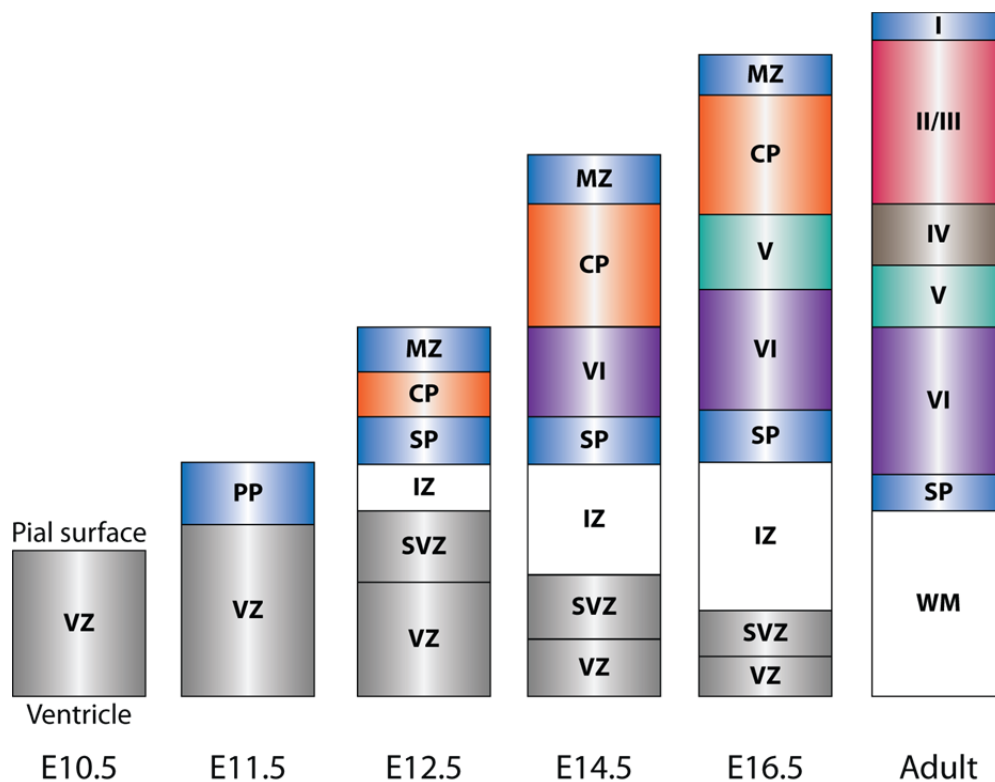


Fig. 1 Inside-out development of the cerebral cortex

The cerebral cortex develops in an inside-out fashion: newborn pyramidal neurons migrate radially from the ventricular regions towards the pial surface, and occupy progressively upper layers in the developing cortex. The earliest born neurons form the preplate (PP) around E11.5 which then splits into the subplate (SP) and the marginal zone (MZ). The intermediate zone (IZ) forms underneath the SP and the cortical plate (CP) forms between SP and MZ. The CP then progressively forms the cortical layers I-VI with layer I being the most superficial one. When neurogenesis is complete, dividing cells in the ventricular (VZ) and subventricular zone (SVZ) undergo terminal differentiation and migrate into the cortex. VZ and SVZ thus disappear and developing axon tracks form the white matter (WM) beneath the CP.

Figure adapted from (Molyneaux et al., 2007).

Neurogenesis in the mouse starts around embryonic day (E) 10.5 and the earliest born neurons form the preplate that then splits into the marginal zone and the subplate. The six layered cortical plate develops in between these two structures (Fig. 1) (Molyneaux et al., 2007).

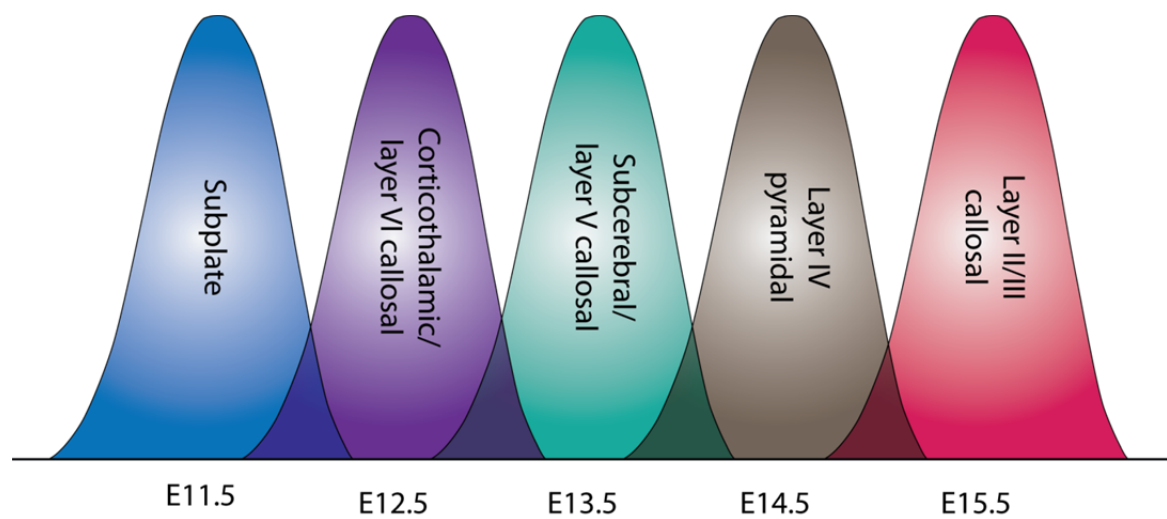


Fig. 2 Generation of cortical projection neurons in the VZ and SVZ

Projection neurons are generated in the VZ and SVZ in overlapping temporal waves. Earliest born neurons form the subplate and later born neurons settle progressively above. Birthdate (during mouse development), cortical location and general projection pattern of each neuronal population are given. Birthdates are approximations given the neurogenic gradients that exist across the cortex, where caudomedial neurogenesis lags behind rostrolateral neurogenesis (Bayer and Altman, 1991). Color coding corresponds to Fig. 1.

Figure adapted from (Molyneaux et al., 2007).

Projection neurons are produced in waves between E11.5 and E17.5 in the mouse, following a tightly regulated temporal program and then migrate into the cortical plate (Fig. 2). The cortical plate develops in an inside-out fashion with the earliest born neurons forming the deepest layer and the later born neurons settling progressively

above (Fig. 1, Fig. 2) (Angevine and Sidman, 1961; Caviness and Takahashi, 1995; Rakic, 1974). The biological significance for the inside-to-outside sequence of neurogenesis and settling of neurons in the cerebral cortex is not clear. It has been hypothesized that this enables later born neurons to interact and communicate with the neurons generated earlier when they pass by each other (Rakic, 2007).

Projection neurons arise from progenitors in the ventricular zone and then mainly migrate radially towards the cortical plate along radial glial fibers (Rakic, 1972, 1974) (Fig. 3 B, see section 1.2 for details). Inhibitory interneurons in the mouse, on the other hand, are born mainly in the medial ganglionic eminence (MGE) in the ventral telencephalon and migrate tangentially towards the cerebral cortex (Fig. 3 A, B) (Anderson, 1999; Casarosa et al., 1999; Horton et al., 1999).

This is one of the major developmental differences between mice and humans, where around 65% of all inhibitory interneurons are born in the subventricular zone and only the remaining 35% have their origin in the GEs (Letinic et al., 2002). Interneurons from the ganglionic eminences (GEs) either migrate into the subventricular zone and lower intermediate zone where they start migrating radially towards the cortical plate to reach their final destination, or they migrate tangentially in the marginal zone and then migrate downwards into the cortical plate (Tanaka et al., 2003; Anderson et al., 2001; Wichterle et al., 2001; Jiménez et al., 2002; Ang et al., 2003).

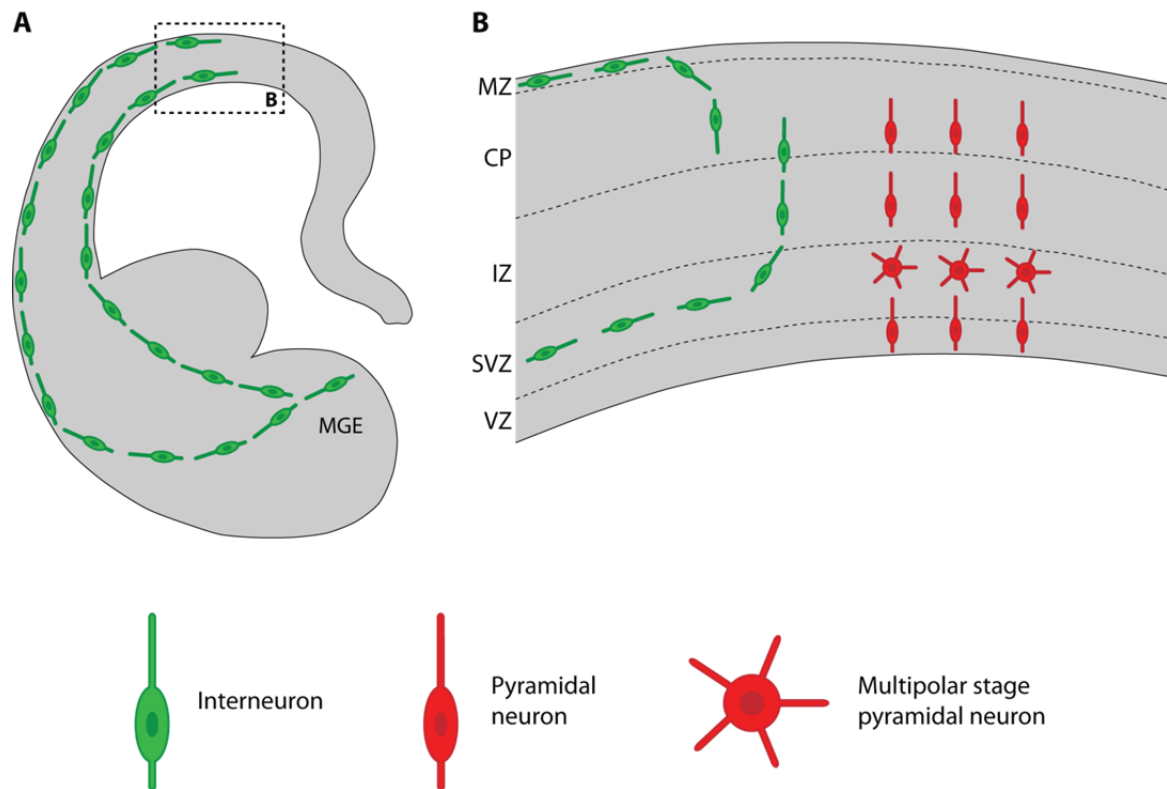


Fig. 3 Migration paths of interneurons and pyramidal neurons

(A) In the mouse, most cortical interneurons (green) are born in the MGE in the ventral midbrain and then migrate tangentially into the cortex through the SVZ or the MZ. (B) Detail of the dashed box in (A). Interneurons (green) arrive in the cortex in the SVZ or the MZ and then mainly start to migrate radially into the cortical plate. Pyramidal neurons (red) are born in the ventricular and subventricular zone and migrate towards the cortical plate. In the SVZ zone they switch to a multipolar stage for a while and then continue migrating radially along radial glia fibers into the cortical plate. CP, cortical plate; IZ, intermediate zone; MGE, medial ganglionic eminence; MZ, marginal zone; SVZ, subventricular zone; VZ, ventricular zone.

1.2. Generation and migration of cortical projection neurons

In the very beginning of the development of the cerebral cortex, there is a single sheet of neuroepithelial cells located at the ventricular surface. These cells mainly undergo symmetric cell divisions to increase the pool of progenitor cells. Some of them also divide asymmetrically to give rise to the earliest born neurons that will then form the preplate (Smart, 1973; Chenn and McConnell, 1995; Götz and Huttner, 2005). Shortly after the onset of neurogenesis, between E10.5 and E12.5, neuroepithelial cells downregulate several epithelial markers and start expressing glial markers. They thereby transform into radial glial cells (RGCs) (Götz and Huttner, 2005). Radial glial cells span the whole cortex with their apical process touching the ventricular surface and the basal process crossing the intermediate zone and cortical plate up to the pial surface (Rakic, 1972). Their cell bodies are located in the ventricular zone where the nuclei show interkinetic movements: they migrate basally for S-phase and undergo mitosis at the apical surface of the ventricular zone. Radial glia cells are the main source of neurons in the developing cerebral cortex (Malatesta et al., 2003; Anthony et al., 2004). They mainly divide asymmetrically to give rise to a neuron and a radial glia cell. A small proportion of cell divisions, on the other hand, is symmetrical, giving rise to two RGCs (Dehay and Kennedy, 2007). Interestingly, they do not retract their processes during cell division, thus allowing simultaneous cell divisions and migration of neurons along the radial glial fiber (Miyata et al., 2001). The neuron that arises from this asymmetric division usually stays in close proximity with the mother cell and migrates along its basal process towards the cortical plate. However, radial glia can also undergo a different asymmetric division. In this case they give rise to an intermediate progenitor cell and a

radial glia cell. Upon division, the intermediate progenitor migrates into the subventricular zone, where it divides symmetrically to give rise to two neurons (Noctor et al., 2004; Miyata et al., 2004).

Whereas neuroepithelial cells are multipotent and can give rise to astroglial cells, oligodendrocytes and neurons, radial glia cells have been shown to be more fate restricted. They usually only have the potential to produce one cell type: astrocytes, oligodendrocytes or neurons, respectively (Götz and Huttner, 2005). When neurogenesis is finished (around E19.5 in the mouse), radial glial cells retract their processes and terminally differentiate into astrocytes (Stipursky et al., 2012).

Upon their generation in the ventricular or subventricular zone, newly generated pyramidal neurons acquire bipolar morphology and start migrating radially, with most neurons migrating along the basal process of their mother cell. Within the subventricular zone, migrating neurons change to a multipolar morphology and halt radial migration. It has been suggested that all neurons undergo this step, although this hasn't been formally proven (LoTurco and Bai, 2006). The cells detach from radial glial fibers and start extending multiple highly motile processes. The cell bodies move in different directions, often without a certain general direction. Over time, multipolar cells slowly migrate towards the intermediate zone. The multipolar stage has been proposed to allow some degree of tangential spread of radially migrating cells (Tan and Breen, 1993; Tabata and Nakajima, 2003; Noctor et al., 2004). Since it has been shown that clonally related projection neurons preferentially connect to each other and share similar functional properties, this would increase the column to column connectivity in the cortex (Yu et al., 2009; Li et al., 2012; Ohtsuki et al., 2012).

Cells spend different periods of time, even up to several days, in the multipolar stage (Tabata and Nakajima, 2003; Tsai et al., 2005). But eventually, all neurons change back to a bipolar morphology, reattach to radial glial fibers and then quickly migrate to the most superficial layer of the developing cortical plate and settle in their final position after detaching again from the glial guide. Some studies suggested that multipolar cells, even though they detach from the glial fiber, stay in contact with their mother cell throughout the whole multipolar stage (Noctor et al., 2004; LoTurco and Bai, 2006). The molecular signals regulating multipolar stage entry and exit have not been understood in detail, yet.

During radial migration, pyramidal neurons have been shown to migrate by two distinct modes: locomotion and somal translocation (Nadarajah et al., 2001). During locomotion, cells extend a leading process along the radial glial fiber and then the nucleus moves forward within this process. Afterwards the trailing process gets retracted and the leading process again extends forward. In the locomotion mode of migration cells typically migrate at speeds of around $10 \mu\text{m h}^{-1}$. During somal translocation, cells first extend a long leading process up to the pial surface and then the nucleus follows smoothly at speeds of $10\text{-}50 \mu\text{m h}^{-1}$ (Nadarajah et al., 2001).

Even though the basic mechanisms of cortical development between rodents and humans are conserved and many of the molecules involved are the same, there are still fundamental differences and not all the data from mice can be directly transferred to human development. The most remarkable evolutionary adaptation of the cortex in higher vertebrates such as carnivores, primates and humans is the massive expansion of surface area that is achieved by folding of the cortex and an accompanying increase in

cell numbers. It has recently been discovered, that the subventricular zone in gyrencephalic species is expanded and can be subdivided into inner (ISVZ) and outer subventricular zone (OSVZ) (Smart, 2002). The ISVZ is comparable to the SVZ in rodents. The OSVZ contains an additional type of RGC, the so called basal RGC (bRGC). bRGCs extend a basal process to the pial surface, but do not connect to the ventricular surface (Reillo et al., 2011; Fietz et al., 2010; Hansen et al., 2010). bRGCs are highly abundant in the OSVZ and add a significant amount of radial fibers to the preexisting scaffold in a basally expanding, fan-like manner, thereby generating tangential expansion of the cortical surface and folding (Borrell and Götz, 2014; Borrell and Reillo, 2012).

1.3. Molecular regulation of neuronal migration

Radial migration of pyramidal neurons from their birthplace in the ventricular or subventricular zone to the cortical plate is regulated by a multitude of factors and, despite extensive research, is still far from being completely understood. Several receptor ligand pairs that were discovered for their involvement in axon guidance have recently been shown to have important functions in the regulation of cell migration as well (Ayala et al., 2007). For example, the soluble brain derived neurotrophic factor (BDNF) and neurotrophin-4 (NT-4) proteins (Brunstrom et al., 1997; Ringstedt et al., 1998) and their main receptor TrkB. Furthermore, there are cell bound guidance molecules like EphrinB2 and its receptor EphB2 that have been shown to regulate migration of neuronal precursors in the rostral migratory stream (Conover et al., 2000) or EphrinB1 which is involved in regulating the tangential spread

of radially migrating neurons in the cortex (Dimidschstein et al., 2013). But the most studied class of molecules involved in regulating cell migration during brain development are cell adhesion molecules (CAMs), their ligands, and the intracellular signaling cascades they are connected to (Solecki, 2012). CAMs can either act homophilically, binding to proteins of the same class in trans (e.g. Cadherins) or heterophilically, binding to a ligand on another cell or to the extracellular matrix (e.g. Integrins). Cell adhesion needs to be tightly regulated during cell migration in order to coordinate directed movement of cells. Cells need to extend a leading process, form adhesions in the front, pull the soma including nucleus and other organelles forward and then release the adhesive contacts in the back to allow retraction of the trailing process (Solecki, 2012). Adhesion can either happen between cells or between a cell and the extracellular matrix. Consequently, one of the most studied molecules involved in cortical migration is the extracellular matrix glycoprotein Reelin. Reelin is produced by Cajal-Retzius cells in the marginal zone and subsequently bound by Integrins on migrating neurons. Reelin has been shown to be important for the termination of migration and detachment from radial glial processes once cells reach the top layer of the cortical plate, thus stopping them from entering the marginal zone (Pinto Lord and Caviness, 1979; Dulabon, 2000).

Many cell adhesion molecules have also been linked to neuronal migration, for example neuronal cell adhesion molecule (NCAM) (Cremer et al., 1994; Hu et al., 1996), N-Cadherin (Franco et al., 2011; Jossin and Cooper, 2011) and Integrins (Anton et al., 1999; Dulabon, 2000). However, the proposed mechanisms of regulation, for example carbohydrate modification of NCAM or transcriptional regulation, take

much longer than the seconds to minutes that are required for the remodeling of adhesion contacts as described in imaging studies (Solecki, 2012). Adhesion receptor trafficking has long been proposed as a possible mechanism for regulation of neuronal migration along radial fibers. First evidence came from electron microscopy (EM) studies showing Clathrin coated vesicles proximal to neuron-glia adhesion sites (Rakic, 1971, 1972; Gregory et al., 1988; O'Rourke et al., 1995). More recently, taking advantage of modern techniques like *in-utero* electroporation and fluorescent live cell imaging, the importance of endocytosis pathways for cell migration in brain development has been conclusively proven (Wilson et al., 2010; Shieh et al., 2011; Kawauchi et al., 2010). For example a pathway involving Dynamin, Rab5 and Rab11 has been shown to regulate surface levels and trafficking of N-Cadherin and thereby radial migration (Kawauchi et al., 2010). Even though different classes of adhesion molecules have been shown to be involved in neuronal migration, only few molecules have been found to date that mediate the adhesive interaction between neurons and radial glia. Two examples of proteins involved in this interaction are Astrotactin (Edmondson, 1988) and the gap junction components Connexin 26 and Connexin 43 (Elias et al., 2007).

Apart from their adhesive functions, most cell adhesion molecules also have an intracellular signaling domain, enabling them to transmit information from external cues into the cell. Thus, several intracellular signaling cascades have also been implicated in the regulation of migration. The vast majority of cases that have been described end up regulating either Actin dynamics or the microtubule network (Ayala et al., 2007). First evidence for the involvement of actin in neuronal migration came from the finding that treatment with Cytochalasin B, a compound that interferes with the assembly of Actin filaments, impairs migration of granule neurons along radial glial processes in the

cerebellum (Rivas and Hatten, 1995). Actin regulators involved in neuronal migration include, among others, the actin crosslinking protein Filamin 1 (Fox et al., 1998), Rho GTPases RhoA, Rac1 and Cdc42 (Dhavan and Tsai, 2001; Luo, 2000; Ayala et al., 2007) and the Ena/VASP complex involved in the formation of filamentous Actin (Krause et al., 2003). Recently, members of the Rnd family of proteins, a family of atypical small GTP-binding proteins, have been shown to regulate different steps of neuronal migration by regulating RhoA activity (Heng et al., 2008; Pacary et al., 2011b; Azzarelli et al., 2014). Most of the Actin regulating proteins are involved in filopodia formation and leading process elongation.

Furthermore, different types of microtubule regulating proteins have been shown to regulate neuronal migration by stabilizing or destabilizing microtubules or regulate microtubule branching. Thus, they are involved in neurite outgrowth and branching, movement of the nucleus and other organelles, or transmission of tension forces from cell adhesions. Among those are classical (MAP1, MAP2 and Tau) and non-classical (Lis1 and DCX) microtubule associated proteins (MAPs) (Ayala et al., 2007). Moreover, both proteins regulating microtubule stability as well as motorproteins play important roles in the migration of neurons via neurite extension, intracellular transport and nucleokinesis (Ayala et al., 2007).

Another important step during radial migration of pyramidal neurons in the cerebral cortex is the multipolar to bipolar transition in the intermediate zone. This step appears to be critical and disruptions can lead to gross developmental abnormalities and disorders in humans (LoTurco and Bai, 2006). Several of the aforementioned molecules, e.g. Lis1, DCX or Filamin 1 have been implicated in multipolar stage exit (Tsai et al., 2005;

Bai et al., 2003; Nagano et al., 2004), but this step is still poorly understood and requires more investigation.

1.4. Cell adhesion in synapse formation

After neurons have reached their final position, they extend processes to their respective target areas. This process is regulated by a wide variety of soluble and membrane bound guidance cues that will not be discussed here since it is beyond the scope of this dissertation. Once the processes arrive in their target region, they need to connect to their respective target cells. How do cells recognize their appropriate partners and establish specific contacts? The influential 'chemoaffinity hypothesis' by Sperry suggested the existence of sets of adhesion molecules that regulate synapse specificity by a lock and key type mechanism (Sperry, 1963). However, the incredible number of neurons and synapses in the CNS of higher vertebrates made clear that expression of specific receptors and ligands on each pair of cells would not be possible. More likely, a restricted set of receptors and ligands is expressed in different compositions in the different subsets of cells and together with other mechanisms like areal restriction, timing, activity dependent stabilization and pruning regulates the specificity of synaptic connections (Shen and Scheiffele, 2010; Scheiffele, 2003; Giagtzoglou et al., 2009).

The formation of a synapse occurs in three main steps (Fig. 4): (A) target selection and establishment of an initial contact between an axon and a dendrite; (B) pre- and

postsynaptic differentiation at the contact site; (C) stabilization and maturation of the synaptic contact (Giagtzoglou et al., 2009).

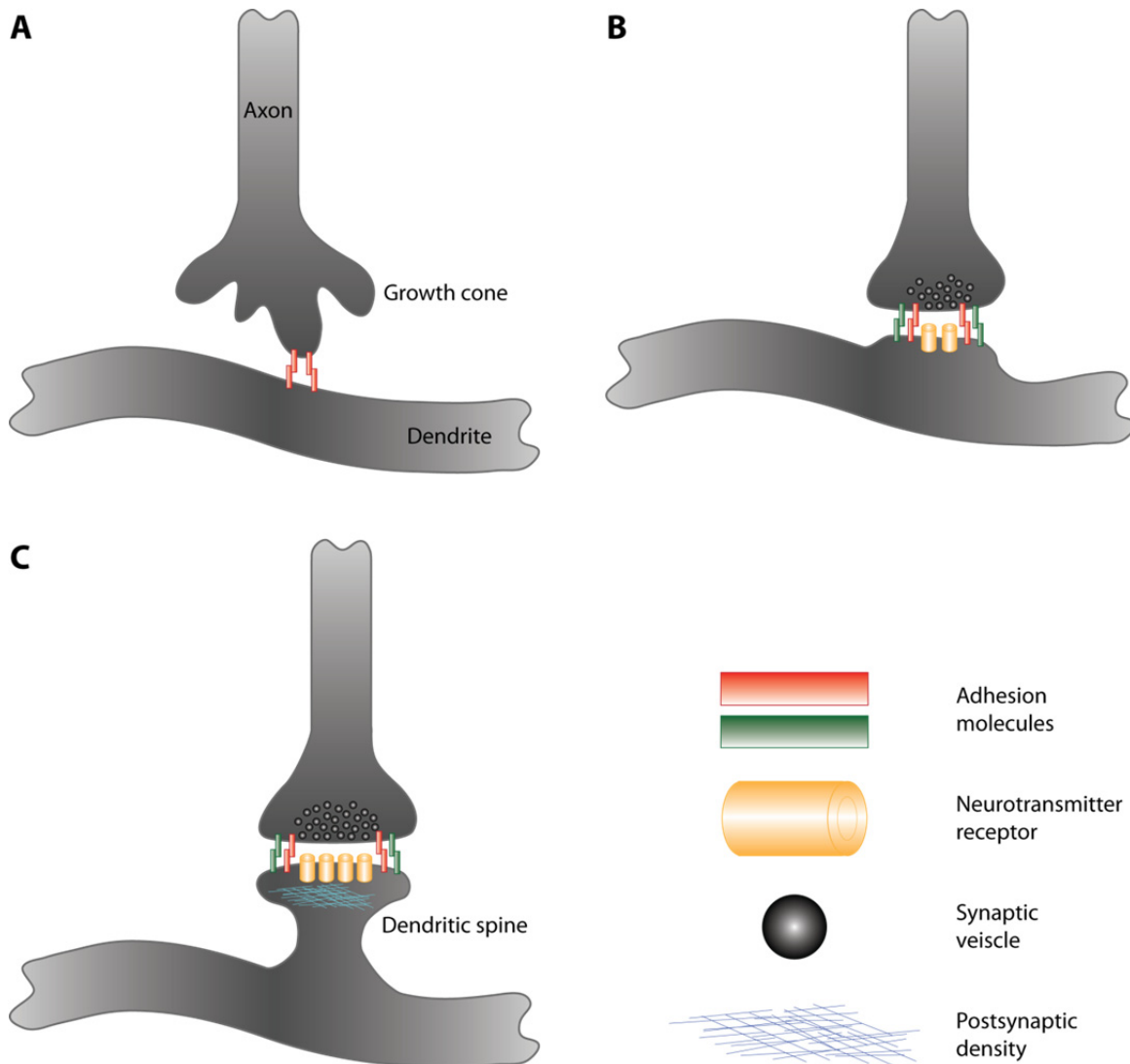


Fig. 4 Synapse formation occurs in three main steps

The general steps during formation of an excitatory synapse are shown: (A) Initial contact of an axon and a dendrite and first adhesive interactions. (B) Pre- and postsynaptic differentiation. More adhesion molecules stabilize the contact, neurotransmitter receptors are recruited to the postsynaptic membrane, synaptic vesicles start clustering at the presynaptic site and the release machinery starts to assemble. (C) Stabilization and maturation of the synapse. More transmitter receptors are inserted in the membrane and their subunit composition changes in some instances. The postsynaptic density forms and matures and the dendritic spine forms.

Different classes of cell adhesion molecules have been implicated in each of these steps. CAMs involved in synapse formation or maintenance can have different functions. They can either act purely adhesive, connecting pre- and postsynaptic membranes or a membrane and the ECM and thus stabilizing the contact and aligning the membranes (examples include N-Cadherin, and several immunoglobulin superfamily proteins), or they can act as synaptic organizers (Yamagata et al., 2003; Siddiqui and Craig, 2011). Synaptic organizing complexes cluster at nascent synaptic sites and induce synaptic differentiation (Siddiqui and Craig, 2011). For example, presynaptic Neurexins expressed in non-neuronal cells cocultured with neurons robustly induce postsynaptic differentiation in crossing dendrites. This effect has been shown to be mediated by binding to, and clustering of Neuroligins on the dendrite (Graf et al., 2004). Conversely, Neuroligins, when expressed in heterologous cells, can induce synaptic vesicle clustering in crossing axons via clustering of Neurexins. Neuroligins are sufficient to promote the formation of a functional active zone capable of vesicle release and reuptake (Scheiffele et al., 2000). Recently, synaptic cell adhesion molecule 1 (SynCAM1) has been discovered to also induce presynaptic differentiation. However, in contrast to the Neuroligin-Neurexin complex, SynCAM1 induces synapses by homophilic binding to other SynCAM1 molecules in trans (Biederer et al., 2002). During the last years, several other transsynaptic adhesion complexes involved in synapse formation have been discovered. These include, amongst others, members of the leucine rich repeat transmembrane protein family (LRRTM) binding Neurexins or Glypican (Linhoff et al., 2009; Ko et al., 2009; de Wit et al., 2009; Siddiqui et al., 2010; de Wit et al., 2013), NGL-3 binding to the protein tyrosine phosphatase receptor LAR (Woo et al., 2009), SALM3 and SALM5 binding to a yet unidentified partner

(Mah et al., 2010) and the transmembrane immunoglobulin superfamily member signal regulatory protein α (SIRP α) (Umemori and Sanes, 2008). The synapse promoting function of SIRP α is at least partially mediated by axonal CD47. However, SIRP α might be more similar to secreted factors like BDNF, NT-3 or FGFs, since its released ectodomain alone can induce synapse formation and its action requires G-protein signaling (Umemori and Sanes, 2008).

The classic synaptic organizers like Neurexins, Neuroligins or SynCAM1 do not directly involve enzymatic activity for their action (Siddiqui and Craig, 2011). Even though the downstream pathways have not yet been completely uncovered, it has been shown that they most likely act by clustering at the developing synaptic site. They then cluster scaffolding proteins such as PSD95 (postsynaptic) or Bassoon and RIM1 (presynaptic) via their PDZ domain binding motif and thus induce clustering of other molecules and signaling complexes (Sheng and Sala, 2001; Schoch et al., 2002; Dick et al., 2003). Furthermore this leads to linkage to the cytoskeleton which is an important step for spine formation and synapse stabilization (Siddiqui and Craig, 2011).

Finally, two interesting facts should be mentioned: first, the synaptogenic potential of the aforementioned proteins appears to be incomplete, since none of them alone is sufficient to induce spine formation, even though they are involved in spine morphogenesis *in vivo* (Ko et al., 2009; Kim et al., 2006; Chih et al., 2005); and second, there seems to be high redundancy in the system since knock-out mice of individual factors often only show subtle defects (Varoqueaux et al., 2006; Pouloupoulos et al., 2009; Gibson et al., 2009; Blundell et al., 2010). The possibility of redundancy is further corroborated by the finding that several synaptogenic factors are often coexpressed at the same synapse (Siddiqui and Craig, 2011). Furthermore, direct

interaction of released or membrane bound presynaptic factors (e.g. Neuronal Pentraxins NARP, NP-1 and NPR or N-Cadherin) with the extracellular, N-terminal domain of GluA α -amino-3-hydroxy-5-methyl-4-isoxazolepropionic acid (AMPA) receptor subunits has been shown as another possible mechanism to drive postsynaptic AMPA receptor clustering and functional synaptic differentiation (O'Brien et al., 1999; Passafaro et al., 2003; Nuriya and Huganir, 2006; Sia et al., 2007; Saglietti et al., 2007), thereby adding another level of complexity to the regulation of synaptic development.

1.5. Leucine-rich repeat proteins in nervous system development

The leucine-rich repeat (LRR) is one of the most common protein motives across species (Björklund et al., 2006). It consists of 11 amino acids with 4 leucines at fixed positions (LxxLxLxxNxL, with x being any amino acid) followed by a C-terminal region of less conserved sequence. Several of these repeats pack tightly against one another to form the LRR domain. LRR domains commonly form a solenoid, horseshoe like structure (Scott et al., 2004; Seiradake et al., 2011; de Wit et al., 2011). The leucine-rich region of each LRR forms a β -strand and the β -strands of all LRRs are aligned and form the concave, structurally conserved side of the horseshoe. This concave surface forms a large binding surface that can bind a wide variety of ligands depending on the amino acid sequence and the number of repeats, whereas the convex side is structurally more variable between different LRR proteins (Kajava, 1998; Kobe, 2001; Kobe and Deisenhofer, 1993, 1994, 1995). Most of the LRR proteins bind their ligands via the concave side of the horseshoe, but there are exceptions (Bella et al., 2008).

LRR proteins have been shown to be involved in several steps of nervous system development in different species, including *C. elegans*, *D. melanogaster* and in the mouse. One of the classic examples is the regulation of midline crossing in the developing spinal cord by the secreted LRR protein Slit and its receptor Robo where Slit prevents Robo expressing axons from crossing the midline (Seeger et al., 1993; Battye et al., 1999; Brose et al., 1999). Furthermore, Slit/Robo signaling is involved in dendrite arborization (Whitford et al., 2002). Another class of LRR proteins, the Trk neurotrophin receptors, is involved in different steps of central and peripheral nervous system development, including neuronal survival, axon outgrowth, axon guidance and target selection (de Wit et al., 2011). In the fly, Capricious and Tartan, two transmembrane LRR proteins, have been shown to regulate targeting of axons and dendrites in different systems, e.g. neuromuscular junction (Shishido, 1998; Kurusu et al., 2008), visual (Shinza-Kameda et al., 2006) and olfactory system (Hong et al., 2009). Capricious and Tartan have been suggested to act homophilically, but this has never been conclusively proven (de Wit et al., 2011).

Several different LRR protein families have also been implicated in synapse formation. Synaptic adhesion-like molecules (SALMs) (Ko et al., 2006; Mah et al., 2010), Netrin-G ligands (NGLs) (Kim et al., 2006; Woo et al., 2009) and leucine-rich repeat transmembrane proteins (LRRTMs) (Linhoff et al., 2009; de Wit et al., 2009; Ko et al., 2009), amongst others, have been shown regulate synapse density.

In contrast to the function of the aforementioned LRR proteins in the formation of synapses, the LRR family member LGI1 has been implicated in the regulation of synaptic function by stabilizing a PSD95 scaffolded ADAM22/Stargazin/AMPA receptor complex at the synapse (Fukata et al., 2006, 2010) and/or by regulating presynaptic release

probability via interaction with the voltage-gated potassium channel subunit Kv1.1 (Schulte et al., 2006; Zhou et al., 2009).

Whereas LGI1 in the CNS appears to be involved in synaptic function, the closely related protein LGI4 has been shown to be important for myelination of axons in the PNS via interaction with ADAM22 (Bermingham et al., 2006; Ozkaynak et al., 2010). In the CNS, on the other hand, LINGO1 is a negative regulator of myelination possibly by interacting with NgR1 and p75^{NTR} (Mi et al., 2004, 2005; Lee et al., 2007).

Several LRR proteins, likely due to their involvement in developmental processes, have also been implicated in different disorders of the nervous system. These include, amongst others, Slitrks in Tourette's syndrome; LGI1 in epilepsy; and NgR, LRRTM1 and Neurexin1 in schizophrenia (de Wit et al., 2011).

1.6. The fibronectin-leucine-rich-repeat-transmembrane (FLRT) family of proteins

One family of LRR proteins that has been described relatively recently are the fibronectin-leucine-rich-repeat-transmembrane proteins (FLRTs). The family consists of three members, FLRT1, FLRT2 and FLRT3 that are 650-675 amino acids (aa) long and share 41-55% identity and 16-20% similarity in humans (Lacy et al., 1999). They are type I transmembrane proteins with an extracellular domain containing 10 leucine-rich repeats flanked N- and C-terminally by a cysteine rich cap region. A fibronectin type III domain is located C-terminally of the LRRs before the transmembrane domain. The short intracellular tail (around 100 aa long) does not contain any typical protein homology

domains apart from a conserved stretch with two lysine residues that are involved in binding small GTPases of the Rnd family (Ogata et al., 2007; Böttcher et al., 2004; Haines et al., 2006; Lacy et al., 1999). Furthermore, the C-terminal domain contains several putative phosphorylation sites and FLRT1 has been shown to be phosphorylated in a fibroblast growth factor (FGF) dependent manner. However, the function of this phosphorylation is not entirely clear to date (Wheldon et al., 2010). In the extracellular juxtamembrane domain, all FLRTs contain a metalloprotease cleavage site. Thus, upon cleavage, the released extracellular domains can act as soluble ligands for Unc5 receptors (Yamagishi et al., 2011). A scheme of the domain structure is shown in Fig. 5.

All FLRTs are expressed in the developing and adult nervous system in the mouse. Expression of FLRTs is highly region specific, with only partial overlap of two FLRTs in specific regions (Yamagishi et al., 2011; Hampel, 2012). For example, during development, FLRT3 is expressed in migrating pyramidal neurons, whereas FLRT2 is only expressed in neurons that already settled in the cortical plate. FLRT3 keeps being expressed when the neurons reach the cortical plate; however, FLRT3-expressing neurons do not acquire FLRT2 expression. In the hippocampus, FLRT1 and FLRT2 are expressed in *Cornu Ammonis 1* (CA1), but not CA3 or dentate gyrus (DG). FLRT3, on the other hand, is expressed in DG and CA3, but not CA1 (Satoru Yamagishi, unpublished data). Furthermore, FLRT3 is expressed in the GE early in development (E13.5 - E14.5) and in the rostral but not in the intermediate thalamus (Hampel, 2012; Leyva-Díaz et al., 2014).

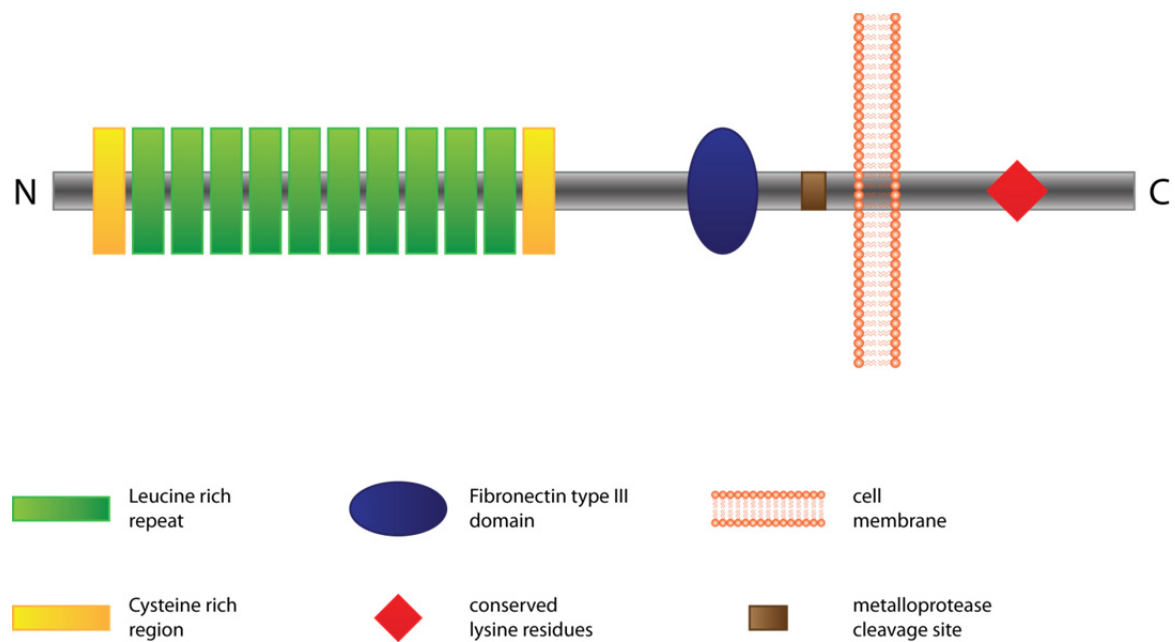


Fig. 5 Domain structure of FLRT family members

In the extracellular domain, FLRTs contain 10 leucine rich repeats (green) flanked N- and C-terminally by a cysteine rich region (yellow). A Fibronectin type III domain (blue) is located between the LRRs and the cell membrane. The short intracellular domain contains several putative phosphorylation sites (not shown) and two conserved lysine residues (red) that are involved in binding of Rnd proteins.

FLRTs have been implicated in several different biological processes in various model systems including mouse, chick, *Xenopus* embryos, primary neurons and cell lines. FLRT3 expression has been shown to be induced by FGF signaling in *Xenopus* embryos (Böttcher et al., 2004) and by Wnt3A during chick limb development (Tomás et al., 2011). In contrast, for both the chick and the *Xenopus* systems, expression of FLRT3 is inhibited by bone morphogenetic protein (BMP) signaling (specifically BMP4 in the chick). In *Xenopus* embryos, repression of FLRT3 by BMP signaling is important for anterior posterior patterning of the embryo (Tomás et al., 2011; Cho et al., 2013). Furthermore, in *Xenopus*, FLRT3 also is a target of the transforming growth factor β

(TGF β) superfamily members Activin/Nodal (Ogata et al., 2007). FLRT3 has also been shown to be upregulated upon infection of endothelial cells with *Enteropathogenic E.coli* (EPEC) or *Enterohemorrhagic E.coli* (EHEC) via the serum response factor (SRF) pathway (Heath et al., 2011). To date, a lot less is known about the regulation of FLRT1 and FLRT2, limiting our understanding of the entire family.

Functionally, FLRTs have been shown to be involved in regulating signaling as well as adhesion and repulsion in different tissues and model organisms. FLRT3 coexpressed with FGF in *Xenopus* embryos induces the expression of Xbra and Xnot. Furthermore, induction of the neuronal markers N-Cadherin and N-Tubulin by FGF signaling requires either FLRT2 or FLRT3 (Böttcher et al., 2004). FLRT3 can bind FGFR1 extracellularly via its FNIII domain and then activate the mitogen activated protein (MAP) kinase pathway via its intracellular domain (Böttcher et al., 2004). Tyrosine phosphorylation of the FLRT1 intracellular domain has been shown to negatively regulate this signaling function (Wheldon et al., 2010). However, the molecular basis of the signaling remains elusive. Furthermore, FLRT2 can interact with the intracellular and extracellular domains of FGFR2 and knock down of FLRT2 lead to a decrease in extracellular signal-regulated kinase (ERK) phosphorylation. The extracellular interaction requires the FLRT2 LRR domain (Wei et al., 2011).

Apart from their function in FGF signaling, FLRTs can interact homophilically via their LRR domains. This adhesive interaction mediates cell sorting in *in vitro* assays and in *Xenopus* embryos. The adhesive function is calcium dependent and does not require the FLRT intracellular domain (Karaulanov et al., 2006). *In vivo*, these adhesive properties have been shown to be important for maintaining tissue integrity and basal membrane stability. Loss of FLRT2 leads to problems in heart development resulting in cardiac

insufficiencies and embryonic death around E11.5/12.5 that can be rescued by expression of FLRT3 (Müller et al., 2011). FLRT3 knock out embryos suffer from ventral closure and headfold fusion defects and die around E10.5 (Maretto et al., 2008; Egea et al., 2008). Thus, functions in later developmental processes could only be revealed using conditional knock out strategies (Yamagishi et al., 2011; Leyva-Díaz et al., 2014).

In *Xenopus* embryos, FLRT3 has been shown to regulate cell adhesion by interacting with the Netrin receptor Unc5B. The LRRs of FLRT3 bind to the Ig domains of Unc5B in *cis* and the intracellular domains of both proteins together bind the small Rho like GTPase Rnd1. This complex regulates C-Cadherin endocytosis and overexpression of FLRT3, Unc5B or Rnd1 leads to a reduction of adhesive forces and detachment of cells from the blastocoel roof (Karaulanov et al., 2009; Ogata et al., 2007). Paraxial Protocadherin (PAPC) can regulate this de-adhesive function by binding to the FLRT3 extracellular domain and thereby inhibiting Rnd1 binding. In *Xenopus* embryos, overexpression of FLRT3 together with PAPC does not lead to cell detachment but rather cell sorting (Chen et al., 2009). Recently, FLRT2 has also been shown to interact with the extracellular matrix protein Fibronectin (FN). Both full length and shed ectodomains were found associated with FN (Flintoff et al., 2014), suggesting involvement of FLRTs in cell-matrix adhesion.

In the nervous system, FLRT3 has been shown to be upregulated in response to sciatic nerve injury in Schwann cells distal of the lesion, in axons and presynaptic terminals of dorsal horn neurons in the spinal cord and in regenerating dorsal root ganglion neurons (Tanabe et al., 2003; Robinson et al., 2004; Tsuji et al., 2004). *In vitro* experiments showed cell autonomous involvement of FLRT3 in neurite outgrowth with

overexpression of FLRT3 increasing the length and number of neurites and siRNA mediated knock down having the opposite effect (Robinson et al., 2004; Hampel, 2012). Non-cell autonomously, FLRT3 can also promote neurite outgrowth in cerebellar granule neurons grown on heterologous cells overexpressing FLRT3 (Tsuji et al., 2004). More recently, FLRT3 has been shown to regulate excitatory synapse development in hippocampus and cortex by binding to the latrotoxin receptor Latrophilin3 in *trans* (O'Sullivan et al., 2012, 2014). In developing thalamocortical axons, FLRT3 regulates attraction to Netrin1 by interacting with Robo1 and regulating surface expression of DCC in the growth cone (Leyva-Díaz et al., 2014). Shed FLRT ectodomains can also induce repulsive signaling into Unc5 expressing cells. This interaction has been shown to induce growth cone collapse in developing axons *in vitro* and inhibit the radial migration of Unc5 expressing pyramidal neurons in the developing cortex (Yamagishi et al., 2011).

Taken together, FLRT family members are involved in a variety of different developmental processes acting as CAMs or as repulsive ligands. Furthermore, they can regulate surface expression of other CAMs or receptors via *cis* interactions and regulation of signaling pathways. However, adhesive properties of FLRT family members in nervous system development have not been studied in detail, and it is not clear how they integrate their adhesive and repulsive functions. The scope of the work presented here was to reveal adhesive functions of FLRT family proteins in central nervous system development, in particular in cortical neuron migration and synapse formation.

1.7. Aims of the study

As discussed above, members of the FLRT family have previously been shown to have adhesive and repulsive properties (Karaulanov et al., 2006; Yamagishi et al., 2011). Furthermore, they are involved in the regulation of cell adhesion by modulating C-Cadherin surface expression (Ogata et al., 2007). Through these functions they are involved in a variety of developmental processes in different organisms and different systems. The general aim of this thesis was to characterize adhesive and repulsive functions of FLRT proteins during central nervous system development.

The first aim of this thesis was to confirm the involvement of FLRT3 in synapse formation (O'Sullivan et al., 2012) and to investigate synaptogenic properties of the other family members.

As mentioned before, FLRTs can act as homophilic cell adhesion molecules or as repulsive ligands for Unc5 positive cells. However, it was not clear before, whether homophilic and heterophilic binding can happen in parallel or if they compete with each other. In collaboration with a structural biology group we found that the homophilic interaction and FLRT-Unc5 binding occur on distinct surfaces of the FLRT LRR domain. Based on these findings, we generated glycosylation mutants of FLRT2, FLRT3 and Unc5D that should specifically abolish homophilic FLRT-FLRT or heterophilic FLRT-Unc5 interactions.

The second aim of this thesis was to validate the functionality and specificity of these mutants in cell based in vitro assays.

The third aim was to conclusively prove that the inhibition of radial migration by overexpression of Unc5D in cortical pyramidal neurons (Yamagishi et al., 2011) is indeed due to binding to FLRT2 by using the Unc5D mutant we generated.

The fourth aim of the thesis was to investigate a cell autonomous role of FLRTs in regulating radial migration in the developing cortex. Using the mutant FLRT constructs we generated, I dissected the involvement of adhesive and repulsive interactions as well as FLRT signaling in the regulation of radial migration.

2. Results

2.1. Involvement of FLRT family members in synapse formation

2.1.1. FLRTs are enriched in synaptic fractions *in vivo*

FLRT3 has previously been shown to be localized to synapses and to be involved in the formation of excitatory synapses via binding to Latrophilin3 (O'Sullivan et al., 2012, 2014). Initial work by Dr. Daniel del Toro Ruiz in our lab confirmed the localization of all FLRT family members to synapses in the mouse brain (Fig. 6).

Hippocampus from P15 mouse brains was dissected and separated using a standard protocol to obtain soluble proteins and synaptosomes. Synaptosomes were further fractionated into synaptic vesicles, synaptic membranes and postsynaptic density (Pérez Otaño et al., 2006). All fractions were subjected to analysis by Western blot using antibodies specific for Synaptophysin and PSD95 to verify successful separation. The PSD95 blot shows a double band with the upper band being an unspecific cross-reactivity with an unknown protein that is enriched in cholesterol rich membranes. This band appears in the synaptic vesicle fraction as well. However, the specific PSD95 band is absent in the synaptic vesicle fraction.

The Western blots confirmed that all FLRT family members are expressed in the hippocampus (Fig. 6, lane 1). Furthermore, all FLRTs are present in the light membrane fraction but not in the cytosolic fraction (Fig. 6, lanes 2 and 3). Upon further fractionation of synaptosomes, all FLRT family members were found to accumulate in the presynaptic side of the synaptic membranes, which is low in cholesterol and

therefore soluble in TritonX-100 (SPM-TX soluble) at low temperatures. Under these conditions, the cholesterol rich postsynaptic membranes precipitate and can thereby be separated. The purity of this fraction can be seen by the presence of Synaptophysin and absence of PSD95 (Fig. 6, lane 6). Conversely, no FLRT family member was detected in the synaptic vesicle fraction (Fig. 6, lane 4). Only FLRT2 can also be found in the PSD fraction (Fig. 6, lane 7). This could either be a specific feature of FLRT2, or could be due to higher expression levels of FLRT2 compared to FLRT1 and FLRT3 which would leave the latter two under the detection limit due to the low amounts of protein available in the PSD fraction.

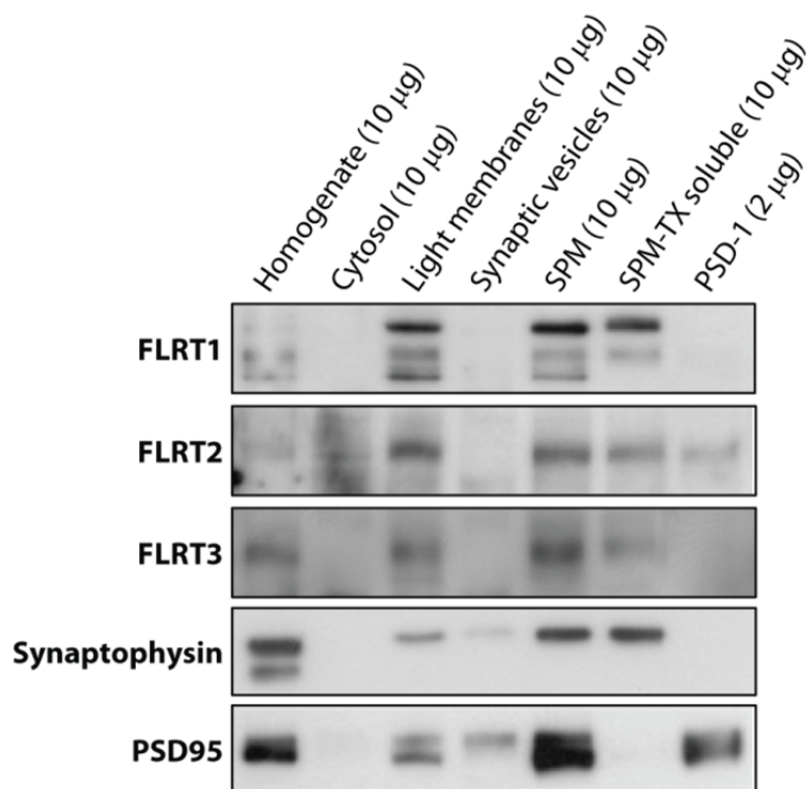


Fig. 6 FLRTs are enriched in synaptic fractions *in vivo*

P15 mouse brains were dissected and hippocampi were separated into different synaptic fractions. Fractions were then subjected to SDS-PAGE and probed with antibodies against FLRT1-3. Antibodies against Synaptophysin and PSD95 were used to confirm purity of the fractions. Note the absence of PSD95 in the presynaptic fraction (SPM-TX soluble) and the absence of Synaptophysin in the postsynaptic fraction (PSD-1), respectively.

Data were generated by Dr. Daniel del Toro Ruiz.

2.1.2. FLRTs do not induce pre- or postsynaptic differentiation in a mixed culture assay

Having confirmed synaptic localization of FLRT proteins I moved on to do functional assays. To investigate the synaptogenic potential of FLRT proteins, I employed a well-established mixed culture assay that combines non-neuronal cells expressing the protein of interest with cultured primary neurons (Biederer and Scheiffele, 2007).

Since we found FLRTs to be mainly expressed presynaptically and FLRT3 was previously shown to be involved in the development of excitatory synapses, I investigated the potential of FLRTs to induce the formation of excitatory postsynaptic specializations (Fig. 7). Thus, I transiently expressed GFP, Neurexin1 β -GFP, Neuroligin1-GFP or FLRT1, 2 or 3 in HEK293 cells and collected the cells after one day of expression using 5 mM EDTA to preserve surface proteins. I then cocultured the cells for two days with DIV10 hippocampal neurons. Samples were then fixed and stained for Flag tag to visualize FLRTs, Map2 to identify dendrites and for PSD95 to mark sites of excitatory postsynaptic differentiation (Fig. 7).

As expected, GFP did not induce any obvious postsynaptic differentiation in dendrites crossing HEK293 cells (Fig. 7 A-D). The same was true for the postsynaptic adhesion molecule Neuroligin1 (Fig. 7 I-L), whereas the positive control Neurexin1 β showed strong clustering of PSD95 at contact sites between dendrites and HEK293 cells (Fig. 7 E-H, arrowheads). This is in line with previous findings (Scheiffele et al., 2000; Graf et al., 2004). None of the FLRTs had any synaptogenic activity in this assay (Fig. 7 M-X).

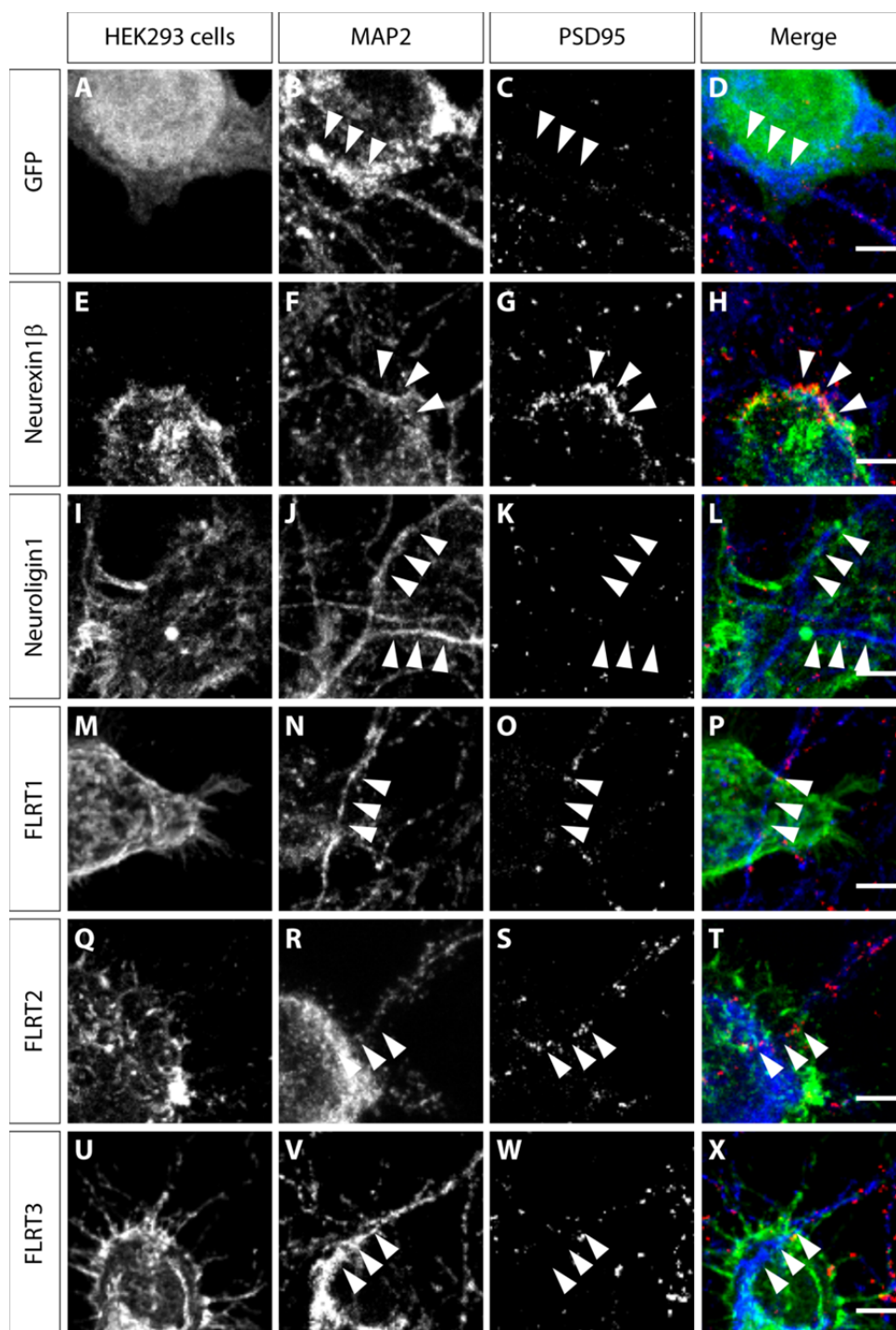


Fig. 7 FLRTs expressed in HEK293 cells do not induce excitatory postsynaptic differentiation in neurons
HEK293 cells were transiently transfected with GFP (A-D), Neurexin1 β -GFP (E-H), Neuroigin1-GFP (I-L), FLRT1 (M-P), FLRT2 (Q-T) or FLRT3 (U-X) and cocultured with DIV10 hippocampal neurons for two days. Samples were fixed and stained for Flag tag (FLRTs, green), MAP2 to identify dendrites (blue) and PSD95 to visualize sites of excitatory postsynaptic differentiation (red). White arrowheads point to Map2-positive dendrites crossing a HEK cell. Note the accumulation of PSD-positive structures on the Neurexin1 β -positive cell (E-H). Scale bars, 5 μ m.

Next, I decided to analyze the ability of FLRTs to induce inhibitory postsynaptic differentiation. To that end I repeated the mixed culture assay but stained for Gephyrin, a postsynaptic scaffolding protein of GABAergic synapses, instead of PSD95 (Fig. 8). Again, as expected, GFP did not induce any Gephyrin clusters in dendrites crossing HEK293 cells (Fig. 8 A-D). Neurexin1 β , which is known to be involved in the formation of excitatory as well as inhibitory synapses (Graf et al., 2004) induced strong clustering of Gephyrin at contact sites between dendrites and HEK cells (Fig. 8 E-H), confirming the reliability of the assay. But again, as with excitatory synapses, FLRTs (Fig. 8 M-X) did not show any Gephyrin clustering activity higher than the negative controls GFP (Fig. 8 A-D) and Neuroligin1 (Fig. 8 I-L).

In the first study showing the involvement of FLRT3 in synapse formation (O'Sullivan et al., 2012), the authors reported mainly postsynaptic localization of FLRT3, in contrast to our results. Therefore, in order to look at the potential of FLRTs to induce presynaptic differentiation in neurons I cocultured DIV8 hippocampal neurons for two days with transfected HEK293 cells and after fixation stained for Flag tag, Map2 and the presynaptic marker Synapsin1 (Fig. 9). For analysis I chose sites of contact between Synapsin1 positive neuronal structures and HEK cells in areas devoid of Map2 staining to ensure the presynaptic differentiation is induced by the adhesion protein expressed on the HEK293 cell and not by axon-dendrite contacts between neurons.

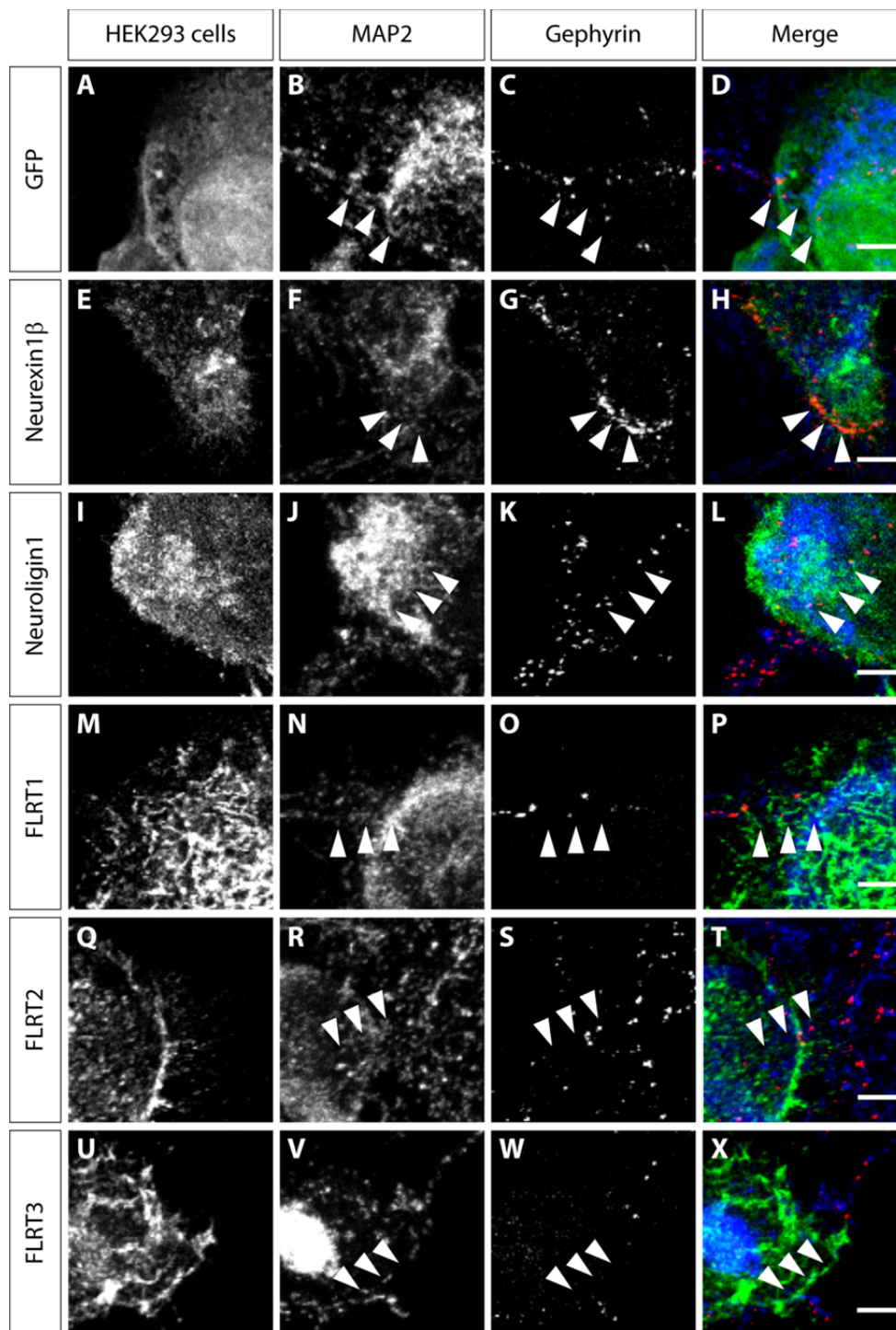


Fig. 8 FLRTs expressed in HEK293 cells do not induce inhibitory postsynaptic differentiation in neurons

HEK293 cells were transiently transfected with GFP (A-D), Neurexin1 β -GFP (E-H), Neuroigin1-GFP (I-L), FLRT1 (M-P), FLRT2 (Q-T) or FLRT3 (U-X) and cocultured with DIV10 hippocampal neurons for two days. Samples were fixed and stained for Flag tag (FLRTs, green), MAP2 to identify dendrites (blue) and Gephyrin to visualize sites of inhibitory postsynaptic differentiation (red). White arrowheads point to Map2-positive dendrites crossing a HEK cell. Note the accumulation of Gephyrin-positive structures on the Neurexin1 β -positive cell (E-H). Scale bars, 5 μ m.

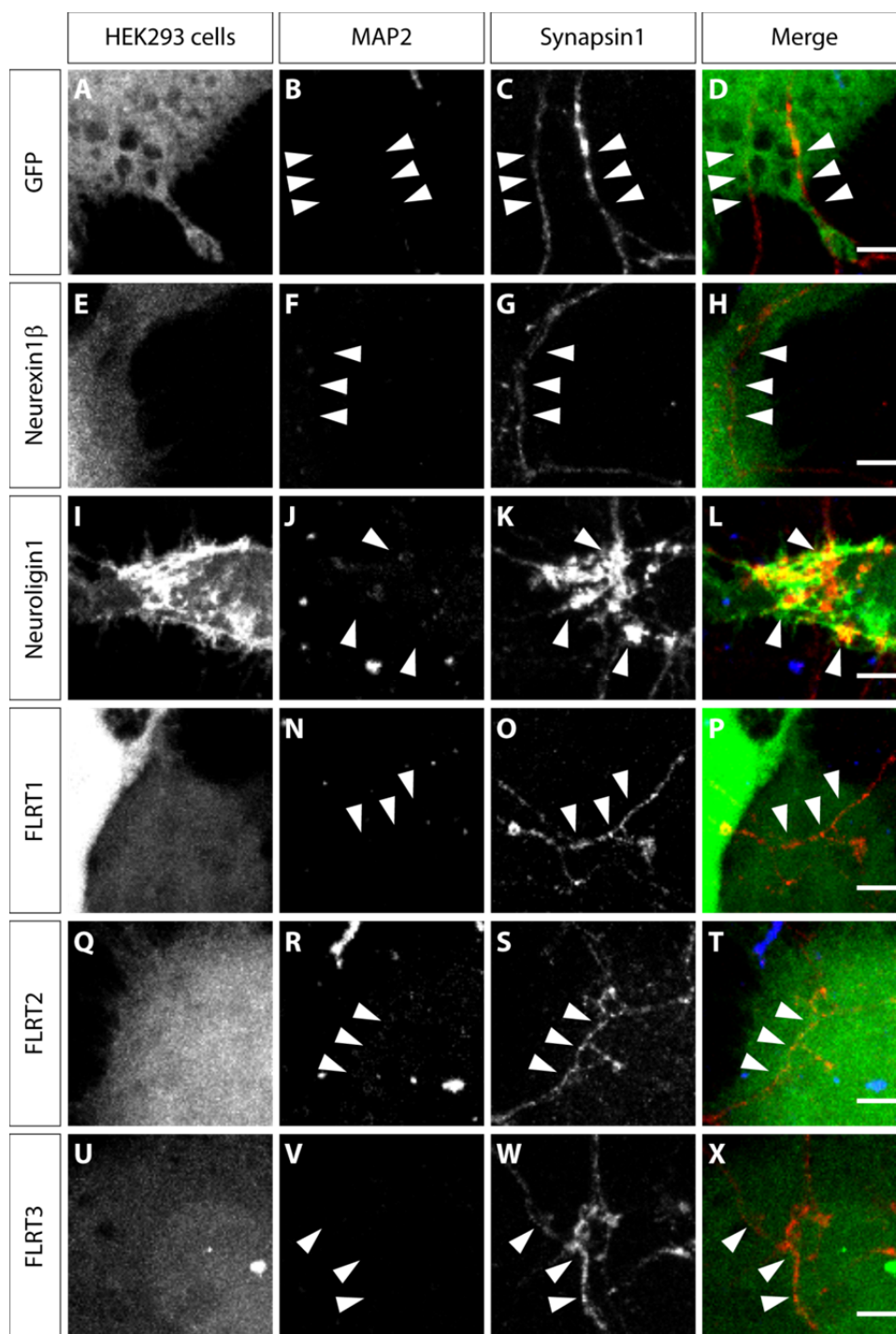


Fig. 9 FLRTs expressed in HEK293 cells do not induce presynaptic differentiation in neurons

HEK293 cells were transiently transfected with GFP (A-D), Neurexin1 β -GFP (E-H), Neuroigin1-GFP (I-L), FLRT1 (M-P), FLRT2 (Q-T) or FLRT3 (U-X) and cocultured with DIV8 hippocampal neurons for two days. Samples were fixed and stained for Flag tag (FLRTs, green), MAP2 to identify dendrites (blue) and Synapsin1 to visualize sites of presynaptic differentiation (red). White arrowheads point to Map2-negative, Synapsin1-positive axons crossing a HEK cell. Note the accumulation of Synapsin1-positive structures on the Neuroigin1-positive cell (I-L). Scale bars, 5 μ m.

The assay showed very strong synaptogenic activity of Neuroligin1 (Fig. 9 I-L) as expected from previous studies (Scheiffele et al., 2000; de Wit et al., 2009), whereas Neurexin1 β did not affect the distribution of Synapsin1 (Fig. 9 E-H) compared to GFP expressing HEK cells (Fig. 9 A-D). Expression of any FLRT in HEK cells did not induce Synapsin1 clustering at contact sites between neurons and HEK cells (Fig. 9 M-X, arrowheads).

In conclusion, I confirmed the published data showing that FLRT3 expressed in heterologous cells does not induce presynaptic differentiation in cocultured primary neurons (O'Sullivan et al., 2012). I extended those findings to the entire FLRT family and furthermore showed that FLRT family members do neither induce excitatory nor inhibitory postsynaptic differentiation when presented to neurons in culture.

2.1.3. FLRT1 and FLRT3 do not regulate excitatory synapse number in primary hippocampal neurons

2.1.3.1. Genetic knock-out of FLRT1 or FLRT3 does not change excitatory synapse number *in vitro*

To investigate the influence of FLRT proteins on synapse formation in neurons I adapted a widely used *in vitro* assay. I grew primary hippocampal neurons isolated from E17.5 mouse embryos in low density culture (approximately 7200 cells/cm²). Low density cultures were necessary to enable imaging and analysis of single neurons. To achieve such low cell numbers, the neurons were cultured on glass coverslips in a sandwich culture on top of primary rat astrocytes (Kaech and Banker, 2006). Neurons were fixed at DIV21 and stained for a presynaptic marker (Synapsin1) and an excitatory postsynaptic marker (PSD95) in parallel to visualize synapses.

Since FLRTs are differentially expressed in mouse hippocampus, the cultures were also stained for Ctip2. Ctip2 is expressed in neurons of the CA1 and dentate gyrus regions of the hippocampus and thus discriminates CA1 from CA3 cells (Fig. 10). Ctip2 positive cells were considered CA1 pyramidal neurons since the majority of dentate granule cells only develop postnatally and in cultures from E17.5 mouse embryos are virtually absent (Banker and Cowan, 1977; Schlessinger et al., 1975).

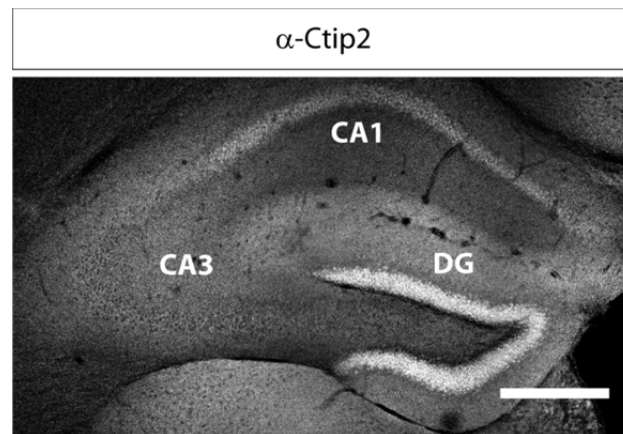


Fig. 10 Distribution of Ctip2-positive cells in hippocampus

Ctip2 antibody staining of a coronal section from hippocampus of a P30 mouse. Note the clear staining in the CA1 and DG regions and the absence of staining in the CA3 region. Scale bar, 500 μ m.

Hippocampal cultures from *FLRT1*^{-/-} embryos and *FLRT1*^{+/+} littermate controls were prepared and cultured for 21 days in the presence of astrocytes. Cells were then fixed, stained and imaged on a confocal microscope. For analysis, maximum projections of confocal stacks were created and Synapsin1 and PSD95 channels were merged using ImageJ software. The number of Synapsin1 puncta, PSD95 puncta and colocalized puncta was determined using the puncta analyzer plugin for ImageJ (Ippolito and Eroglu, 2010). Afterwards, the length of all neurites of the cell was measured using the NeuronJ plugin for ImageJ (version 1.4.2, written by Eric Meijering) and number of puncta per 10 μ m neurite length was calculated. An example of the quantification is shown in Fig. 11.

Previous work from our lab (Satoru Yamagishi, unpublished results; Hampel, 2012) has shown differential expression of FLRT proteins in the hippocampus with FLRT1 being exclusively expressed in the CA1 region while FLRT3 is present in the CA3 and dentate gyrus regions.

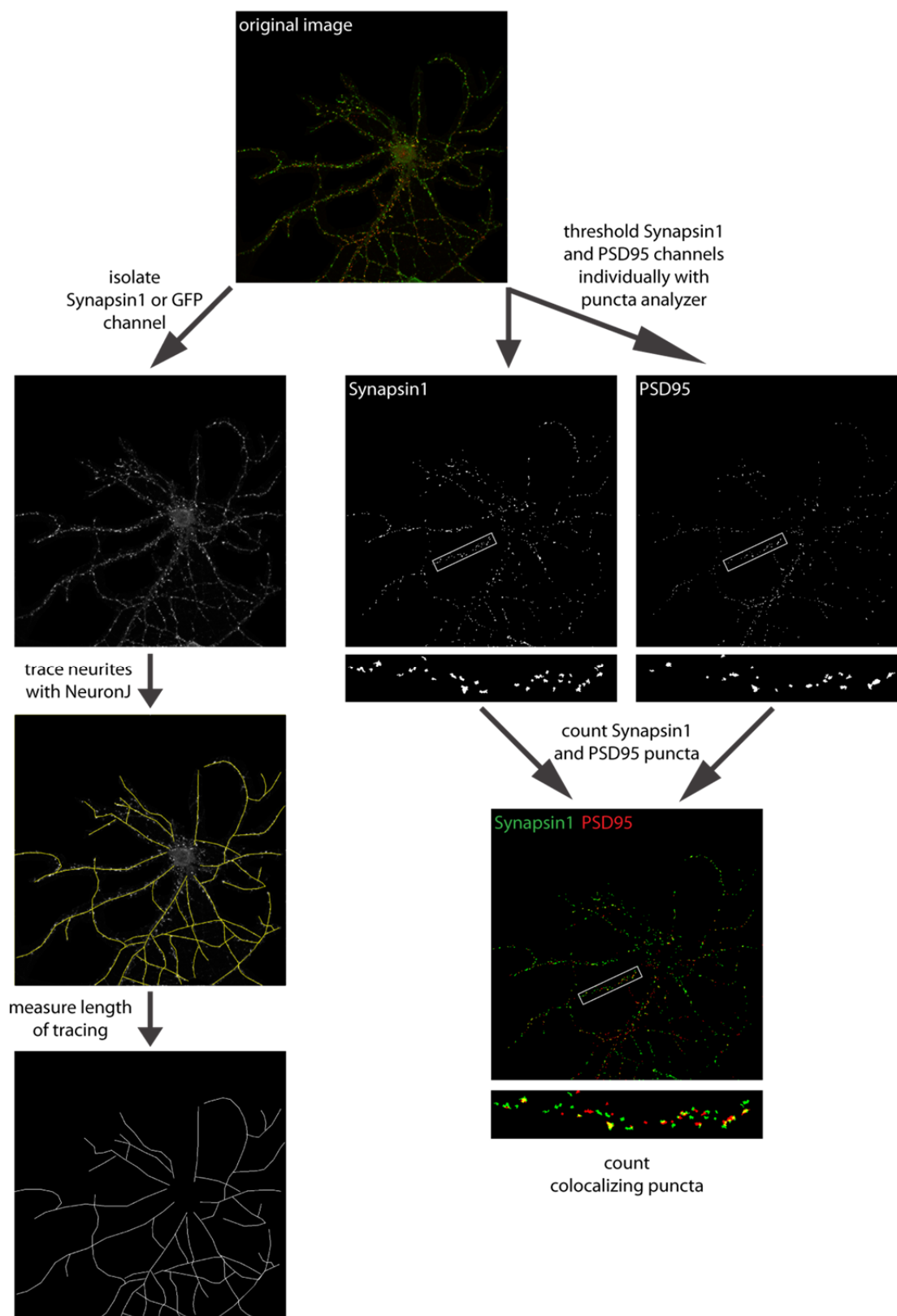


Fig. 11 Example of synapse quantification in primary neurons

The steps of synapse quantification in primary neurons from the original image to the traced neuronal arbor and thresholded Synapsin1 and PSD95 puncta are shown by a representative example.

Results

Thus, I chose Ctip2 positive neurons to analyze synapse density of FLRT1 knock-out cells. As shown in Fig. 12, knock-out of FLRT1 did not change the density of Synapsin1-positive (Fig. 12 A, D) or PSD95-positive (Fig. 12 B, E) puncta on these neurons. Moreover, FLRT1 knock-out also had no effect on the density of colocalized puncta as well (Fig. 12 C, F).

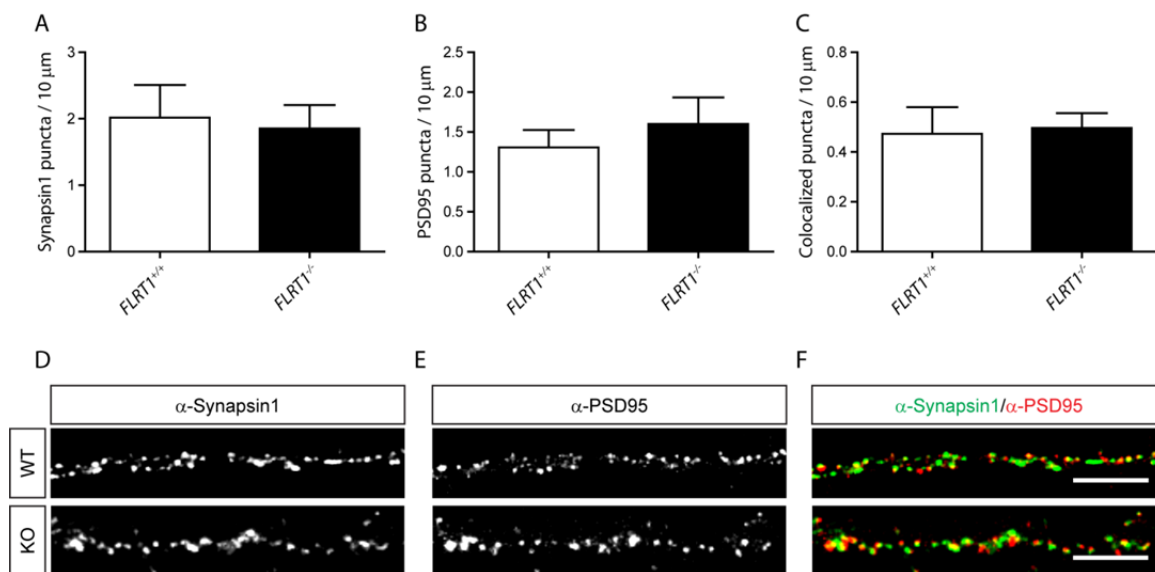


Fig. 12 Genetic knock-out of FLRT1 does not change synapse number in primary hippocampal neurons
Hippocampal neurons were prepared from E17.5 *FLRT1*^{-/-} mouse embryos or *FLRT1*^{+/+} littermate controls and fixed at DIV21. Cells were stained for Synapsin1 (D, green in F), PSD95 (E, red in F) and Ctip2. Synapsin1-positive puncta (A, D), PSD95-positive puncta (B, E) and colocalized puncta (C, F) per 10 μm neurite length were counted on Ctip2-positive cells. Results represent mean ± SEM of three independent experiments (≥ 20 cells per experiment). Statistical significance was calculated using Student's T-test. Scale bars, 10 μm.

Next, I decided to investigate the effect of FLRT3 knock-out on synapse density in primary neurons. First I analyzed the identity of FLRT3-positive neurons in culture. To this end, I made use of the *FLRT3*^{lacZ} mouse line (Egea et al., 2008) that expresses β-galactosidase under the control of the FLRT3 promoter and thus allows

identification of FLRT3-positive cells in wild-type and knock-out situations. X-Gal staining of a coronal hippocampal section from a P30 *FLRT3^{lacZ/+}* confirmed the expression of FLRT3 in CA3 and DG (Fig. 13 A). The expression of Ctip2 exclusively in CA1 and DG is shown by antibody staining in Fig. 10. I then cultured neurons from *FLRT3^{lacZ/+}* embryos for 21 days, fixed and stained them for NeuN and Ctip2. I performed X-Gal staining as well to identify β -galactosidase positive cells. An example image of NeuN-positive (red), Ctip2-negative cells expressing β -galactosidase is shown in Fig. 13 B. The white arrowheads point to prominent spots of X-Gal staining. A Ctip2-positive cell (green) expressing low levels of β -galactosidase can also be seen on the right side of the image. I then quantified the number of cells expressing the different markers and found 41.3% of NeuN-positive cells in culture to be Ctip2-negative (Fig. 13 C). 78.2% of the Ctip2-negative cells were X-Gal-positive (Fig. 13 D). Thus, I quantified the density of Synapsin1 and PSD95-positive as well as colocalized puncta on Ctip2-negative cells in cultures from FLRT3 knock-out embryos (Fig. 14). Because *FLRT3^{-/-}* embryos die around E10.5 from defects in ventral closure, headfold fusion and definitive endoderm migration (Maretto et al., 2008; Egea et al., 2008), the *FLRT3^{lx/lx}* mouse line (Yamagishi et al., 2011) was used for all FLRT3 knock-out experiments. To achieve nervous system specific knock-out of FLRT3 I bred the *FLRT3^{lx/lx}* mice to a mouse line expressing Cre recombinase under the control of the Nestin promoter (Tronche et al., 1999).

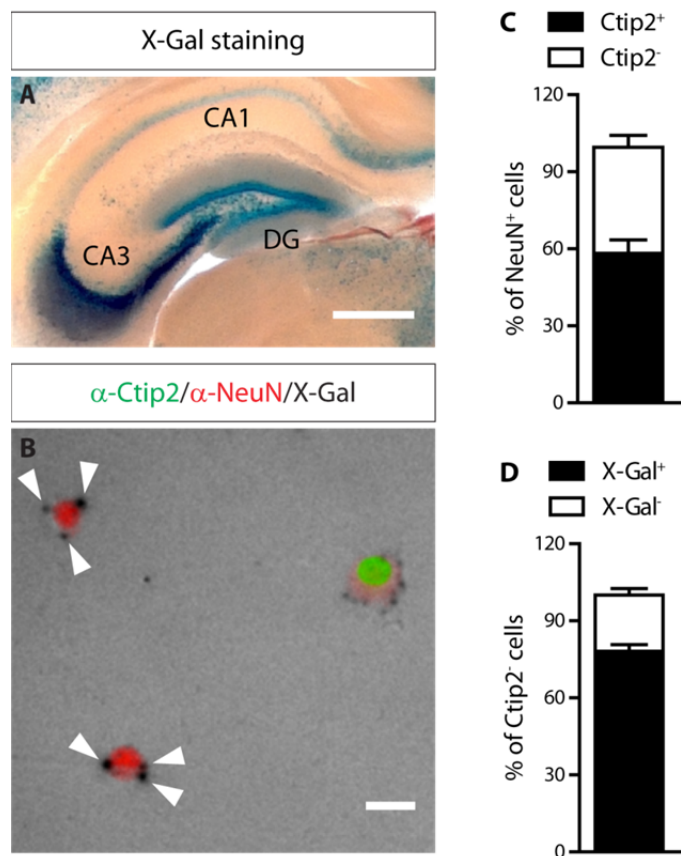


Fig. 13 Distribution of FLRT3-positive cells in hippocampus and primary culture

(A) X-Gal staining of a coronal section from hippocampus of a P30 *FLRT3^{lacZ/+}* mouse. (B) DIV21 hippocampal neurons stained for NeuN (red), Ctip2 (green) and X-Gal (black). White arrowheads point to X-Gal-positive spots on Ctip2-negative neurons. (C) Quantification of NeuN-positive cells expressing Ctip2. (D) Quantification of Ctip2-negative cells expressing β -galactosidase. Values in C and D represent mean \pm SEM of two experiments (≥ 98 NeuN⁺ cells per experiment). Scale bars, 500 μ m in (A) and 10 μ m in (B).

X-Gal staining (A) was performed by Dr. Daniel del Toro Ruiz.

I prepared cultures from *FLRT3^{lx/lx}/NesCre⁺* embryos and *FLRT3^{lx/lx}* littermate controls at E17.5 and analyzed the neurons at DIV21. Complete loss of FLRT3 protein in *FLRT3^{lx/lx}/NesCre⁺* mouse brain and primary neurons from those mice has been shown previously (Yamagishi et al., 2011). Genetic knock-out of FLRT3 did not change the density of Synapsin1-positive puncta compared to control neurons (Fig. 14 A, D). There

was no statistically significant change in the density of PSD95-positive puncta (Fig. 14 B, E) or colocalized Synapsin1/PSD95 puncta (Fig. 14 C, F) as well.

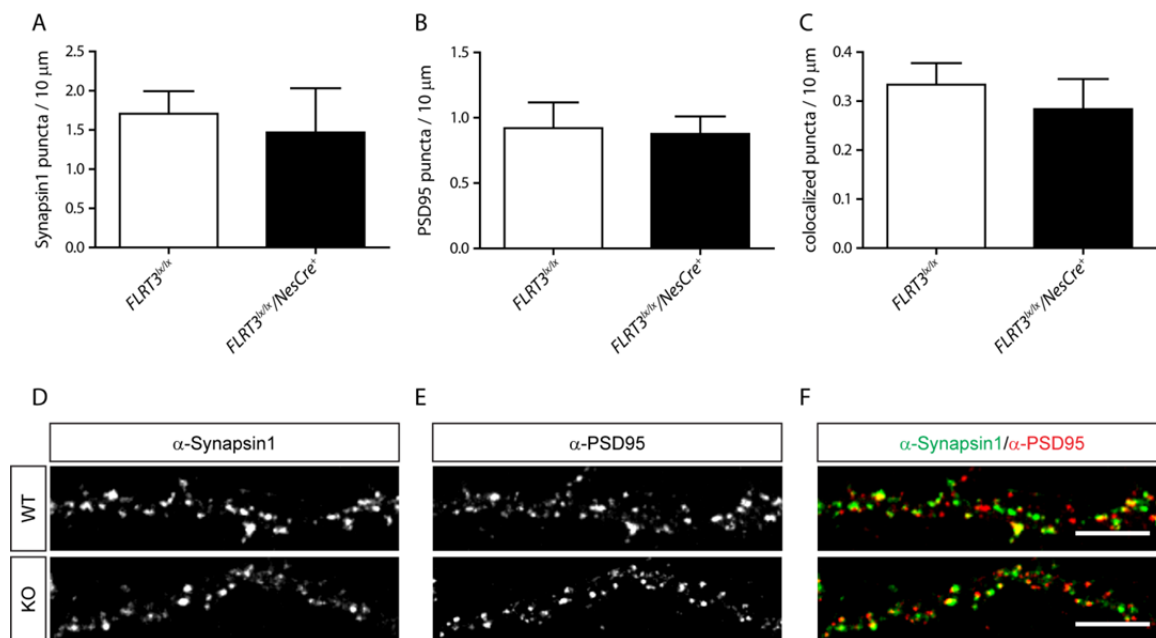


Fig. 14 Conditional genetic knock-out of FLRT3 does not change synapse number in primary hippocampal neurons

Hippocampal neurons were prepared from E17.5 $FLRT3^{lox/lox}/NesCre^{+}$ mouse embryos or $FLRT3^{lox/lox}$ littermate controls and fixed at DIV21. Cells were stained for Synapsin1 (D, green in F), PSD95 (E, red in F) and Ctip2. Synapsin1-positive puncta (A, D), PSD95-positive puncta (B, E) and colocalized puncta (C, F) per 10 μm neurite length were counted on Ctip2-negative cells. Results represent mean ± SEM of three independent experiments (≥ 20 cells per experiment). Statistical significance was calculated using Student's T-test. Scale bars, 10 μm.

2.1.3.2. Sparse knock-out of FLRT3 does not change excitatory synapse number *in vitro*

My results up to this point were in clear contrast to previously published work that showed an involvement of FLRT3 in the formation of excitatory synapses

(O'Sullivan et al., 2012, 2014). The main difference between the experimental approaches was the use of shRNA knock-down of FLRT3 in the published work and genetic ablation of FLRT3 in my experiments. The two approaches lead to two major differences between the experiments: first, NesCre expression starts around E9.5, whereas the knock-down approach is limited to the day of neuronal culture. Thus, compensatory mechanisms could potentially diminish the effects induced by genetic ablation of FLRT3. Second, the knock-out with Cre recombinase targets all neurons, since Nestin is expressed in all neuronal precursors (Zimmerman et al., 1994; Tronche et al., 1999), whereas shRNA mediated knock-down only suppresses gene expression in a limited number of transfected neurons. It has been shown that neurons from Neuroligin1, Neuroligin2, Neuroligin3 triple knock-out mice have normal numbers of synapses and normal synaptic ultrastructure (Varoqueaux et al., 2006) and deletion of Neuroligin1 in hippocampus or amygdala does not change synapse density in the mouse (Varoqueaux et al., 2006; Kim et al., 2008; Blundell et al., 2010), even though Neuroligins are well established synaptogenic proteins. A recent report showed that rather than the absolute levels of Neuroligin1 regulating synapse density, the intercellular differences in its expression determines the number of synapses, with high-expressing cells making more synapses than low-expressing neighboring cells (Kwon et al., 2012).

In consideration of those findings, I decided to take a similar approach. To achieve sparse knock-out of FLRT3, I prepared neurons from *FLRT3^{lx/lx}* embryos and transfected them with a plasmid encoding Cre recombinase and GFP under control of the CAG promoter before plating, making use of the low transfection efficiency of primary neurons. I then analyzed Synapsin1 and PSD95 puncta density as well as density of colocalized puncta on Ctip2-negative, GFP-positive neurons (Fig. 15).

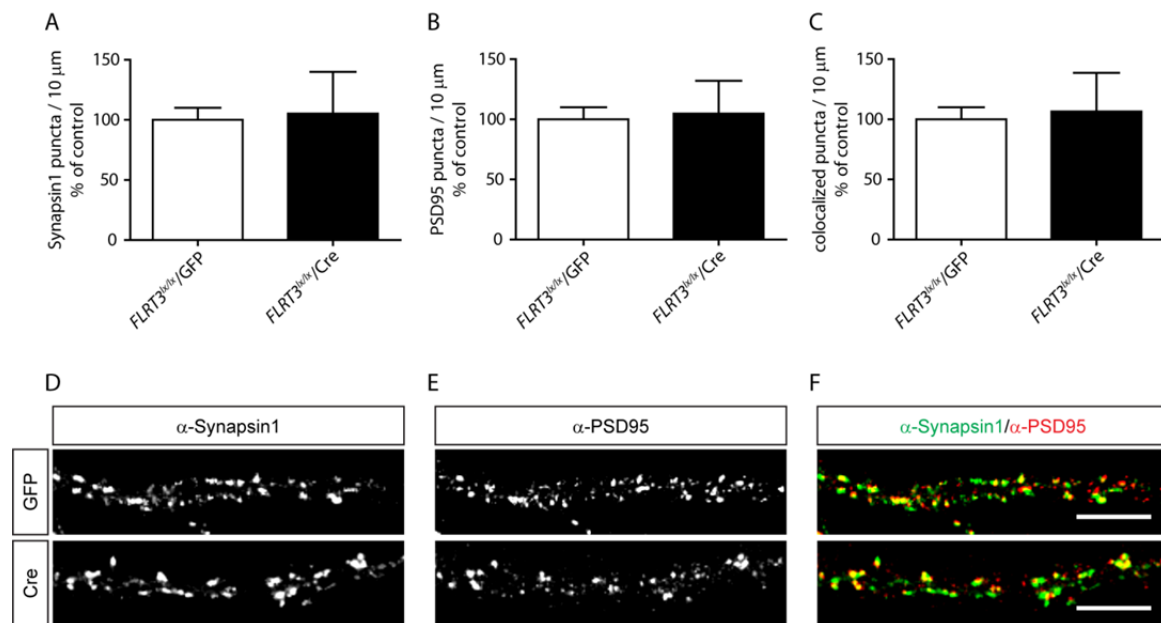


Fig. 15 Sparse knock-out of FLRT3 does not change synapse number in primary hippocampal neurons

Hippocampal neurons were prepared from E17.5 *FLRT3*^{lox/lox} mouse embryos and transfected with a pCAG-Cre-IRES-GFP construct or a GFP control plasmid using Amaxa™ before plating. Cells were fixed at DIV21 and stained for Synapsin1 (D, green in F), PSD95 (E, red in F) and Ctip2. Synapsin1-positive puncta (A, D), PSD95-positive puncta (B, E) and colocalized puncta (C, F) per 10 μm neurite length were counted on Ctip2-negative, GFP-positive cells. Results represent mean ± SEM of three independent experiments (≥ 20 cells per experiment). Statistical significance was calculated using Student's T-test. Scale bars, 10 μm.

As shown in Fig. 15 A and D, expression of Cre recombinase had no effect on the density of Synapsin1 puncta compared to expression of GFP alone. Also the density of PSD95 puncta (Fig. 15 B, E) or colocalizing Synapsin1/PSD95 puncta (Fig. 15, C, F) was unaffected by Cre mediated deletion of FLRT3 in these neurons. These results show that loss of FLRT3 even in only a subset of neurons also does not impair their ability to make synapses compared to surrounding FLRT3-positive cells.

Since available FLRT3 antibodies do not reliably detect endogenous FLRT3, I could not confirm the loss of FLRT3 protein in Cre transfected neurons. However, the *FLRT3*^{lox} allele

has been shown to be efficiently excised by Cre recombinase (Yamagishi et al., 2011). Furthermore, I tested the activity of the Cre recombinase by cotransfecting HEK293 cells with pCAG-Cre-GFP and a plasmid containing a lox-stop-lox-mCherry sequence. I found virtually all GFP-positive cells to also be mCherry-positive with no GFP-negative cells being mCherry-positive (data not shown), confirming the functionality of the Cre construct. These findings confirm that the lack of phenotype is not due to a problem with the knock-out strategy.

2.1.3.3. Overexpression of FLRT3 does not change excitatory synapse number *in vitro*

Next I decided to take a gain-of-function approach and overexpress FLRT3 in hippocampal neurons. For that purpose, I prepared hippocampal neurons from wild-type mouse embryos at E17.5 and transfected the cells with a pCAG-FLRT3-IRES-GFP construct or a GFP control plasmid using Amaxa™ before plating. At DIV21 I fixed and stained the cells and analyzed Synapsin1 and PSD95 puncta density (Fig. 16).

Overexpression of FLRT3 in hippocampal neurons did not result in a statistically significant change of the density of Synapsin1-positive puncta (Fig. 16 A, D), or the density of PSD95-positive puncta (Fig. 16 B, E). Moreover, the density of colocalized puncta did not change upon ectopic expression of FLRT3 (Fig. 16 C, F).

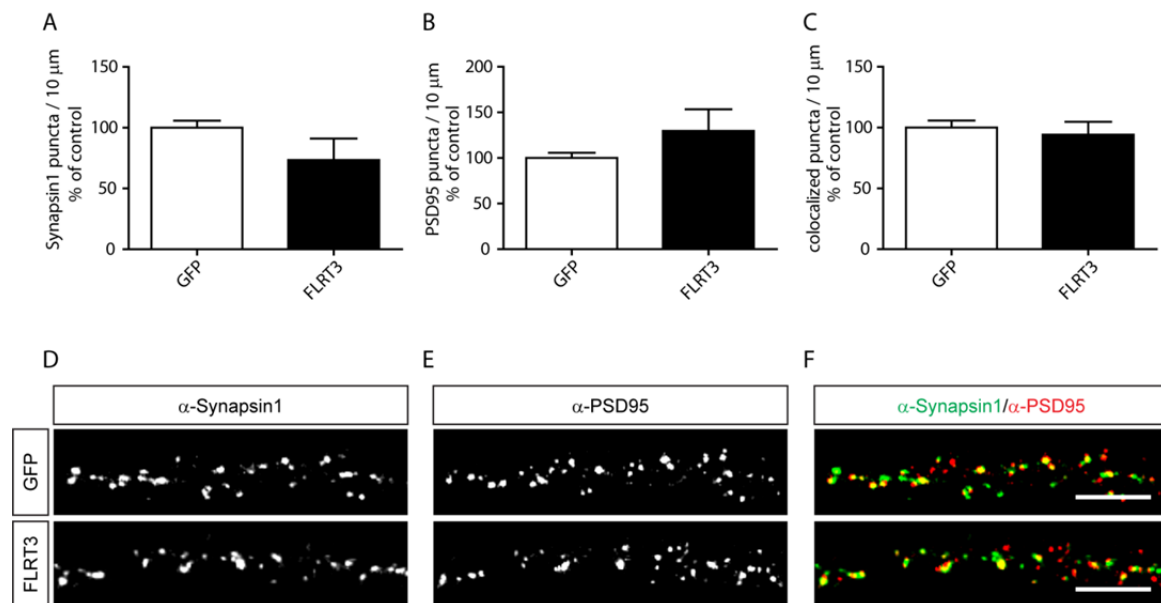


Fig. 16 Overexpression of FLRT3 does not change synapse number in primary hippocampal neurons

Hippocampal neurons were prepared from E17.5 mouse embryos and transfected with a pCAG-FLRT3-IRES-GFP construct or a GFP control plasmid using Amaxa™ before plating. Cells were fixed at DIV21 and stained for Synapsin1 (D, green in F) and PSD95 (E, red in F). Synapsin1-positive puncta (A, D), PSD95-positive puncta (B, E) or colocalized puncta (C, F) per 10 μm neurite length were counted on GFP-positive cells. Results represent mean ± SEM of three independent experiments (≥ 20 cells per experiment). Statistical significance was calculated using Student's T-test. Scale bars, 10 μm.

2.1.4. Knock-out of FLRT1 and FLRT3 does not change expression of synaptic proteins in hippocampus *in vivo*

Since changes in the expression levels of FLRT proteins in primary neurons did not show any effect on excitatory synapse density in my hands, I decided to investigate the involvement of FLRTs in synapse formation *in vivo*. First, I took a biochemical approach. For that purpose, I isolated brains from four P20/P21 mice and dissected out the hippocampi. The hippocampi were then cut into 1 mm thick sections using a tissue chopper and the sections were manually dissected into CA1, CA3 and DG regions under a dissection microscope. Material of both hippocampi from one mouse was pooled and further processed.

First I performed Western blot analysis to confirm successful separation of the regions (Fig. 17). Ctip2 was used as a marker of CA1 and DG regions and Prox1, a marker of DG cells only, was used to further distinguish regions. As shown in Fig. 17, Ctip2 is present in samples from the CA1 and DG regions, whereas high levels of Prox1 can only be found in samples from the DG with low level contamination in samples CA1 and CA3.

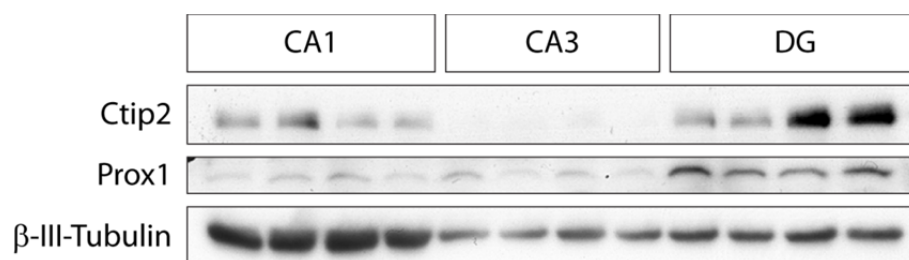


Fig. 17 Validation of hippocampal microdissection

Hippocampi from four mice were dissected out at P20 and further dissected into CA1, CA3 and DG regions. Each brain was processed separately and used as independent sample. Samples were then subjected to SDS-PAGE and probed with antibodies against Ctip2 and Prox1 to verify good separation of the different regions and β -III-Tubulin to confirm equal loading. DG, dentate gyrus.

Having confirmed successful separation of the three main hippocampal regions, I went on to check expression levels of synaptic proteins in FLRT knock-out mouse brains. I dissected hippocampi from four *FLRT3^{lox/lox}/NesCre⁺* mice and four *FLRT3^{lox/lox}* controls, respectively. I then blotted for the synaptic markers Munc13-1, Synapsin1, Synaptophysin and Snap25 (Fig. 18, left side). These proteins have different functions in the presynapse. Snap25 is a vSNARE and thus involved in the docking and fusion of vesicles. Munc13-1 has been shown to be involved in the priming of vesicles, whereas Synaptophysin can interact with Dynamin at high calcium concentration and has been implicated in the endocytosis of synaptic vesicles. Synapsin1 is a phosphoprotein on the surface of synaptic vesicles and has been shown to be involved in the modulation of neurotransmitter release.

As expected, none of the markers showed a change in expression levels between FLRT3 knock-out and wild-type mice in the CA1 region, which, as it is devoid of FLRT3 expression, functions as an internal control (Fig. 18 A). Furthermore, in FLRT3 knock-out mice the FLRT3-expressing regions CA3 and DG did not show the lower levels of synaptic proteins that would be expected if there were fewer synapses present (Fig. 18 B, C).

I repeated the same experiment using two FLRT1 knock-out mice and two controls (Fig. 18, right side). In case of a strong effect of FLRT1 on synapse numbers, synaptic proteins should be reduced in samples from the CA1 region. On the other hand, no effect should be seen in CA3 and DG regions which do not express FLRT1. As shown in Fig. 18 A-C, no obvious change in the levels of Munc13-1, Synapsin1, Synaptophysin or Snap25 was found in any of the regions of the hippocampus in *FLRT1^{-/-}* mice.

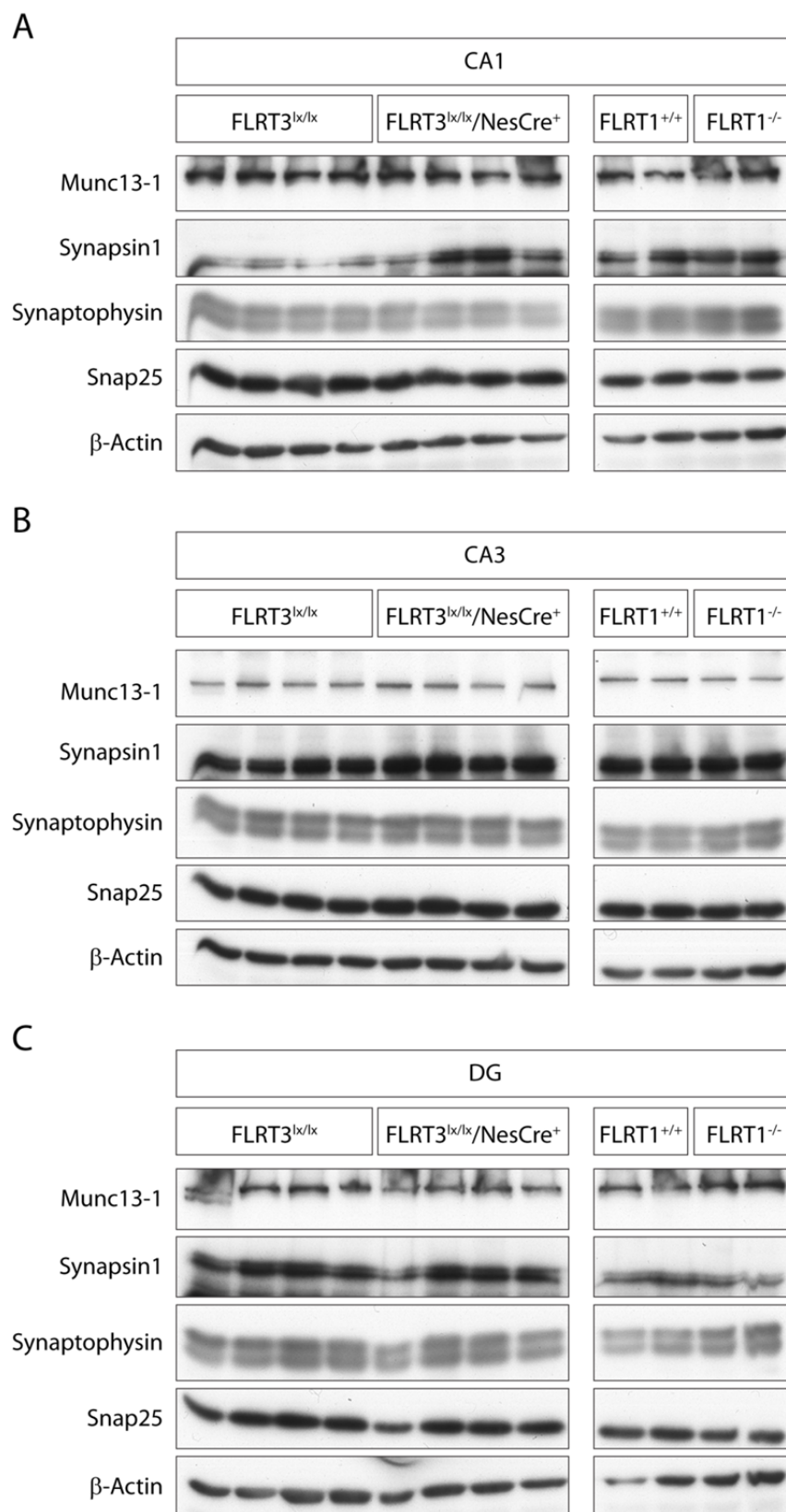


Fig. 18 Analysis of synaptic proteins in microdissected hippocampus

Hippocampi from P20/P21 mice were dissected into CA1, CA3 and DG and the samples were subjected to SDS-PAGE and blotted on PVDF membranes. Membranes were probed with antibodies against synaptic proteins, and β -Actin to confirm equal loading.

2.1.5. Knock-out of FLRT3 does not change synapse density in the hippocampus *in vivo*

Since the biochemical approach described before is not very sensitive, it might not be sufficient to uncover weak effects of FLRT family members on the number of synapses. Thus I decided to use a much more sensitive method to directly quantify synapses in the mouse brain. To this end, transmission electron microscopy was performed on coronal sections of the hippocampus from P20 $FLRT3^{lx/lx}/NesCre^+$ mice and $FLRT3^{lx/lx}$ controls. Images were taken from the stratum radiatum of CA1 and CA3 and the middle molecular layer of the DG. I then manually counted the number of synaptic structures in the images. For quantification, two well aligned membranes and a clearly stained postsynaptic density were considered a synapse (Fig. 19 A, white arrowheads).

I did not find a statistically significant difference in the number of excitatory synapse densities in the CA3 or DG regions between $FLRT3^{lx/lx}/NesCre^+$ and control mice, similar to what I quantified in the CA1 region that was used as an internal control as it does not express FLRT3 (Fig. 19 B).

In summary, in contrast to previously published results (O'Sullivan et al., 2012, 2014) that showed involvement of FLRT3 in the development of excitatory synapses *in vitro* and in hippocampus and cortex *in vivo*, I could not find any evidence for a function of FLRT family members in excitatory synapse development using a variety of different assays, perhaps highlighting the differences between knock-out and knock-down model systems.

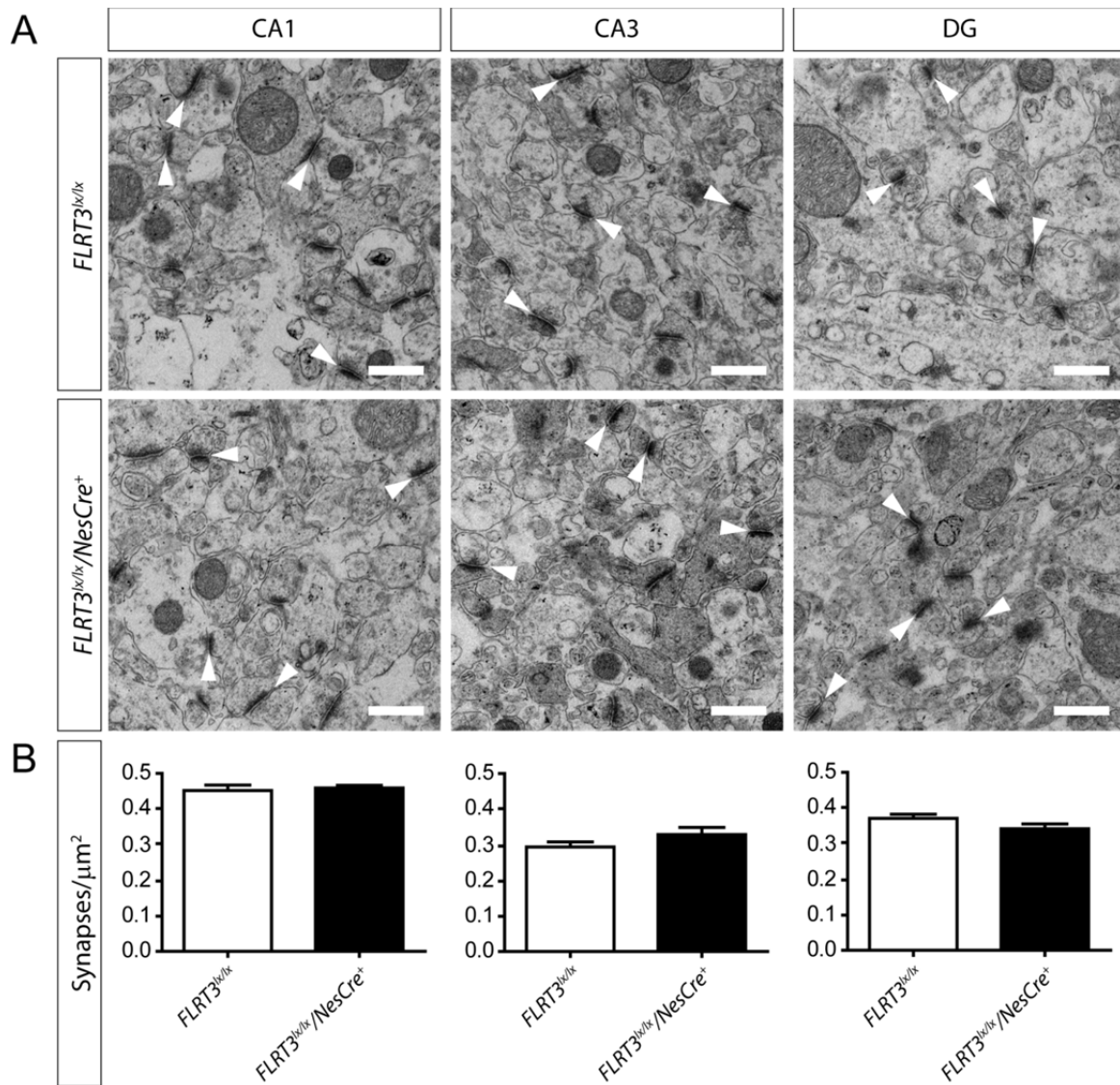


Fig. 19 Ultrastructural quantification of synapses in the hippocampus

Coronal sections from hippocampus of *FLRT3^{lox/lox}/NesCre⁺* mice and *FLRT3^{lox/lox}* controls at P20 were imaged by transmission electron microscopy at 25,000x magnification. Images were taken from stratum radiatum of CA1, CA3 and the middle molecular layer of DG. (A) Representative example images from *FLRT3* WT and KO mice. (B) Quantification of images. Synapses were counted manually in ImageJ and total numbers were normalized to area. White arrowheads in (A) point to examples of synapses. Results represent mean \pm SEM of 4 animals. Statistical significance was calculated using Student's T-test. Scale bars, 0.5 μ m.

Thin sectioning, staining and imaging were done by Marianne Braun and Ursula Weber from the EM facility of the MPI for Neurobiology.

2.2. Involvement of FLRT family members in neuronal migration during cortex development

2.2.1. Generation of a variety of FLRT and Unc5 binding mutants based on crystal structures

Recent work has shown that FLRT proteins can interact either homophilically or form heterophilic complexes with cell surface receptors of the Unc5 family (Karaulanov et al., 2006; Söllner and Wright, 2009; Karaulanov et al., 2009). In case of heterophilic interaction, soluble FLRT ectodomains act as repulsive guidance cues for Unc5 expressing neurons (Yamagishi et al., 2011). But the structural determinants of these interactions are still unknown. To gain insight into this interaction, we collaborated with structural biologist Dr. Elena Seiradake in the lab of Prof. E. Yvonne Jones at the University of Oxford, UK, who has solved the crystal structures of the FLRT (Fig. 20 A) and Unc5 (Fig. 20 C) ectodomains. She has also solved the structure of an FLRT2-Unc5D complex, however only at low resolution. The high resolution data from the uncomplexed ectodomains was sufficient, however, to assign amino acid locations to the complex. A summary of the structural data is shown in Fig. 20.

The FLRT leucine-rich repeats (LRRs) formed a horseshoe shape similar to other LRR containing proteins (Scott et al., 2004; Seiradake et al., 2011; de Wit et al., 2011) and the Unc5 immunoglobulin (Ig) domains revealed the classical, compact globular structure of previously crystalized Ig domains (Coles et al., 2011; Chothia and Jones, 1997). The data showed that the FLRT LRRs bind to the Ig1 domain of Unc5 via the lateral side of the horseshoe (Fig. 20 E), whereas the homophilic FLRT-FLRT interaction uses the concave side of the LRR structure (Fig. 20 D). The homophilic interaction data is comparable to

other LRR proteins (Islam et al., 2013). FLRT2 and FLRT3 LRR domains from different species show a high degree of conservation especially in the regions that appear to be important for the interactions described here (Fig. 20 B). This could explain the binding promiscuity between different FLRT and Unc5 isoforms (Yamagishi et al., 2011; Söllner and Wright, 2009).

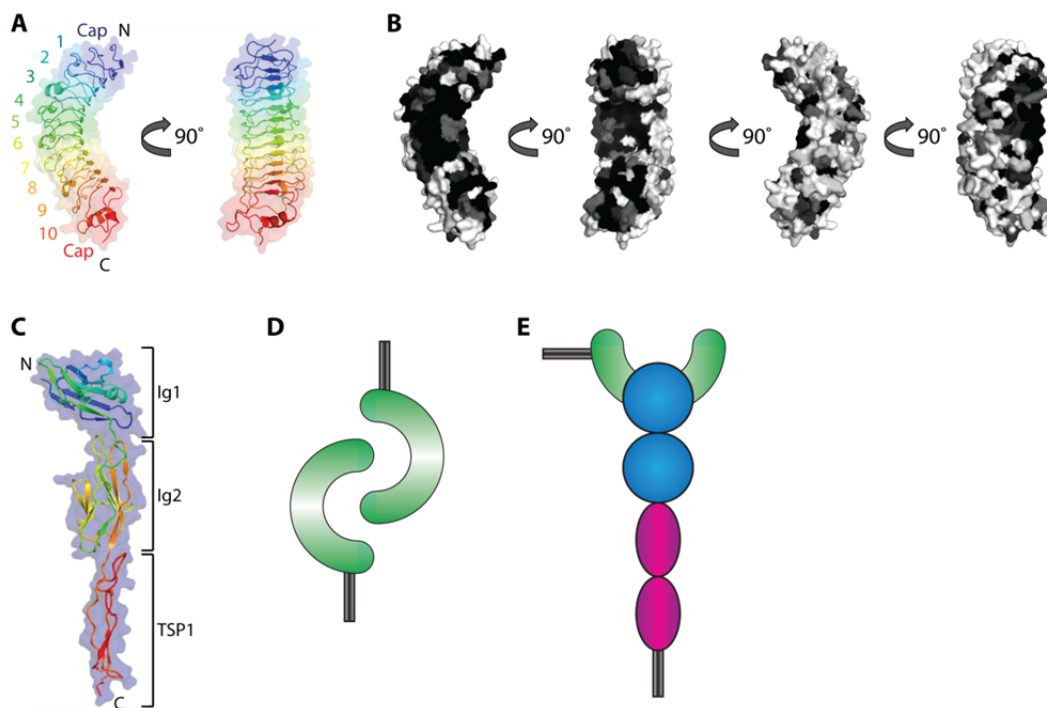


Fig. 20 Summary of structural data

(A) FLRT3 LRR coloured according to the rainbow. Blue, N-terminus; red, C-terminus. The LRR motifs are numbered 1-10 and the positions of the Cysteine-rich cap structures are indicated. (B) Surface views of the FLRT3 LRR domain, colored according to sequence conservation within FLRT2/3 from mouse, fish, frog and bird. Black, highest conservation; white, lowest conservation. (C) Structure of the complete human Unc5A ectodomain. Note that human Unc5A contains only one TSP domain. (D) Schematic representation of the FLRT LRR homophilic interaction. (E) Schematic representation of the interaction of the FLRT LRR domain with the Unc5 ectodomain.

Structural data and panels A-C were generated by Dr. Elena Seiradake.

Having found that the FLRT LRR domain uses structurally distinct surfaces for homophilic and heterophilic interactions, we decided to make use of this fact by designing specific glycosylation mutants of FLRT2 and FLRT3 that should inhibit homophilic interaction without interfering with heterophilic binding, and *vice versa*. To add an N-glycosylation site at the protein surface region of choice, we introduced the sequence Asp-X-Thr/Ser, where X can be any amino acid other than proline. We introduced such a glycosylation site at the lateral side of the FLRT LRR domain, harboring the Unc5-binding site, to inhibit FLRT-Unc5 interaction (Fig. 21 A). This mutant will be referred to as FLRT2/3^{UF}. To inhibit FLRT-FLRT interactions, we introduced a glycosylation site at the concave side of the horseshoe structure and named this mutant FLRT2/3^{FF} (Fig. 21 A). Furthermore, we introduced a glycosylation site into Ig1 (the outermost Ig domain of the extracellular domain) of Unc5D to inhibit Unc5D-FLRT2 interaction (Unc5D^{UF}, Fig. 21 B). Insertion of glycosylation sites at surface-exposed binding sites of proteins has been shown to interfere with protein-protein interactions without disturbing protein folding and function *per se* (Seiradake et al., 2011; Islam et al., 2013). All constructs were inserted into the pHL-mVenus vector. This added a C-terminal mVenus tag to the protein to easily visualize expression in imaging experiments. Furthermore, an N-terminal HA tag was added to allow reliable examination of surface expression of the constructs.

First I tested the surface expression of all constructs upon overexpression in COS7 cells by staining for the N-terminal HA tag without permeabilizing the cells. All constructs were well expressed on the surface (data not shown). An example of the experiment is shown in Fig. 22. Immunostaining against the HA tag (Fig. 22 B) shows clear staining of the transfected cell that is shown by mVenus fluorescence (Fig. 22 A). However, even though the cell shows clear mVenus fluorescence, it is negative for staining against the

intracellular mVenus tag (Fig. 22 C). This confirms the integrity of the cell membrane and ensures that the HA staining detects surface proteins only.

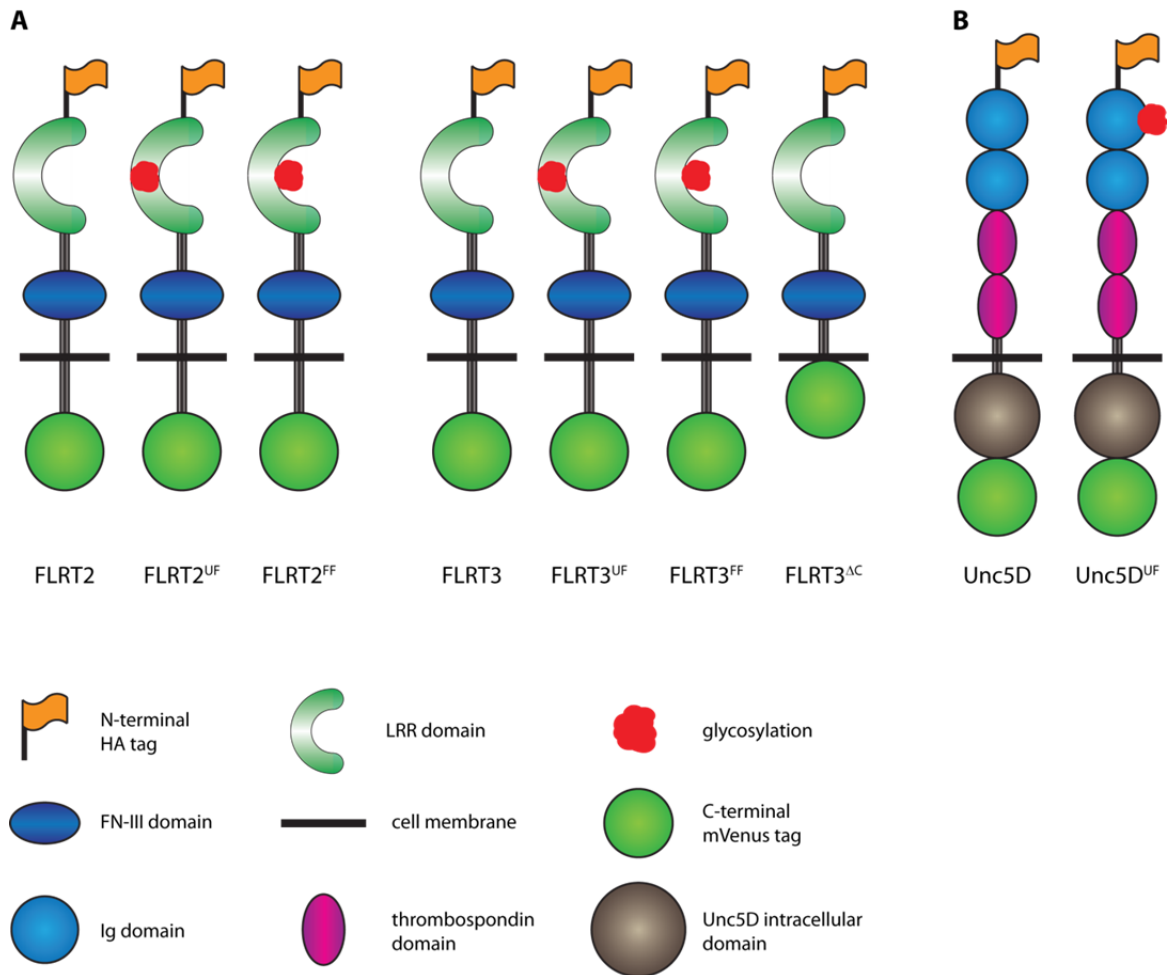


Fig. 21 Overview of FLRT and Unc5D binding mutant constructs

A schematic overview of the FLRT2, FLRT3 (A) and Unc5D (B) constructs used is shown. The red dot represents the site of N-glycosylation to specifically disrupt binding.

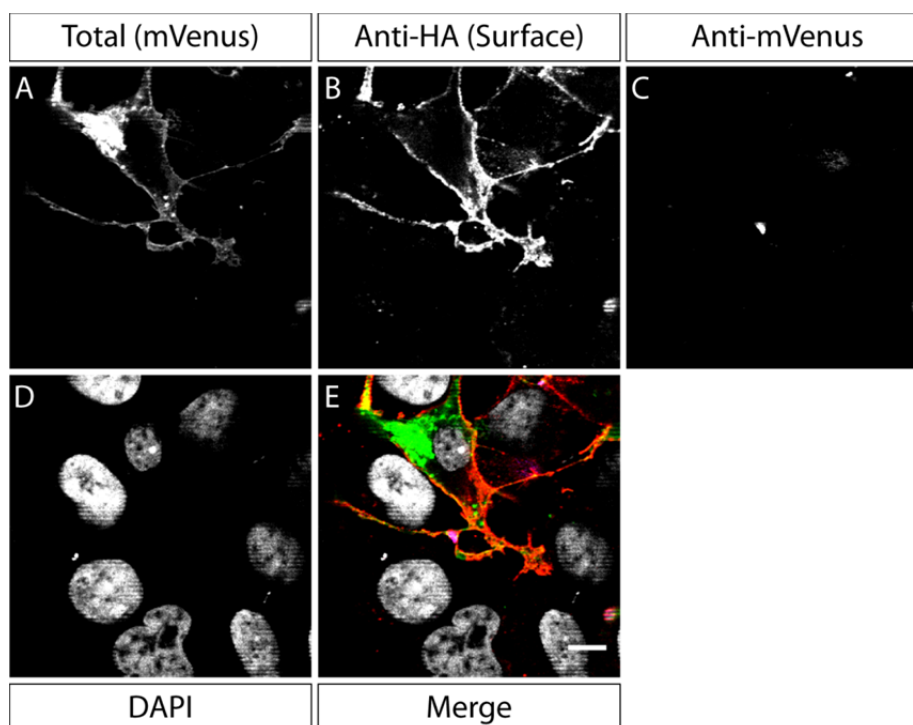


Fig. 22 Surface staining of mVenus constructs

Constructs were expressed in COS7 cells. Cells were fixed after one day of expression and stained against the extracellular HA tag and against the intracellular mVenus without permeabilizing. Cells were then counterstained with DAPI and imaged on a confocal microscope. (A) Total construct expression (mVenus fluorescence, green in merge). (B) Anti-HA staining (surface, red in merge). (C) Anti-mVenus staining (blue in merge). (D) DAPI staining (gray in merge). (E) merge. Note the absence of surface staining in nontransfected cells and the absence of anti-mVenus staining in the transfected cell. Scale bar, 10 μm .

To confirm the specificity of the glycosylation mutants I performed surface binding assays as previously described (Yamagishi et al., 2011). The constructs were transfected into COS7 cells and after one day of expression, cells were incubated with Fc-tagged soluble extracellular domains of their respective binding partners that were preclustered using fluorescently labelled anti-human Fc antibodies. As a control, cells were incubated with preclustered human Fc.

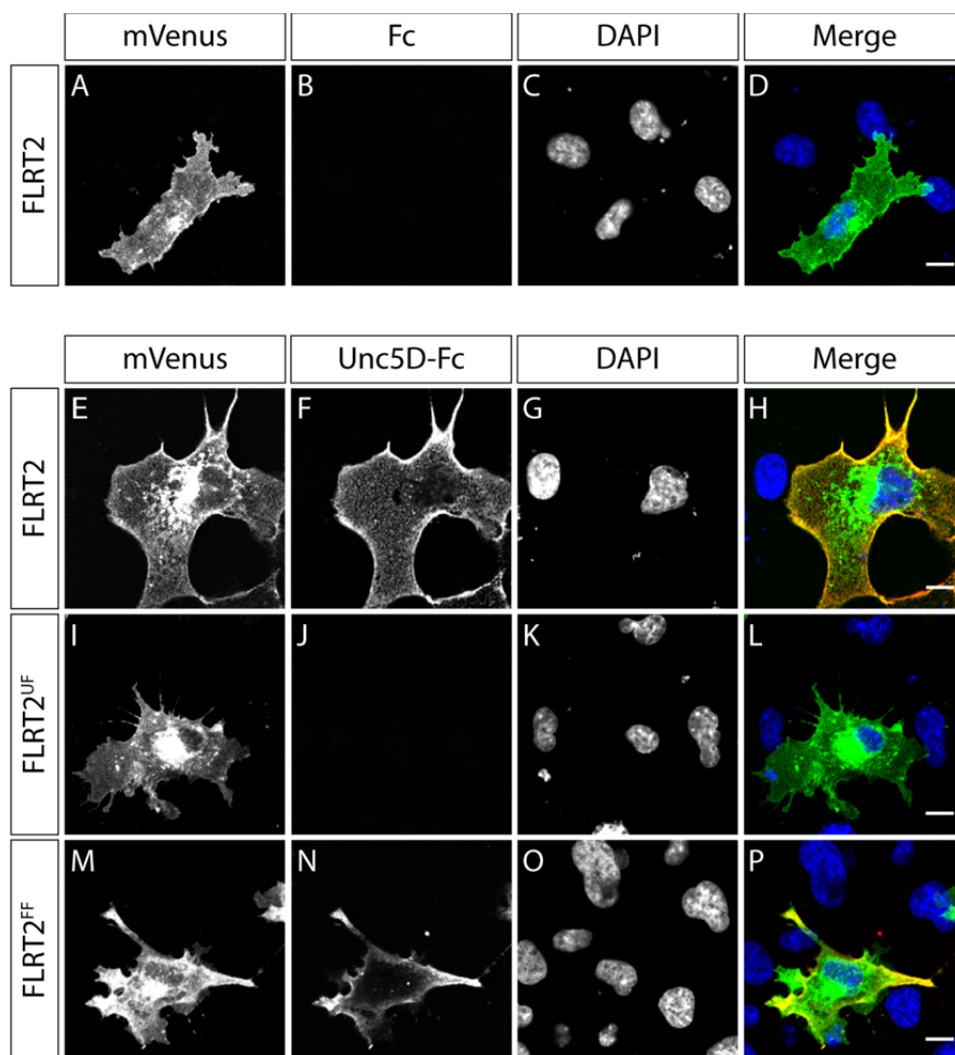


Fig. 23 Validation of FLRT2 binding mutants

COS7 cells were transfected with the constructs indicated on the left. After one day of expression, cells were incubated with human Fc (A-D) or soluble Unc5D extracellular domain fused to human Fc (E-P) preclustered with fluorescently labelled anti-human Fc antibody. Cells were then fixed and counterstained with DAPI. Samples were imaged on a confocal microscope. In the merges, mVenus fluorescence is depicted in green and Fc or Unc5D-Fc is shown in red. Scale bars, 10 μ m.

Fig. 23 A-D confirms the absence of unspecific background binding of clustered human Fc to FLRT2-expressing COS7 cells. Clustered Unc5D extracellular domain strongly binds to wild-type FLRT2 without detectable background binding to neighboring non-transfected cells (Fig. 23 E-H). Insertion of a glycosylation site in the FLRT2-Unc5D

interaction surface completely abolished binding of Unc5D to FLRT2^{UF} (Fig. 23 I-L), whereas mutation of the FLRT-FLRT interaction surface did not have any effect on Unc5D binding to FLRT2^{FF} (Fig. 23 M-P).

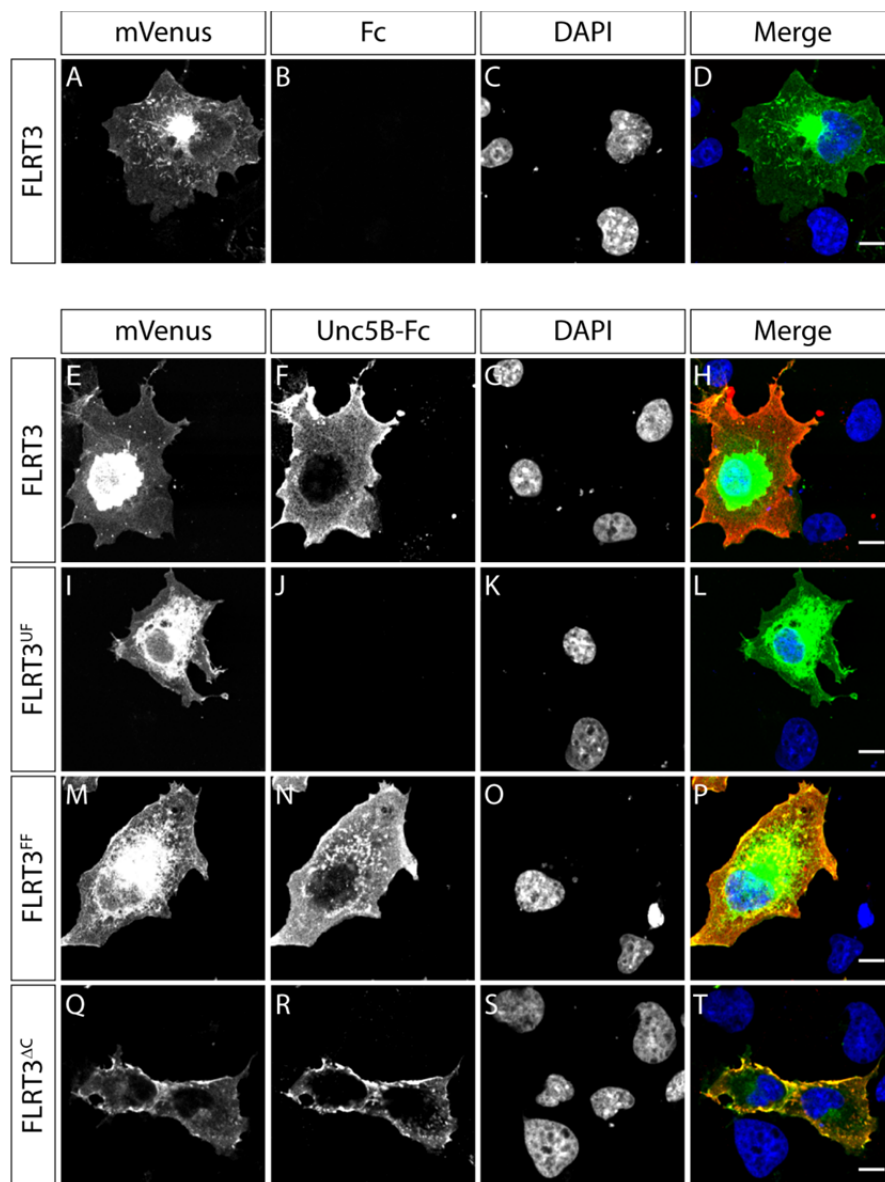


Fig. 24 Validation of FLRT3 binding mutants

COS7 cells were transfected with the constructs indicated on the left. After one day of expression, cells were incubated with human Fc (A-D) or soluble Unc5B extracellular domain fused to human Fc (E-T) preclustered with fluorescently labelled anti-human Fc antibody. Cells were then fixed and counterstained with DAPI. Samples were imaged on a confocal microscope. In the merges, mVenus fluorescence is depicted in green and Fc or Unc5B-Fc is shown in red. Scale bars, 10 μ m.

I also tested the binding of Unc5B-Fc to the FLRT3 constructs (Fig. 24). As expected, no binding of human Fc alone was detectable (Fig. 24 A-D). Unc5B-Fc efficiently bound to wild-type FLRT3 whereas binding to surrounding nontransfected cells was absent (Fig. 24 E-H). As predicted by the crystallographic data, insertion of a glycosylation site in the inside of the LRR horseshoe structure did not interfere with the binding of Unc5B to FLRT3 (Fig. 24 M-P) whereas a glycosylation on the lateral side of the LRR domain completely abolished binding (Fig. 24 I-L). Also deletion of the entire intracellular domain of FLRT3 (FLRT3^{ΔC}) did not have any influence on Unc5B binding (Fig. 24 Q-T).

To confirm functionality of the Unc5D mutant constructs, COS7 cells were transfected with wild type Unc5D or Unc5D^{UF} and binding of FLRT2-Fc was tested after one day of expression (Fig. 25). Binding of Fc to Unc5D was under the detection limit (Fig. 25 A-D). As reported previously (Yamagishi et al., 2011), FLRT2 ectodomain strongly bound to wild-type Unc5D (Fig. 25 E-H), whereas the Unc5D^{UF} mutation completely abolished binding of FLRT2 (Fig. 25 I-L).

FLRT-FLRT homophilic binding cannot be tested using the surface binding assay, presumably due to the weak nature of the interaction (Yamagishi et al., 2011). Thus, we employed a cell aggregation assay (Karaulanov et al., 2006) to test the potential for homophilic binding of our FLRT mutants. HEK cells were transfected with the FLRT3 constructs and collected using 5 mM EDTA to preserve surface proteins. Cells were then incubated in BSA coated 24 well plates for 6 days under constant orbital shaking to allow aggregate formation. Samples were then fixed and imaged (Fig. 26).

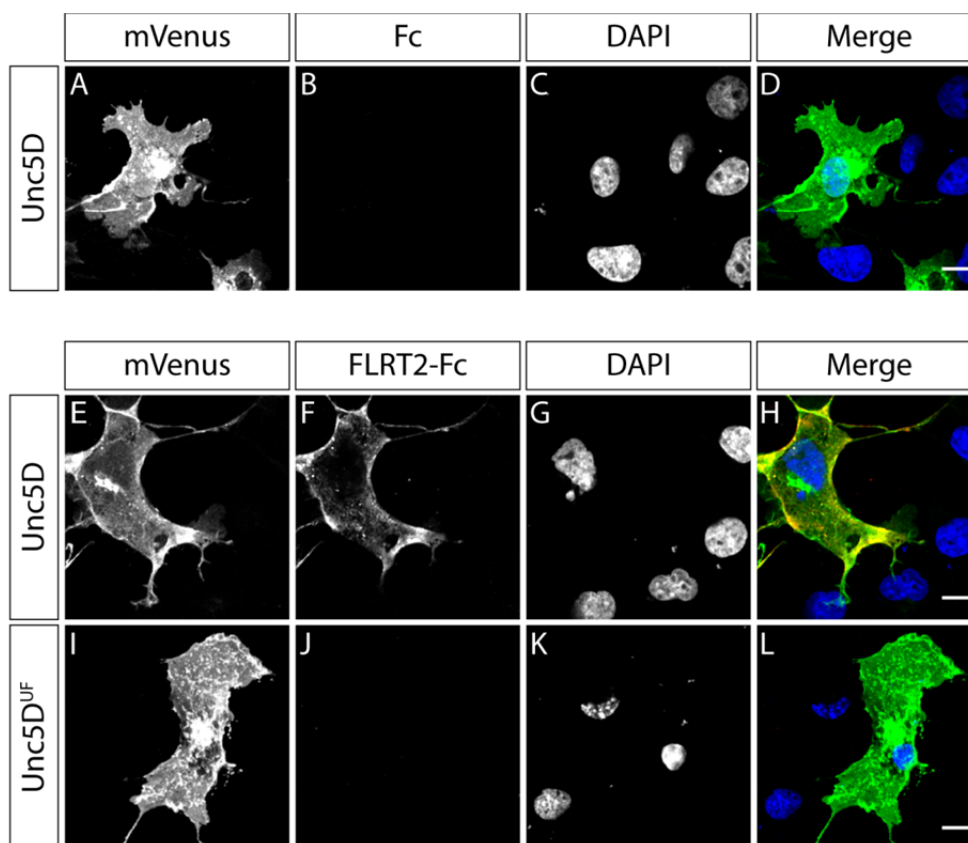


Fig. 25 Validation of the Unc5D binding mutant

COS7 cells were transfected with the constructs indicated on the left. After one day of expression, cells were incubated with human Fc (A-D) or soluble FLRT2 extracellular domain fused to human Fc (E-L) preclustered with fluorescently labelled anti-human Fc antibody. Cells were then fixed and counterstained with DAPI. Samples were imaged on a confocal microscope. In the merges, mVenus fluorescence is depicted in green and Fc or FLRT2-Fc is shown in red. Scale bars, 10 μm .

As shown before (Karaulanov et al., 2006; Hampel, 2012), overexpression of FLRT3 in HEK cells lead to formation of GFP-positive cell clusters within the aggregates (Fig. 26 B, F). In contrast to previously published results (Egea et al., 2008; Hampel, 2012), FLRT3 overexpression did not change aggregate size. Overexpression of the FLRT3^{FF} mutant (Fig. 26 D, H) lead to a more dispersed distribution of GFP-positive cells in the aggregates comparable to GFP expression (Fig. 26 A, E) an effect that was not apparent

Results

upon overexpression of FLRT3^{UF} (Fig. 26 C, G). Quantification of the size of GFP-positive cell clusters within the aggregate revealed statistically significant bigger clusters when FLRT3 or FLRT3^{UF} were overexpressed as compared to GFP or FLRT3^{FF} (Fig. 26 I). Overexpression of FLRT3^{FF} did not result in cluster sizes significantly different from GFP and clusters of FLRT3 cells were not significantly different in size from FLRT3^{UF} (Fig. 26 I). The same was true for FLRT2 and its mutants (data not shown).

Taken together, these results confirmed that the FLRT^{UF} mutants abolished the binding of Unc5s to FLRTs without interfering with FLRT homophilic binding. The FLRT^{FF} mutants on the other hand had no effect on FLRT-Unc binding but efficiently disrupted FLRT-FLRT binding.

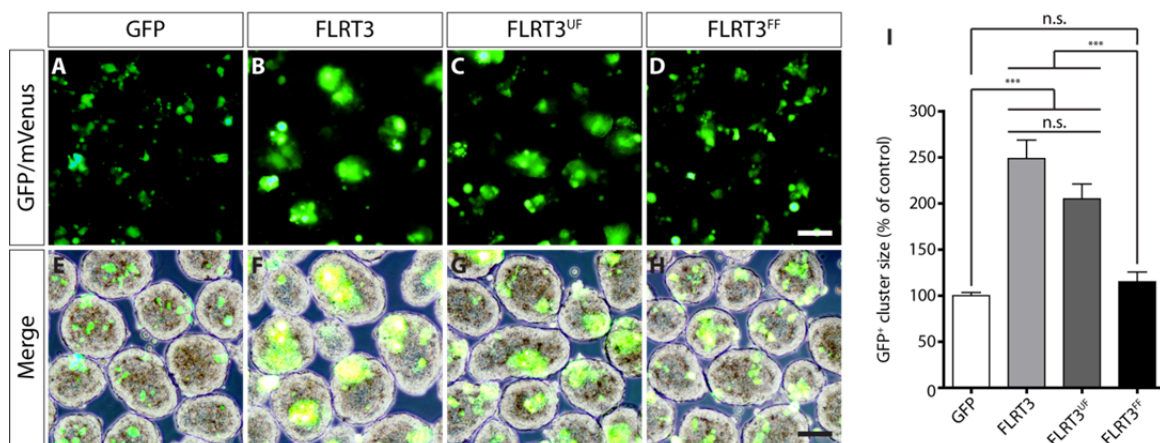


Fig. 26 Validation of homophilic binding of FLRT mutants

HEK293 cells were collected one day after transfection using 5 mM EDTA and incubated for 6 days in BSA coated 24 well plates under constant orbital shaking. (A-D) Representative images of clusters of GFP-positive cells. (E-H) Merges of the GFP channels from A-D with brightfield images of the same field to visualize cell aggregates. (I) Quantification of GFP⁺ cluster size normalized to the size of clusters in the GFP transfection. Results represent mean \pm SEM of 3 independent experiments. Statistical significance was determined by ANOVA with Tukey's post test (***) $p \leq 0.001$; n.s., not significant). Scale bars, 50 μ m.

Data were generated by Dr. Gönül Seyit-Bremer.

2.2.2. Unc5D-induced inhibition of migration is partially dependent on FLRTs

Next, I tested the mutants described above *in vivo*. To this end, I transiently overexpressed the constructs in the developing cortex by *in utero* electroporation of mouse embryos. For these experiments, the constructs were subcloned into the pCAG-IRES-EGFP vector. This vector contains a modified chicken β -actin promoter with a cytomegalovirus-immediate early enhancer, which confers high and long-lasting *in vivo* expression of both the protein of interest and EGFP (Cancedda et al., 2007). First, I tested for equal expression levels of the overexpressed constructs by Western blotting in HEK293 cells (Fig. 27) and surface expression by immunostaining in COS7 cells (Fig. 28).

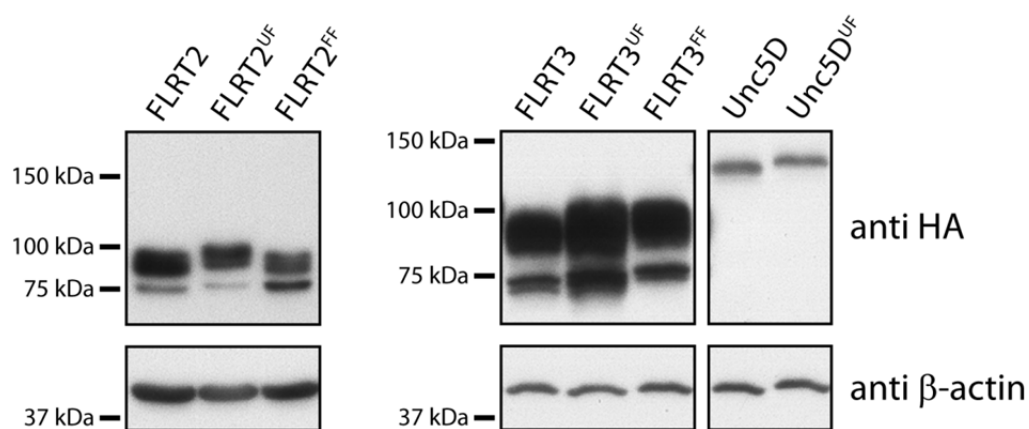


Fig. 27 Expression analysis of pCAG-IRES-EGFP constructs by Western blotting

Constructs were expressed in HEK293 cells. Lysates were subjected to SDS-PAGE and blotted onto PVDF membranes. Membranes were probed with antibodies against the HA tag, and against β -Actin as a loading control.

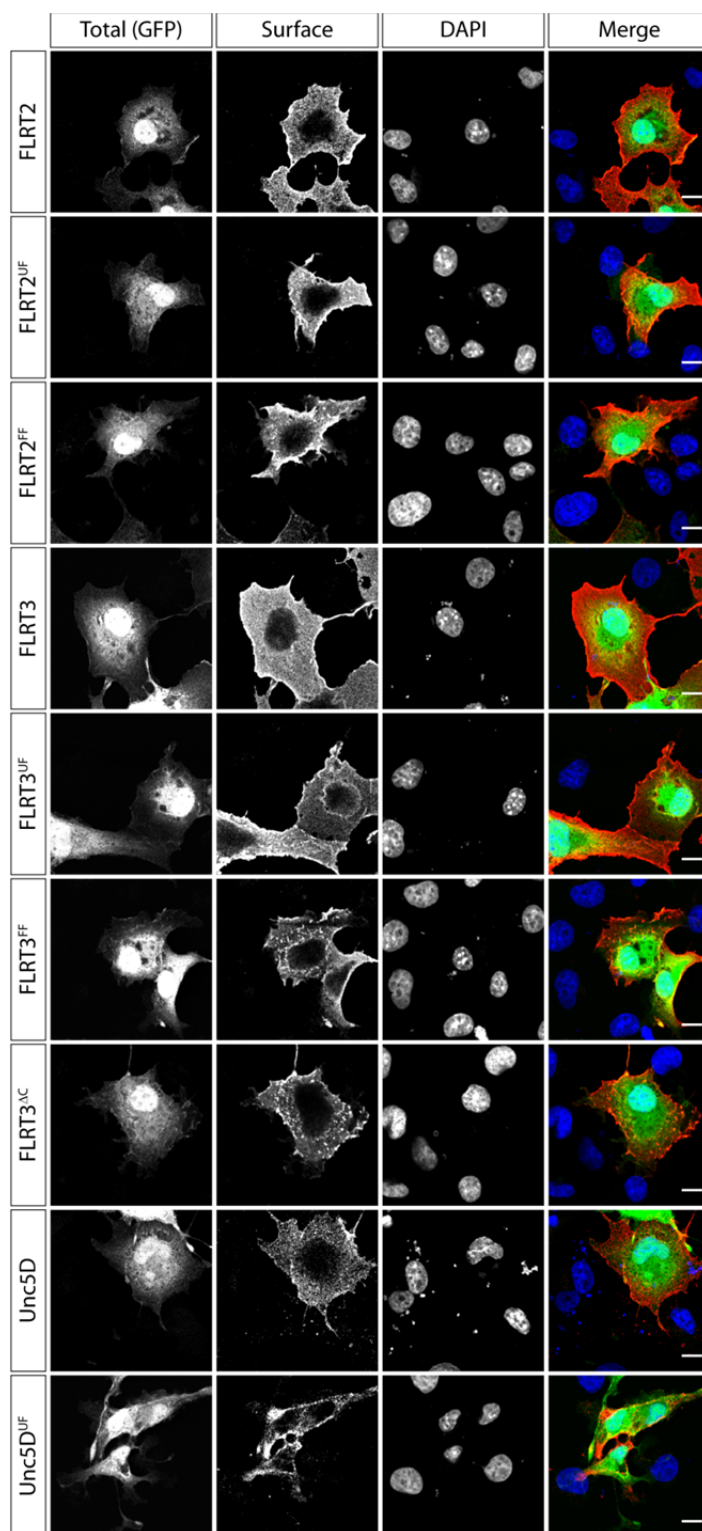


Fig. 28 Surface expression of pCAG-IRES-EGFP constructs

Constructs were expressed in COS7 cells. Cells were fixed after one day of expression and stained against the N-terminal HA tag without permeabilizing. Cells were then counterstained with DAPI and imaged on a confocal microscope. Total construct expression (GFP fluorescence) is shown in the first column (green in merge). Surface staining is shown in the second column (red in merge). Scale bars, 10 μ m.

It has recently been shown that soluble FLRT2 ectodomains that are shed from FLRT2-expressing neurons in the cortical plate inhibit the migration of Unc5D-positive neurons. Overexpression of Unc5D in migrating neurons slowed down the migration of the cells towards the cortical plate (Yamagishi et al., 2011). To test if the delayed migration of overexpressing cells is due to interaction with FLRT2, I overexpressed Unc5D or Unc5D^{UF} in E13.5 mouse embryos. Expression of GFP alone was used as a control. After three days of expression the embryos were fixed at E16.5. Coronal sections of brains were cut and imaged on a confocal microscope and the distribution of cells between ventricular/subventricular zone, intermediate zone and cortical plate was analyzed with ImageJ.

Upon overexpression of GFP alone, 86.5% of all GFP-positive cells reached the cortical plate after three days (Fig. 29 A, E), as compared to only 38.8% when Unc5D was overexpressed (Fig. 29 B, E; $p \leq 0.001$). Significantly more cells were found in the ventricular/subventricular zone and intermediate zone in Unc5D-overexpressing embryos compared to GFP-expressing embryos (19.7% versus 0.6%, $p \leq 0.01$ and 41.9% versus 13%, $p \leq 0.001$, respectively). Overexpression of the Unc5D^{UF} mutant (Fig. 29 C, E) partially rescued the migration defect of Unc5D but did not restore migration to GFP levels (11.6% of cells in VZ/SVZ, 33.1% of cells in IZ and 55.3% of cells in CP). These experiments confirmed that Unc5D-induced reduction of radial migration is indeed, at least partially, mediated by repulsive activity of FLRT2. The results further suggest that overexpression of Unc5D has other effects on the neurons that also interfere with radial migration.

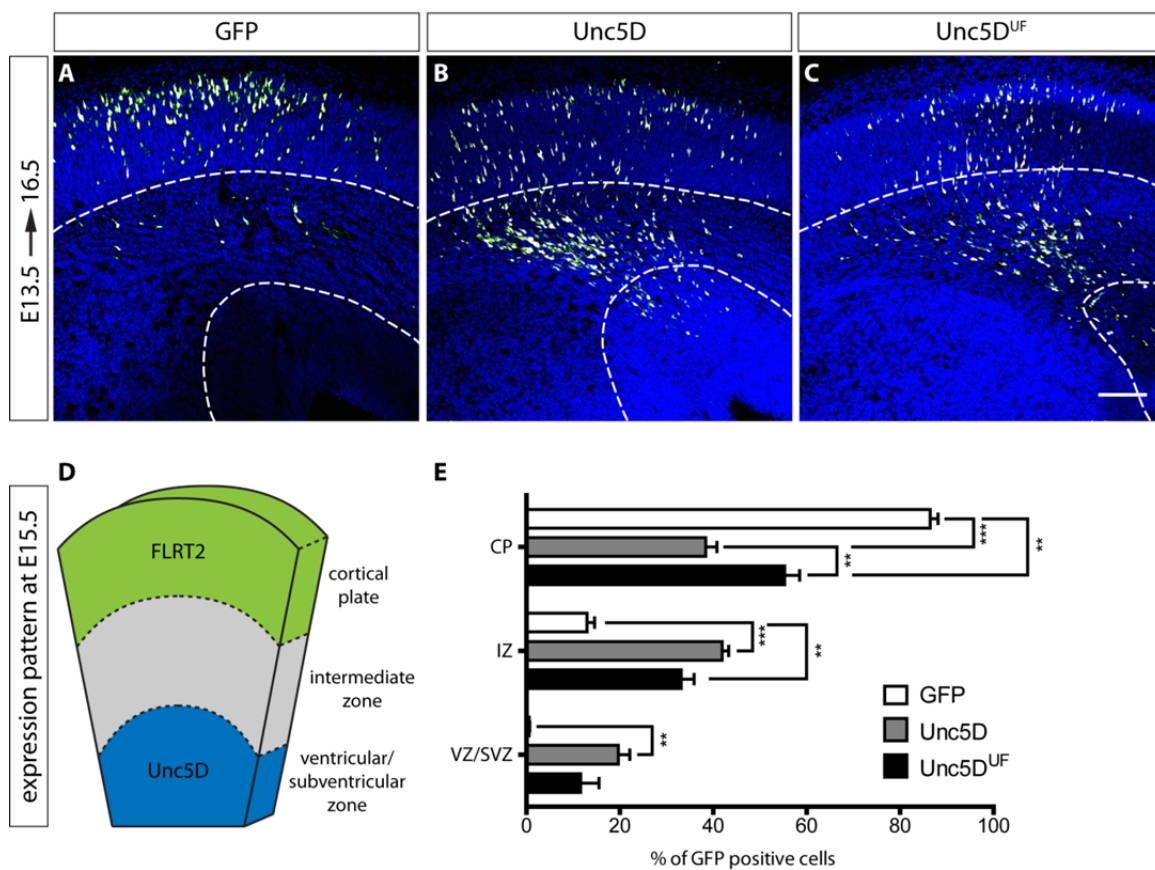


Fig. 29 Inhibition of migration by Unc5D is partially mediated by FLRTs

Mouse embryos were electroporated at E13.5 and brains were fixed at E16.5. Representative images of GFP (A), Unc5D (B) or Unc5D^{UF} (C) are shown. (D) Cartoon of the expression pattern of FLRT2 and Unc5D at E15.5. (E) Quantification of the distribution of cells in the cortex. Results represent mean \pm SEM of at least 4 embryos from a minimum of 2 independent electroporations. 3-4 adjacent coronal sections from the somatosensory cortex were analyzed and averaged per embryo. Statistical significance was determined by ANOVA with Bonferroni multiple comparison post test (** $p \leq 0.01$, *** $p \leq 0.001$). Dashed white lines show the borders between cortical areas as determined by DAPI staining. VZ/SVZ, ventricular/subventricular zone; IZ, intermediate zone; CP, cortical plate; scale bar, 100 μ m.

2.2.3. Loss of FLRT3 does not affect radial migration of neurons

To investigate if FLRTs also have a cell-autonomous effect on the migratory behavior of FLRT-expressing, pyramidal neurons, I performed both loss of function and gain of function experiments. FLRT3 is expressed in migrating neurons that are born around E13.5 and migrate towards the cortical plate during the following days. At the same time, Unc5B is expressed in the cortical plate and could thus induce signaling into FLRT3-expressing cells when they enter the cortical plate (Fig. 30 E). Furthermore, FLRTs have been shown to act as homophilic cell adhesion molecules (Karaulanov et al., 2006) and to be involved in regulation of cadherin trafficking (Chen et al., 2009), and thus could also be involved in cell migration via these functions.

For loss of function studies I again utilized the *FLRT3^{lx/lx}* mice (Yamagishi et al., 2011). I electroporated plasmids encoding Cre recombinase fused to GFP (Cre-GFP) or GFP alone into E13.5 *FLRT3^{lx/lx}* or wild-type embryos and analyzed the brains at E16.5. Expression of Cre-GFP in WT embryos (Fig. 30 B, F) had no statistically significant effect on the distribution of GFP-positive cells between ventricular/subventricular zone, intermediate zone and cortical plate compared to overexpression of GFP alone (Fig. 30 A, F). GFP-transfected cells in *FLRT3^{lx/lx}* embryos (Fig. 30 C, F) showed a similar distribution as GFP-transfected cells in wild-type embryos, confirming that the *FLRT3^{lx}* allele does not influence the behavior of the cells by itself. Expression of Cre-GFP in *FLRT3^{lx/lx}* embryos also did not influence the migration of GFP-positive cells compared to controls (Fig. 30 D, F).

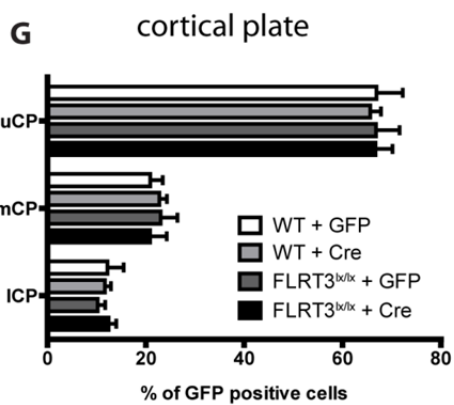
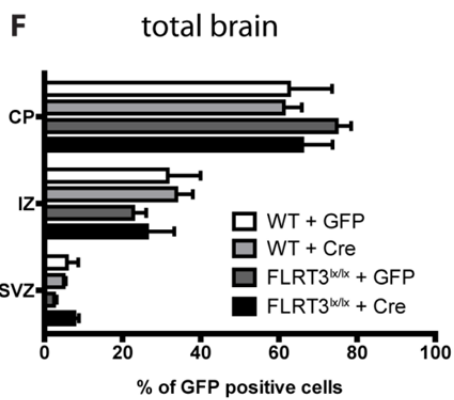
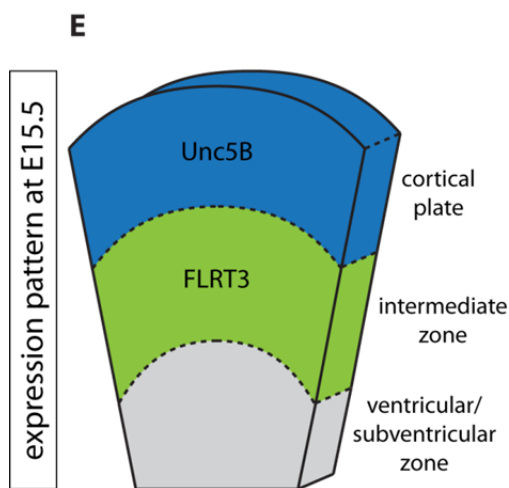
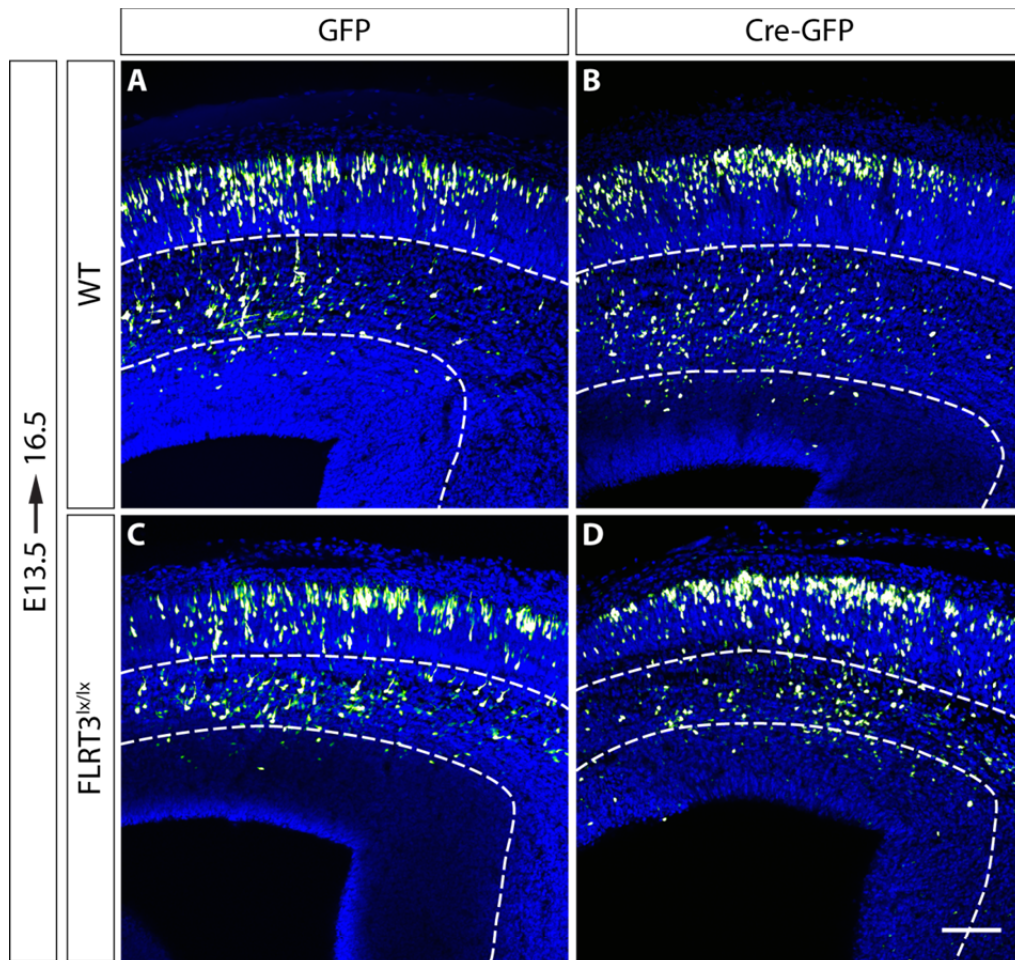


Fig. 30 Loss of FLRT3 does not influence radial migration of neurons

FLRT3^{lx/lx} and wild-type mouse embryos were electroporated at E13.5 with plasmids encoding Cre recombinase fused to GFP or GFP alone and brains were fixed at E16.5. Representative images of GFP (A, C) and Cre-GFP (B, D) are shown. (E) Cartoon of the expression pattern of FLRT3 and Unc5B at E15.5. (F) Quantification of the distribution of cells in the cortex. (G) Quantification of the distribution of cells within the cortical plate. Cortical plate was divided into three equally sized bins and the distribution of cells was quantified. Results represent mean \pm SEM of at least 4 embryos from a minimum of 2 independent electroporations. 3-4 adjacent coronal sections from the somatosensory cortex were analyzed and averaged per embryo. Statistical significance was determined by ANOVA with Bonferroni multiple comparison post test. Dashed white lines show the borders between cortical areas as determined by DAPI staining. VZ/SVZ, ventricular/subventricular zone; IZ, intermediate zone; CP, cortical plate; scale bar, 100 μ m.

Since Unc5B is only expressed in the cortical plate and there is no evidence for ectodomain shedding of Unc5s (Yamagishi et al., 2011), I reasoned that an effect of FLRT3-Unc5B interaction might only appear within the cortical plate. To investigate this possibility I analyzed the distribution of GFP-positive cells within the cortical plate. To this end, I divided the cortical plate into three equally sized bins and quantified the distribution of cells between these bins. As shown in Fig. 30 G, loss of FLRT3 had no effect on the migration of cells within the cortical plate.

To rule out that the lack of phenotype is due to a problem with the Cre recombinase construct, I cotransfected HEK293 cells with pCAG-Cre-GFP and a plasmid containing a lx-stop-lx-mCherry sequence. I found virtually all GFP-positive cells to also be mCherry-positive with no GFP-negative cells being mCherry-positive (data not shown), confirming the functionality of the Cre construct.

2.2.4. Ectopic expression of FLRT2 or FLRT3 interferes with radial migration independently of Unc5s

Next, I examined if there was a gain of function effect produced when overexpressing FLRT3 in the cortex of E15.5 wild-type embryos and analyzing them at E18.5. Upon overexpression of GFP, 36.2% of the transfected cells reached the cortical plate, 60.4% migrated into the intermediate zone and 3.3% of the cells still remained in the ventricular/subventricular zone after three days (Fig. 31 A, E). When FLRT3 was overexpressed, only 1.9% of GFP-positive cells migrated into the cortical plate, whereas 90.2% of cells stayed in the intermediate zone forming a sharp border within the IZ. 8% of the cells remained in the VZ/SVZ (Fig. 31 B, E). To explore the possibility that Unc5D binding to FLRT3 induced this strong reduction in migration, I overexpressed FLRT3^{UF} in E15.5 embryos. As shown in Fig. 31 C and E, the effect of FLRT3^{UF} overexpression was indistinguishable from overexpression of wild-type FLRT3. These results showed that ectopic expression of FLRT3 inhibits radial migration of pyramidal neurons independently of Unc5s.

To test if the inhibition of migration is specific for FLRT3 that is normally expressed in migrating neurons or if it is a general feature of FLRT family members I overexpressed GFP, FLRT2 or FLRT2^{UF} in the developing cortex. FLRT2 had the same effect on the neurons as FLRT3 (Fig. 31 F, G, I), and was similarly independent of binding to Unc5s, as shown with the expression of FLRT2^{UF} (Fig. 31 H, I).

Data for Fig. 31 and Fig. 32 were generated in within the same experiment. However, for more clear presentation of the conclusion, the experiment was split into two graphs. Therefore, the same controls (images and data) are presented in both figures.

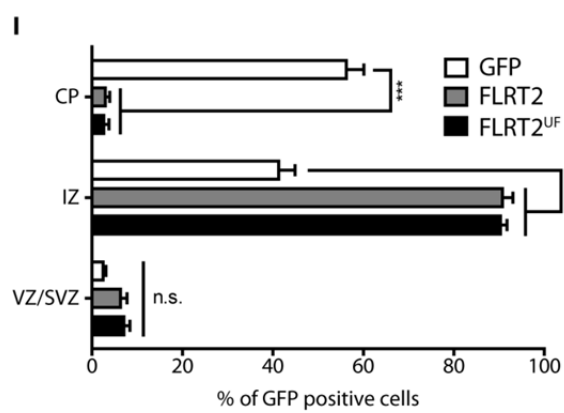
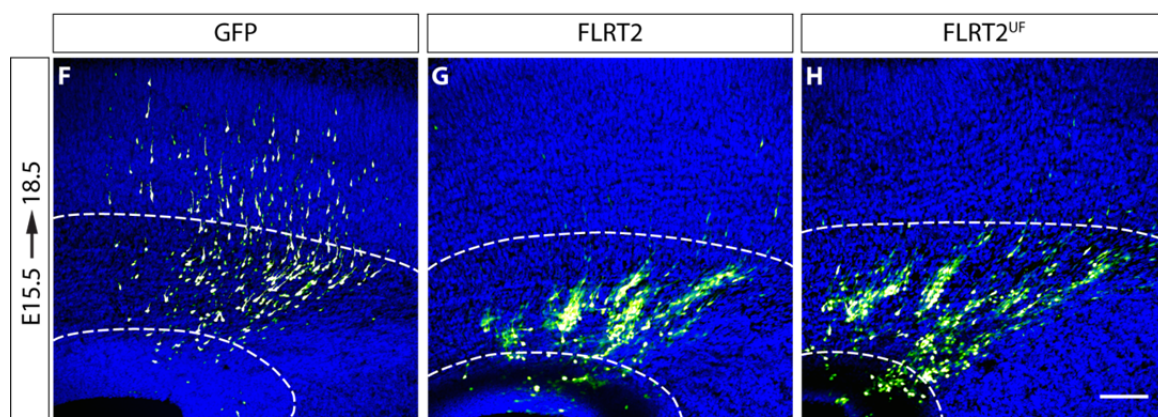
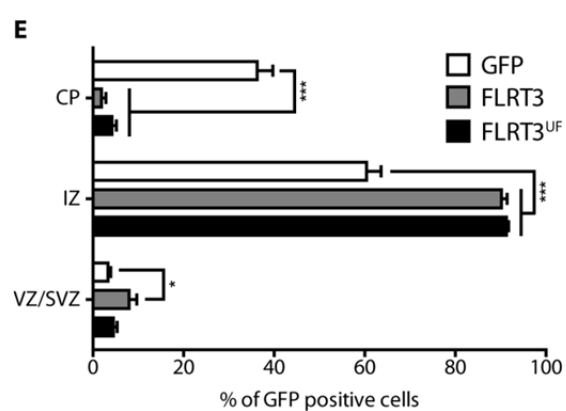
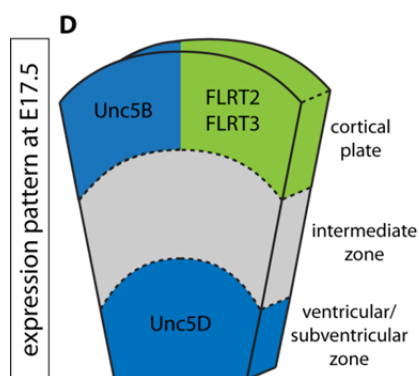
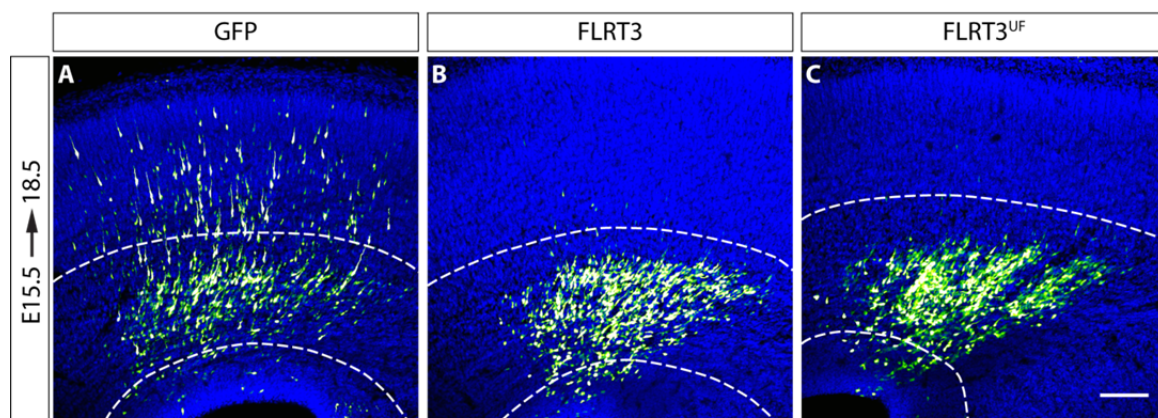


Fig. 31 Ectopic expression of FLRT2 or FLRT3 interferes with radial migration independently of Unc5s

Mouse embryos were electroporated at E15.5 and brains were fixed at E18.5. Representative images of GFP (A, F), FLRT3 (B), FLRT3^{UF} (C), FLRT2 (G) or FLRT2^{UF} (H) are shown. (D) Schematic representation of the expression pattern of FLRTs and Unc5s in the cortex at E17.5. (E, I) Quantification of the distribution of cells in the cortex. Results represent mean \pm SEM of at least 4 embryos from a minimum of 2 independent electroporations. 3-4 adjacent coronal sections from the somatosensory cortex were analyzed and averaged per embryo. Statistical significance was determined by ANOVA with Bonferroni multiple comparison post test (n.s., not significant; * $p \leq 0.05$; *** $p \leq 0.001$). Dashed white lines show the borders between cortical areas as determined by DAPI staining. VZ/SVZ, ventricular/subventricular zone; IZ, intermediate zone; CP, cortical plate; scale bars, 100 μm .

2.2.5. Homophilic binding of FLRTs is involved in inhibiting radial migration

Since FLRTs can also act as homophilic cell adhesion molecules, I next investigated if homophilic binding is involved in inhibiting migration of neurons overexpressing FLRTs. For that purpose I electroporated E15.5 embryos with FLRT3^{FF}. While overexpression of wild-type FLRT3 lead to an almost complete loss of migration into the cortical plate (Fig. 32 B, E), expression of the FLRT3^{FF} mutant partially rescued this effect (Fig. 32 C, E). In the case of FLRT3^{FF}, 13.4% of all GFP-positive cells reached the cortical plate while 77.2% of the cells remained in the intermediate zone compared to 1.9% in the CP and 90.2% in the IZ in the case of FLRT3. But the rescue was not complete as both the intermediate zone and the cortical plate were significantly different compared with expression of GFP alone (60.4% and 36.2% of cells, respectively; Fig. 32 A, E). The same was true for overexpression of FLRT2. The FLRT2^{FF} mutant showed approximately 50% rescue of the phenotype induced by wild type FLRT2 but was still significantly different from GFP alone (Fig. 32 F-I).

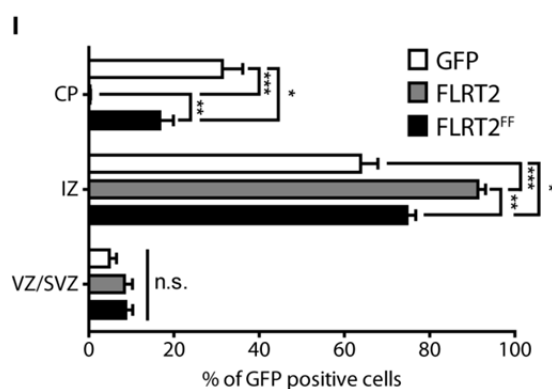
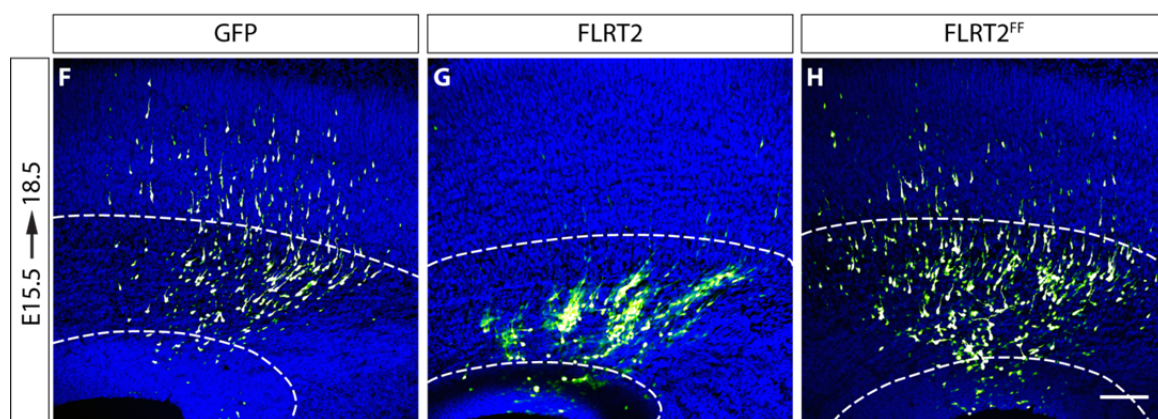
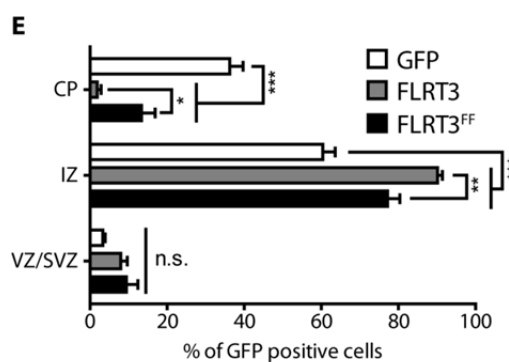
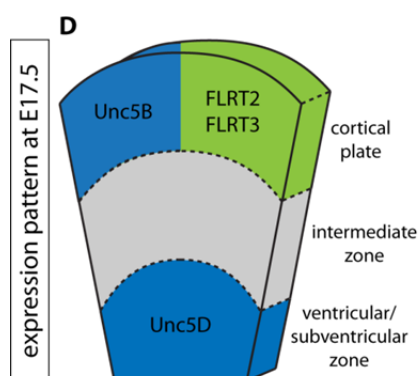
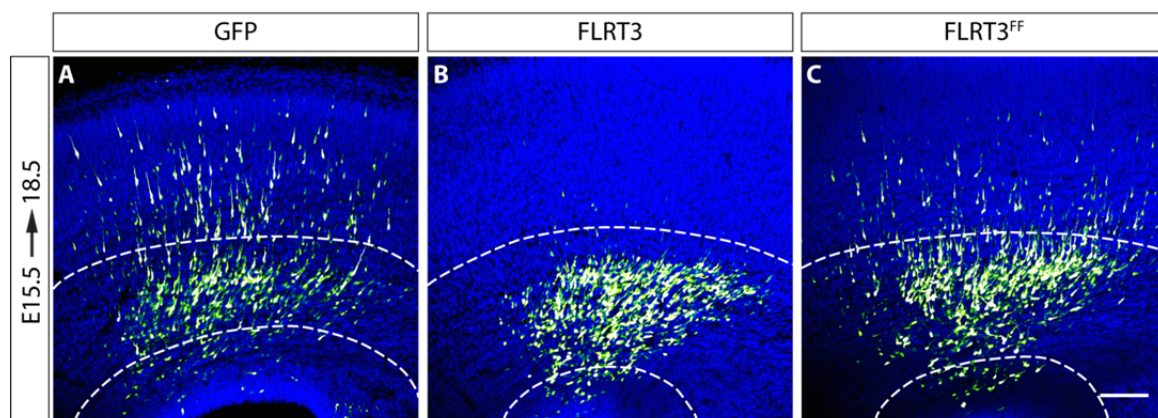


Fig. 32 Homophilic binding of FLRTs is involved in inhibiting radial migration

Mouse embryos were electroporated at E15.5 and brains were fixed at E18.5. Representative images of GFP (A, F), FLRT3 (B), FLRT3^{FF} (C), FLRT2 (G) or FLRT2^{FF} (H) are shown. (D) Schematic representation of the expression pattern of FLRTs and Unc5s in the cortex at E17.5. (E, I) Quantification of the distribution of cells in the cortex. Results represent mean \pm SEM of at least 4 embryos from a minimum of 2 independent electroporations. 3-4 adjacent coronal sections from the somatosensory cortex were analyzed and averaged per embryo. Statistical significance was determined by ANOVA with Bonferroni multiple comparison post test (n.s., not significant; * $p \leq 0.05$; ** $p \leq 0.01$; *** $p \leq 0.001$). Dashed white lines show the borders between cortical areas as determined by DAPI staining. VZ/SVZ, ventricular/subventricular zone; IZ, intermediate zone; CP, cortical plate; scale bars, 100 μ m.

These results indicated that homophilic FLRT-FLRT interactions inhibit radial migration of neurons in the cortex. It is not clear yet if the FLRT-FLRT interactions occur between FLRT expressing cells or between cell-bound FLRTs and shed ectodomains, either from overexpressing cells or from FLRTs expressed in the cortical plate (Fig. 32 D). However, other mechanisms must also be involved, since interfering with homophilic binding did not completely abolish the effect of FLRT overexpression.

2.2.6. FLRT3 signaling is involved in the inhibition of migration

Having found that interfering with FLRT-FLRT homophilic binding only partially rescued the inhibition of migration by FLRTs, next I investigated whether FLRT3 signaling also plays a role in this effect. FLRTs have been shown to regulate FGF signaling and to be phosphorylated in an FGF dependent manner (Wheldon et al., 2010; Wei et al., 2011). Furthermore, FLRT3 has been shown to regulate Cadherin trafficking together with Rnd1

(Ogata et al., 2007). To this end, we engineered a FLRT3 construct lacking the entire intracellular region (FLRT3^{ΔC}) to abolish all signaling induced by FLRT3. As shown above, this construct was well expressed on the surface of COS7 cells (Fig. 28) and bound soluble Unc5B ectodomains (Fig. 24).

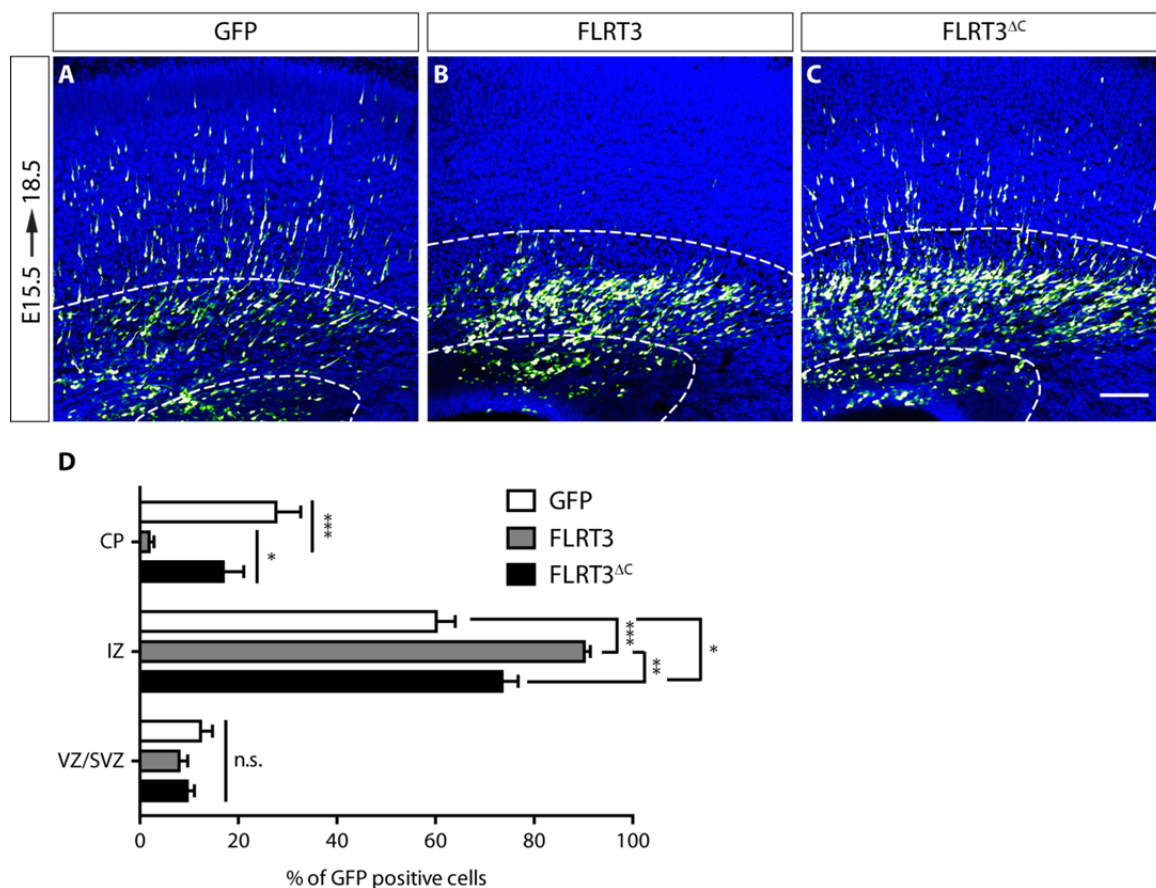


Fig. 33 The FLRT3 intracellular domain is involved in regulating migration in the cortex

Mouse embryos were electroporated at E15.5 and brains were fixed at E18.5. Representative images of GFP (A), FLRT3 (B) or FLRT3^{ΔC} (C) are shown. (D) Quantification of the distribution of cells in the cortex. Results represent mean ± SEM of at least 4 embryos from a minimum of 2 independent electroporations. 3-4 adjacent coronal sections from the somatosensory cortex were analyzed and averaged per embryo. Statistical significance was determined by ANOVA with Bonferroni multiple comparison post test (n.s., not significant; * p ≤ 0.05; ** p ≤ 0.01; *** p ≤ 0.001). Dashed white lines show the borders between cortical areas as determined by DAPI staining. VZ/SVZ, ventricular/subventricular zone; IZ, intermediate zone; CP, cortical plate; scale bars, 100 μm.

When overexpressed in the cortex of E15.5 mouse embryos, FLRT3^{ΔC} showed a significant rescue of the migrational defect induced by FLRT3 (16.9% vs. 1.9% of cells in the CP and 73.5% vs. 90.2% of cells in the IZ, respectively; Fig. 33, B-D). Compared to overexpression of GFP, the rescue induced by lack of the C-terminus was not complete (Fig. 33, A, C, D), suggesting that the FLRT-FLRT trans interaction that was still taking place is, at least partially, inhibiting migration by adhesive forces that do not require signaling.

2.2.7. Overexpression of FLRT3 does not change cell fate

To exclude the possibility that overexpression of FLRT3 inhibited radial migration of cells by changing cell fate, I performed immunostaining against Cux1 on sections from GFP or FLRT3 overexpressing embryos (Fig. 34). Cux1 is an early marker of neuronal differentiation. It is expressed in migrating pyramidal neurons and in pyramidal neurons of layers II-IV of the cerebral cortex but not in cortical interneurons (Nieto et al., 2004).

Upon GFP overexpression, both cells in the cortical plate as well as in the intermediate zone were clearly positive for Cux1 (Fig. 34 A, A', white arrowheads). When FLRT3 was expressed, virtually all GFP-positive cells remained in the intermediate zone (Fig. 34 B), however, most of the GFP⁺ cells were still positive for Cux1 (Fig. 34 B'). Quantification of GFP-positive cells expressing Cux1 showed no difference in the proportion of double positive cells between GFP and FLRT3 overexpression (Fig. 34 C; 94.3% versus 95% of all GFP⁺ cells positive for Cux1). This result indicated that overexpression of FLRT3 does not

change the fate of neurons thereby interfering with radial migration, but rather had a direct effect on migration itself.

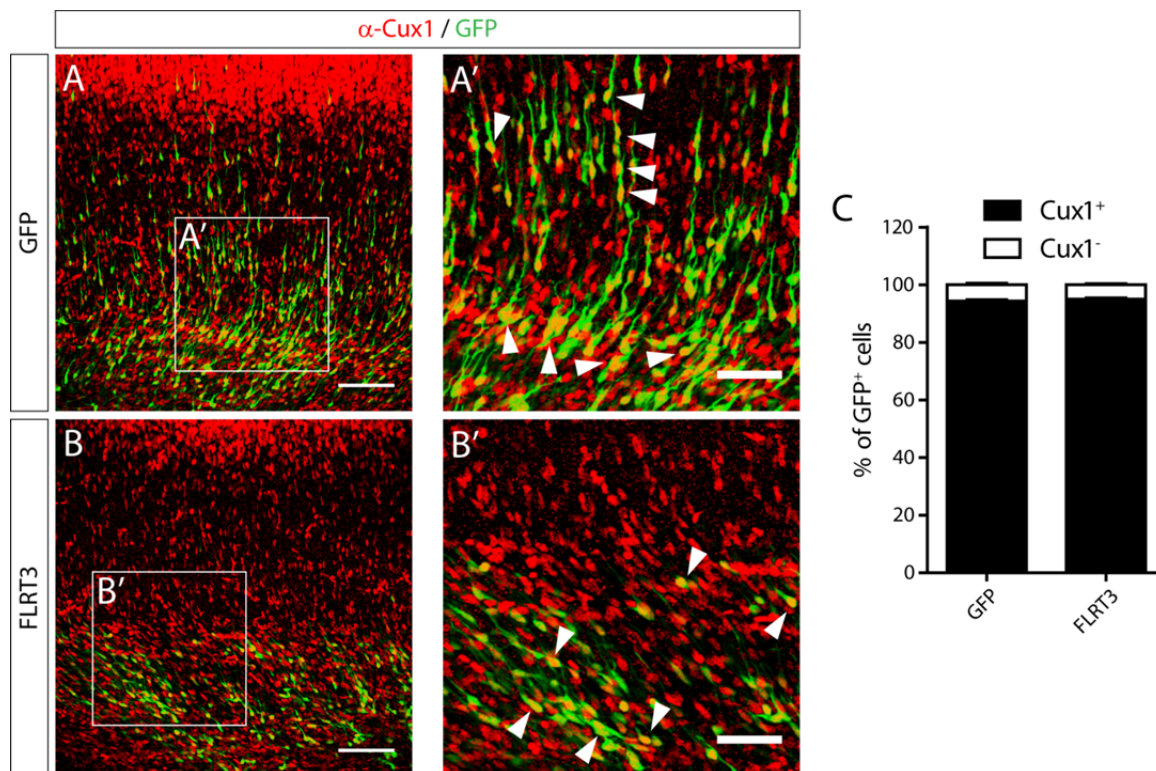


Fig. 34 Overexpression of FLRT3 does not change cell fate

Mouse embryos were electroporated at E15.5 with GFP (A, A') or FLRT3 (B, B'), brains were fixed at E18.5 and stained for Cux1. White arrowheads indicate examples of GFP⁺, Cux1⁺ cells. (C) Quantification of GFP-positive cells positive (black) or negative (white) for Cux1. Results represent mean \pm SEM of 3 (GFP) and 4 (FLRT3) embryos from 2 independent electroporations. 3 adjacent coronal sections from the somatosensory cortex were analyzed and averaged per embryo. Overall, more than 1200 GFP-positive cells were analyzed for each genotype. No statistically significant difference was found with Student's T-test. Scale bars, 100 μ m (A, B), 50 μ m (A', B').

3. Discussion

3.1. FLRTs in synapse development

FLRT family members are widely expressed in the developing and adult mouse brain. Two recent studies from the same laboratory showed localization of FLRT3 to excitatory synapses in the rat brain and involvement of FLRT3 in the development of excitatory synapses in mouse hippocampus and cortex via binding to the latrotoxin receptor Latrophilin3 (O'Sullivan et al., 2012, 2014). We confirmed localization of all three FLRT family members to excitatory synapses in hippocampus (Fig. 6) and cortex (data not shown) by biochemical fractionation of P15 mouse brains. In contrast to the previous report that showed mainly postsynaptic localization of FLRTs however, we found all FLRTs to be enriched in the Triton X-100 soluble fraction. This fraction is usually considered to contain mainly presynaptic components. However, proteins located in perisynaptic regions of the postsynapse, for example NMDA receptors would also be enriched in this fraction. The PSD fraction is defined by its detergent insolubility at low temperatures due to the high cholesterol content of the membrane, but this applies only to the PSD region and not to all postsynaptic membranes *per se*. We found low amounts of FLRT2 in the PSD fraction. This could be a special feature of FLRT2 or alternatively, all FLRTs could be present in the PSD but FLRT1 and FLRT3 are expressed at lower levels compared to FLRT2 and thus under the detection limit (Fig. 6) given the low amounts of total protein available for the PSD fraction.

Moreover, we analyzed P15 mouse brains whereas O'Sullivan and colleagues (2012) used P21 rat brains for their experiments. So another possible explanation for the

contradictory results is that FLRTs are indeed located postsynaptically but they are present perisynaptically at earlier stages of development and get shuttled into the PSD at later stages. Alternatively, FLRTs could also be expressed pre- and postsynaptically and it depends on the fractionation protocol used where they are mainly detected.

Having confirmed the synaptic localization of FLRT proteins, I went on to do functional assays to investigate their role in synapse development and to dissect the contributions of adhesive and repulsive functions during this process. However, in contrast to the previously published reports I could not confirm the involvement of FLRT1 or FLRT3 in synapse development using loss of function and gain of function approaches in primary neurons (Fig. 12, Fig. 14 - Fig. 16) or biochemical (Fig. 18) and ultrastructural analysis of hippocampus (Fig. 19) in knock-out mice. Possible reasons for these discrepancies are discussed below.

In line with the findings of O'Sullivan and colleagues (O'Sullivan et al., 2012), FLRTs expressed in HEK293 cells did not induce pre- or postsynaptic differentiation in contacting primary neurons, suggesting that they are not key components of initial steps of synapse formation. These results are not too surprising considering the domain structure of FLRTs. Since they lack common protein-protein interaction motifs in their intracellular domain (Lacy et al., 1999; Böttcher et al., 2004; Haines et al., 2006) they are unlikely to be involved in the assembly of the intracellular protein complexes required for a functional presynaptic release machinery or the formation of a postsynaptic density. They could of course interact heterophilically with other proteins in *trans* or form homotypic clusters and then recruit other proteins via extracellular interactions. For example in *Xenopus* embryos FLRT3 has been shown to bind to Unc5B in *cis* via the

extracellular LRR domain to regulate cell adhesion (Ogata et al., 2007; Karaulanov et al., 2009). However, FLRTs expressed in heterologous cells appear not to be sufficient to induce synaptic differentiation. This does not mean, however, that they cannot be involved in synapse formation. Other membrane proteins critical for proper synapse development or maintenance such as N-Cadherin, N-CAM, L1-CAM or EphrinB1 do not have synaptogenic activity in coculture assays (Scheiffele et al., 2000; Sara et al., 2005).

Thus I investigated the importance of FLRT1 and FLRT3 for synapse formation in primary neurons, but genetic knock-out of either did not change the number of excitatory synapses *in vitro*. Also sparse knock-out of FLRT3 by transfection of Cre recombinase into *FLRT3^{lox/lox}* neurons or overexpression of FLRT3 did not alter the number of synapses on these neurons compared to GFP control transfections. Furthermore, I was not able to detect loss of synapses *in vivo* in FLRT3 knock-out mice, an effect that had been observed upon shRNA mediated knock-down of FLRT3 (O'Sullivan et al., 2012, 2014). There are several possible explanations for this discrepancy of results. First of all, the loss of synapses reported could be due to off-target effects of the shRNA used to knock down FLRT3 in the published studies. Off-target effects are a well-recognized problem when using RNA interference to knock down gene products (Alvarez et al., 2006; Mishra et al., 2008; Echeverri et al., 2006). However, this is an unlikely scenario since an shRNA resistant FLRT3 construct was successfully used to rescue the effects induced by knocking-down FLRT3. The use of an RNAi resistant rescue construct is considered to be a sufficient proof of the specificity of the effect and is the gold standard control for RNAi experiments to date (Echeverri et al., 2006).

Another difference between my experiments and the published studies is the timing of deletion of FLRTs. In my genetic knock-out strategies, embryos either lack FLRT expression from fertilization on (FLRT1, full knock-out) or starting from around E9.5, when NesCre expression starts (Tronche et al., 1999) (FLRT3, nervous system specific knock-out). In the RNAi approach on the other hand, knock-down is limited to the time of cell preparation. This leaves a long time window for possible compensatory mechanisms mitigating the effect of loss of FLRTs. Compensation of effects after genetic knock-out has been shown before, for example in PSD95 knock-out mice (Elias et al., 2006; Fitzjohn et al., 2006). However, this explanation is unlikely as well since electroporation of Cre recombinase into *FLRT3^{lx/lx}* neurons at the time of neuronal culture also did not show an effect on synapse development in these neurons.

Moreover, O'Sullivan and colleagues used P0 rat pups for their neuronal cultures and analyzed synapse density on dentate gyrus granule neurons, whereas I cultured neurons from E17.5 mouse embryos and analyzed CA3 neurons since DG cells are virtually absent from embryonic neuronal cultures (Banker and Cowan, 1977; Schlessinger et al., 1975). This experimental difference could possibly account for the contradictory *in vitro* results.

Also for the in the *in vivo* experiments there are substantial differences in the experimental setup between my work and that of the studies published previously. I used genetic knock-out of FLRT3 in the entire nervous system from E9.5, whereas the other studies used *in utero* electroporation at E15.5 or virus injection at P5 to sparsely knock down FLRT3 by RNAi. This leaves a relatively long time window for compensatory mechanisms to take place. Furthermore, I used P20 mice for my biochemical and electron microscopy experiments, whereas O'Sullivan and colleagues performed spine

counts and electrophysiological measurements on 14 to 16 days old mice (O'Sullivan et al., 2012).

Methodologically, I quantified synapses based on ultrastructure whereas the other studies looked at dendritic spines and electrophysiological recordings, but I did not quantify dendritic spine density in FLRT3 knock-out mice. This could be achieved by crossing the FLRT3 KO mice to a fluorescent reporter mouse line, for example GFP-M mice (Feng et al., 2000), that randomly and sparsely labels cells in hippocampus and cortex, and then count spines on labeled cells. It is possible that by doing that I would see an effect of FLRTs on spine development or maturation rather than absolute synapse number.

I also did not examine the possibility of FLRT3 being involved in other synaptic parameters such as presynaptic release probability, postsynaptic receptor trafficking or causing subtle changes in synaptic structure. This could be done by detailed analysis of synaptic ultrastructure measuring, for example width of the synaptic cleft, PSD length, size and number of synaptic vesicles, or by electrophysiological measurements. Changes in these parameters could be indicative of disturbed synaptic function rather than an overall loss of synapses. Several proteins have been shown to be important for synaptic function and to regulate synaptic morphology without changing number of synapses, e.g. Neuroligins or Cntnap4 (Varoqueaux et al., 2006; Karayannis et al., 2014).

In summary, I could not confirm the published results on the involvement of FLRT3 in synapse formation and did not find evidence for FLRT1 being critically involved in synapse development. However, this could be due to differences in experimental paradigms and developmental stages of the animals used in the different studies.

Furthermore, my results do not exclude the possibility that FLRTs have other functions in synaptic development or physiology that do not lead to reduced synaptic density upon loss of FLRTs. One other possibility is that due to overlapping expression of FLRTs in the hippocampus, especially during late embryonic and early postnatal development (Satoru Yamagishi and Daniel del Toro, unpublished results), another FLRT could compensate for the loss of FLRT3 and thus strong phenotypes would only be found in double knock-out animals.

3.2. FLRT-FLRT and FLRT-Unc5 interactions occur via distinct surface domains and can be uncoupled

FLRTs have been shown to act as homophilic adhesion molecules and as repulsive ligands for Unc5 expressing cells (Karaulanov et al., 2006; Yamagishi et al., 2011). Both, the homophilic and heterophilic interactions have been mapped to the LRR domain of FLRTs and Unc5s bind to the FLRT LRRs via their Ig1 domain (Karaulanov et al., 2006, 2009). However, it has not been investigated whether these two interactions can happen in parallel or if they compete with each other. Thus we set out to determine the structural determinants of FLRT-FLRT and FLRT-Unc5 binding. To this end, we solved the crystal structures of complete FLRT and Unc5 ectodomains and of a FLRT-Unc5 complex. The crystal structures revealed a typical horseshoe shape for FLRT LRRs that has been shown for other LRR domains (Scott et al., 2004; Seiradake et al., 2011; Bella et al., 2008). The Ig domains of Unc5s on the other hand showed the well-known, compact globular structure of other Ig domains (Coles et al., 2011;

Chothia and Jones, 1997). Furthermore, the structures showed homophilic interaction of FLRT LRRs via the concave surface on the inside of the horseshoe, whereas the Unc5 Ig1 domain bound to the lateral side of the LRR domain. The homophilic interaction via the concave side of the horseshoe is in line with published results for other LRR domain containing proteins (Islam et al., 2013). By designing glycosylation mutants of FLRTs and Unc5s, we were able to specifically disrupt FLRT-FLRT interaction without affecting FLRT-Unc5 interaction, and *vice versa*. This strategy has been shown before to successfully inhibit protein-protein interactions without generally affecting protein folding, trafficking or function (Seiradake et al., 2011; Islam et al., 2013). The functionality of the mutants was confirmed by surface binding and cell aggregation assays. These mutants allowed us to uncouple adhesive and repulsive functions of FLRTs in *in vitro* (Daniel del Toro, data not included in this thesis) and *in vivo* assays.

In initial surface binding experiments I also investigated the published interaction of the Latrophilin3 ectodomain with FLRTs (O'Sullivan et al., 2012). I could confirm strong binding of Latrophilin3 to all FLRTs (data not shown). Thus, Latrophilins should always be kept in mind when interpreting data obtained with FLRTs and their mutants, especially because of broad Latrophilin expression in the mouse brain (Lein et al., 2007; Silva and Ushkaryov, 2010).

Furthermore, there might be other extracellular, yet unidentified binding partners of FLRTs. Binding of those could also be differentially affected by the FLRT^{FF} and FLRT^{UF} mutants described here and thus should also be kept in mind. Some other possible binding partners of FLRTs have been described in binding screens of zebrafish LRR and Ig domain membrane proteins (Söllner and Wright, 2009; Martin et al., 2010), including Boc and Pdgfrl. However, the functional relevance of those interactions has not been

tested yet, so it will be interesting in the future to investigate possible functions of other FLRT binding partners in development if there is promising overlap in the expression patterns. The mutants established here could then be useful tools to elucidate the functional roles of such interactions if they specifically abolish binding of certain proteins but not others, and thus help extend the knowledge about FLRTs in other systems as well.

3.3. FLRTs in cortical development

FLRTs have recently been shown to be involved in different steps of nervous system development. The released ectodomain of FLRT2 was shown to act as a repulsive ligand for Unc5D positive neurons by delaying their exit from the multipolar stage (Yamagishi et al., 2011). Furthermore, FLRT3 is involved in the guidance of developing thalamocortical axons by regulating attraction to Netrin1 via interaction with Robo1 (Leyva-Díaz et al., 2014). However, in contrast to FLRT2, which is expressed in pyramidal neurons only after they settle in the cortical plate, FLRT3 is expressed in migrating neurons (Yamagishi et al., 2011; Hampel, 2012). Given the prominent functions of FLRTs as homophilic adhesion molecules (Karaulanov et al., 2006; Müller et al., 2011), as binding partners of Rnd proteins (Karaulanov et al., 2009; Chen et al., 2009) and as regulators of cell adhesion via regulation of cadherin surface expression (Karaulanov et al., 2009; Chen et al., 2009), I set out to investigate cell autonomous FLRT functions in radially migrating pyramidal neurons in the developing cortex.

3.3.1. FLRT2 inhibits radial migration via Unc5D

FLRT2 has been proposed to act as a repulsive ligand for Unc5D expressed in migrating neurons, preventing those neurons from prematurely entering the cortical plate (Yamagishi et al., 2011). However, it has not been formally proven that this effect is dependent on Unc5D-FLRT2 interaction. I used *in utero* electroporation experiments to address this problem. Whereas overexpression of wild-type Unc5D in migrating neurons strongly reduced the migration of cells towards the cortical plate compared to GFP overexpression, expression of the non-FLRT binding mutant Unc5D^{UF} reduced this inhibitory effect (Fig. 29). This shows that the inhibitory effect of Unc5D on radial migration is indeed partially dependent on interaction with FLRT2. But the rescue is not complete when this interaction is abolished. Thus, there must be other effects of Unc5D overexpression that inhibit radial migration. There are four prominent features of Unc5s that could account for this effect. First, Unc5s have been shown to act as dependence receptors. In the absence of their main ligand Netrin1 they induce apoptosis via a death domain in their intracellular tail (Llambi et al., 2001; Williams et al., 2003; Tanikawa et al., 2003; Delloye-Bourgeois et al., 2009; Takemoto et al., 2011). Hence, cells overexpressing Unc5D could die or be less healthy overall and thus migrate slower. However, this hypothesis is unlikely since I could not observe an overt decrease in the numbers of transfected cells upon overexpression of Unc5D or Unc5D^{UF} compared to GFP control, even though I did not quantify this. Furthermore, we did not find increased apoptosis of COS7 cells transfected with Unc5B or Unc5D compared to GFP control transfections (Gönül Seyit-Bremer, unpublished results). Second, in *Xenopus* Unc5B has been shown to interact with FLRT3 and Rnd1 to regulate cell adhesion

(Karaulanov et al., 2009). A similar interaction of Unc5D with Rnds could possibly influence the adhesive properties of migrating neurons and thereby influence their migratory behavior. Deregulated adhesion has already been shown to disrupt cortical migration and development. For example, Integrin $\alpha1\beta3$ is required for neuron-glia interaction during radial migration and genetic ablation of Integrin $\alpha1$ leads to abnormal cortical layering (Anton et al., 1999). Third, proteins of the Rnd family have been shown to be involved in regulating different steps of radial migration (Heng et al., 2008; Pacary et al., 2011; Azzarelli et al., 2014). Rnd proteins are atypical small Rho GTPases. They lack intrinsic GTPase activity and are constitutively active once they bind GTP. Their activity is mainly regulated by expression and degradation, phosphorylation or subcellular localization (Riento et al., 2005; Chardin, 2006; Madigan et al., 2009). Since Unc5B can physically bind Rnd1 (Karaulanov et al., 2009), overexpression of Unc5D could also have an effect on the distribution of Rnds in neurons and thereby disturb their normal migration. Fourth, Unc5D has been proposed to prevent neurons from exiting the multipolar stage (Miyoshi and Fishell, 2012), although the authors do not provide a biological mechanism by which Unc5D achieves this function. Thus, overexpression of Unc5D could delay migration of neurons by extending the multipolar phase. I did not perform a detailed morphological analysis of the cells overexpressing Unc5D and thus cannot provide data for this hypothesis. This could, however, be done in the future.

3.3.2. Loss of FLRT3 does not influence radial migration

Having shown that FLRT2 indeed inhibits radial migration of pyramidal neurons by binding to Unc5D, I explored the possibility whether FLRT3 that is expressed in migrating neurons in the intermediate zone at E14.5, could cell-autonomously regulate the migration of these cells. I electroporated *FLRT3^{lx/lx}* embryos at E13.5 with a plasmid encoding Cre recombinase and GFP or a GFP control plasmid. Analyzing the distribution of GFP positive cells at E16.5, I could not detect any difference between GFP and Cre transfected embryos (Fig. 30). I excluded the possibility that the lack of phenotype is due to a problem with the Cre plasmid by confirming the expression of Cre recombinase by Western blotting of HEK293 cell lysates after transfection of the plasmid and by coexpression of the Cre plasmid and an *lx-stop-lx-mCherry* plasmid in COS7 cells (data not shown). These experiments confirmed expression and activity of the recombinase.

The results are not surprising since FLRT3 knock-out mice do not show gross abnormalities in cortex architecture and the radial distribution of FLRT3 positive cells in these brains is normal as well (Hampel, 2012; Daniel del Toro, unpublished results). There are three likely explanations for the lack of a phenotype in these experiments. First, FLRT3 could not be required for the regulation of radial migration but rather be involved in the tangential distribution of radially migrating cells. This would be in line with work by Dr. Daniel del Toro and Tobias Ruff in our lab (unpublished data). They found β -galactosidase positive cells in FLRT3 knock-out mice and GFP-positive cells upon overexpression of FLRT3 to be unevenly distributed tangentially in the cortical plate and this effect is abolished by overexpression of the FLRT3^{FF} mutant. However, the tangential clustering phenotype in FLRT3 knock-out mice is restricted to the very lateral

and posterior part of the cortex and this region I did not analyze in my *in utero* electroporation experiments. Strikingly, this resembles the effect seen by knock-out or overexpression of EphrinB1 (Dimidschstein et al., 2013) or in EphrinA1/3/5 triple knock-out mice (Torii et al., 2009). In these studies the authors show that EphrinAs and EphrinB1 do not regulate the radial migration of pyramidal neurons but rather determine the tangential distribution of clonally related cells thereby regulating the columnar structure of the cortex (Rakic, 1988). In this scenario, FLRTs would have a double role where the shed ectodomains act as repulsive ligands for Unc5D positive neurons regulating radial migration and cell bound FLRTs in migrating neurons regulate tangential spread of cells by adhesive interactions.

Second, FLRT3 expressing cells in the cortex could be interneurons. Thus, electroporation of Cre recombinase into the ventricular zone would not hit the right cells. Work by Dr. Falko Hampel in our lab showed expression of FLRT3 in the ganglionic eminences at E13.5 (Hampel, 2012). This would be the correct time for the development of interneurons that reach the intermediate zone at E14.5. However, the *in situ* hybridization and X-Gal staining experiments did not reveal FLRT3-positive cells migrating out of the GE towards the cortex making this explanation less likely, but the identity of FLRT3 positive cells could be easily determined by immunostaining for markers of pyramidal neurons and interneurons. Furthermore, electroporation of the GE is easily achievable by changing the angle of the electrode during IUE experiments. Thus, Cre-mediated deletion of FLRT3 in developing interneurons could be used to analyze the migration pattern of these cells and to further test this hypothesis.

Third, the loss of FLRT3 could be compensated by FLRT1 which is widely expressed in the developing cortex. We have not formally proven that FLRT1 and FLRT3 are expressed in

the same cells in cortex, but the expression pattern strongly supports this possibility. In this case, FLRT1 could take over the function of FLRT3 in migrating neurons and the reduction in total FLRT levels might not be strong enough to have an effect on the migration of these cells. This is a likely option since compensation is a common phenomenon in many systems and it is often necessary to knock down several members of a protein family to achieve strong phenotypes. This is for example true for Neuroligins. Even though Neuroligins are highly active in synapse formation assays *in vitro*, single Neuroligin knock-out mice do not show strong phenotypes. Neuroligin1/2/3 triple knock-out mice, however, die shortly after birth due to respiratory failure induced by synaptic defects (Varoqueaux et al., 2006). Furthermore, preliminary unpublished data from Dr. Daniel del Toro showed that the tangential spreading phenotype is aggravated in FLRT1/FLRT3 double knock-out brains. This hypothesis could be easily tested by analyzing brains of FLRT1/FLRT3 double knock-out embryos or electroporating Cre recombinase into $FLRT1^{-/-}/FLRT3^{lx/lx}$ embryos.

3.3.3. Overexpression of FLRTs inhibits radial migration by homophilic adhesion and via the intracellular domain

To gain more insight into adhesive and repulsive functions of FLRTs in cortical development I performed a gain of function approach and overexpressed wild type and mutant FLRTs by *in utero* electroporation. I found a strong effect of FLRT overexpression in radially migrating neurons. Whereas a large proportion of GFP overexpressing cells reached the cortical plate after three days, virtually all cells overexpressing FLRT2 or FLRT3 stayed in the intermediate zone forming a sharp border approximately at the level

90

of the subplate (Fig. 31). This effect was independent of interaction with Unc5s as shown by the lack of rescue upon overexpression of the FLRT^{UF} mutants but partial dependence on FLRT-FLRT homophilic binding. Overexpression of the FLRT^{FF} mutants resulted in an approximately 50% rescue of the migrational delay induced by wild-type FLRTs (Fig. 32). Furthermore, deletion of the intracellular domain of FLRT3 (FLRT3^{ΔC}) also partially rescued the effect of FLRT3 overexpression (Fig. 33). The gain-of-function results show that two properties of FLRTs are likely to influence the radial migration of cortical neurons. First, homophilic adhesion can inhibit the migration if not well balanced, and second, the intracellular domain can either signal by itself or regulate the intracellular distribution of other signaling components, for example Rnd proteins, to influence migration. Furthermore, FLRT1 has been shown to physically interact with FGF receptors, be phosphorylated in an FGF-dependent manner, and regulate FGF signaling (Wheldon et al., 2010; Wei et al., 2011). Thus, also disrupted FGF signaling could influence the migration of cells.

Different cell adhesion molecules have been shown to be important for proper radial migration of cortical neurons. Prominent examples are Integrin $\alpha 1\beta 3$ which is involved in neuron-glia interaction (Anton et al., 1999), N-Cadherin which has been shown to be important for radial orientation of movement and glia independent somal translocation (Franco et al., 2011; Jossin and Cooper, 2011), or Integrin $\alpha 3\beta 1$ that was shown to bind the extracellular matrix protein Reelin and regulate the termination of migration and detachment from radial glial fibers (Dulabon, 2000). However the question remains how overexpression of FLRTs inhibits radial migration? There are several different possible explanations to this. The first possibility is a mechanism similar to FLRT2-induced repulsion of Unc5D positive neurons. Since Unc5B is expressed in the cortical plate it

could bind to FLRTs expressed in migrating neurons and induce a repulsive signal in these cells, thereby inhibiting their migration. However, the lack of rescue by overexpression of the FLRT^{UF} mutant that is deficient in binding to Unc5s but not to FLRTs rules out this option. Partial rescue of the migration defect by overexpression of the FLRT^{FF} mutant suggests a strong involvement of homophilic FLRT-FLRT interactions in inhibiting radial migration upon FLRT overexpression. Increased adhesive forces between overexpressing cells could make those cells stick to each other and thereby delay their migration by preventing either proper attachment to radial glial fibers or their movement away from each other. Overexpression of FLRTs could also directly increase the adhesion to radial glial fibers and thereby inhibit migration along the fibers. This explanation is, however, less likely since, according to our expression studies, radial glia cells do not endogenously express FLRTs and embryos with ectopic glial expression were excluded from my analysis. Embryos with glial expression could be clearly identified GFP expression in radial fibres, a condition that only happened in a very small number of embryos. Another possibility could be that FLRTs can also act as heterophilic CAMs binding to a yet unidentified ligand expressed in radial glia cells. This adhesive interaction could then inhibit the migration of FLRT-overexpressing cells. To exclude the possibility that low levels of FLRTs are also overexpressed in radial glia cells some experiments should be repeated with a plasmid that restricts expression to postmitotic neurons, for example using a construct containing the NeuroD1 promoter instead of the CAG promoter (Heng et al., 2008).

One intriguing explanation would also be that FLRTs expressed ectopically in migrating neurons interact with endogenous FLRTs on other cells. It has been shown previously that neurons in the rostral thalamus express high levels of FLRT3

(Leyva-Díaz et al., 2014). These neurons send thalamocortical projections into the cortex and the axon bundles pass through the cortex at the level of the subplate. Thus, FLRT positive migrating neurons could come into contact with the FLRT3-expressing thalamocortical axons and stop migrating due to excessive adhesion. This could explain the sharp border formed by the FLRT-overexpressing neurons. This hypothesis could be easily tested by overexpressing FLRTs in FLRT3 knock-out embryos. Another possibility would be to perform the electroporation at E13.5 instead of E15.5 because the thalamocortical projections only reach the cortex around E15.5 (López-Bendito and Molnár, 2003). In this case, most of the transfected cells would have migrated past the subplate once the thalamocortical axons arrive there. Thus, the transfected cells would not come in contact with those projections and would not get stuck. Furthermore, antibody staining of thalamocortical axons should be performed to confirm that neurons overexpressing FLRTs actually stop at the level of the thalamocortical projections.

Since it is well established that FLRTs can be shed from cells and also act as soluble ligands (Yamagishi et al., 2011) the option that overexpression of FLRTs leads to an excess of released ectodomain that can bind other receptors or adhesion molecules on migrating neurons and thereby exert a dominant negative effect should be considered as well. This hypothesis could be tested by engineering a cleavage resistant construct (Yamagishi et al., 2011) and overexpress this by *in utero* electroporation. In case the soluble ectodomains have a non-cell autonomous effect, this construct should at least partially, rescue the migration defect.

Interestingly, not only the FLRT^{FF} mutants partially rescued the migration defect induced by FLRT overexpression, but also FLRT3^{ΔC} showed a reduced effect compared to WT FLRT3. This is striking since the FLRT intracellular domain does not have well characterized signaling functions or common protein homology domains (Lacy et al., 1999; Böttcher et al., 2004; Haines et al., 2006). However, FLRTs have been shown to interact with Rnd proteins and to regulate cell adhesion via control of C-Cadherin surface expression (Ogata et al., 2007; Karaulanov et al., 2009). Furthermore, Paraxial Protocadherin (PAPC) has been shown to physically interact with FLRT3, thereby inhibiting binding of Rnd1 and reducing the deadhesive effect of FLRT3 to allow physiological cell sorting (Chen et al., 2009).

An interesting hypothesis is that FLRT3 in neurons could regulate surface expression of N-Cadherin and thereby regulate radial migration, similar to the situation in *Xenopus* embryos. Deregulated (surface)-expression of N-Cadherin or interference with N-Cadherin trafficking by downregulation of Rab GTPases has been shown to inhibit radial migration of pyramidal neurons (Kawauchi et al., 2010; Jossin and Cooper, 2011; Shikanai et al., 2011). Thus, overexpression of FLRT3 could, either in cooperation with Rnd proteins, or with other as yet unidentified binding partners, lead to a reduced surface expression of N-Cadherin or interfere with proper N-Cadherin trafficking and thereby inhibit neuronal migration.

Rnds are atypical small GTPases without intrinsic GTPase activity thus rendering them constitutively active. Their activity is mainly regulated by translation and degradation or by localization (Riento et al., 2005; Chardin, 2006; Madigan et al., 2009). Rnds have been shown to be involved in regulation of the actin cytoskeleton in a variety of different cell types including neurons (Chardin, 2006). They have been shown to interact with Plexins

and thereby regulate neurite outgrowth and branching, axon guidance and neuron migration (Oinuma et al., 2004; Zanata et al., 2002; Azzarelli et al., 2014). Furthermore, they are involved in actin stress fiber formation and linkage of Actin fibers to focal adhesions (Nobes, 1998). Via regulation of the actin cytoskeleton, Rnds have been shown to regulate cell adhesion to the ECM as well as cell migration (Nobes, 1998; Guasch et al., 1998). They are well known regulators of radial migration in the developing cortex (Heng et al., 2008; Pacary et al., 2011a; Azzarelli et al., 2014). Since the FLRT intracellular domain can interact with Rnd proteins, overexpression of FLRTs could also lead to a relocation of Rnds from the cytoplasm to the cell membrane and thus regulate adhesive properties of neurons and their migration. This effect would be abolished by deletion of the FLRT3 C-terminus.

The above mentioned hypotheses could be tested in further IUE experiments by simultaneously overexpressing FLRTs and N-Cadherin or Rnds or engineering a FLRT mutant lacking the two lysine residues involved in binding of Rnd proteins. Furthermore, overexpression of a FLRT^{ΔC/FF} double mutant would be interesting. If such a mutant would fully rescue the FLRT overexpression phenotype, this would rule out the possibility of further interactions taking place to inhibit cell migration upon FLRT overexpression.

3.3.4. FLRT3 does not change cell fate of developing pyramidal neurons

Several molecules, for example the protocadherins DCHS1 and FAT4, have been shown to interfere with cortical development by changing cell fate or disrupting differentiation

rather than directly inhibiting migration (Cappello et al., 2013). To rule out this possibility I investigated the molecular identity of the cells by immunostaining for the upper layer marker Cux1 three days after overexpression FLRT3. Even though the vast majority of FLRT3 expressing cells did not leave the intermediate zone they showed the same proportion of Cux1-positive cells as GFP transfected cells. Thus I concluded that overexpression of FLRTs does not change differentiation or fate of the cells but rather interferes with their migration by changing their adhesive properties and deregulating intracellular signaling pathways, most likely cytoskeletal dynamics. Thus it would be very important to investigate the behavior of FLRT overexpressing cells at later stages of development. Does overexpression of FLRTs only delay the migration of cells or do the cells terminate migration at the subplate forever? If the cells do not resume their migration at some point it would be interesting to investigate if they start making projections and if so, where they project to. For example in a mosaic knock-out model of Ndel1 it has been reported that pyramidal neurons, even though they were misplaced due to migrational defects, still established projections to their respective target area (Hippenmeyer et al., 2010). If they do not make projections, the cells might eventually die due to a lack of synaptic activity or incorrect surrounding environment. If the cells eventually resume migration it would be very interesting to see where they migrate to. Do they end up in the right place or do they settle ectopically on top of their normal location in layer II/III? These questions should be addressed in future experiments.

3.4. Conclusions and outlook

FLRTs have already been shown to be involved in a wide variety of processes ranging from regulation of FGF signaling to cell adhesion and cell sorting in different tissues. In the nervous system, FLRTs have been shown to regulate cell migration, axon guidance and synapse formation. I set out to untangle adhesive and repulsive functions of FLRTs in different paradigms during nervous system development, namely synapse formation and cortical migration.

I could not confirm the previously described involvement of FLRT3 in synapse formation *in vitro* and *in vivo*. This could, however, be due to technical differences between my experiments and the published work.

Three interesting questions could be addressed in future experiments: First, the electrophysiological properties of the hippocampus in FLRT knock-out mice could be measured to detect more subtle changes in synaptic physiology in these mice. Second, detailed ultrastructural analysis of the hippocampus could be performed to investigate changes in synaptic ultrastructure. And third, quantification of synapses could be performed in FLRT1/3 double knock-out mice to exclude the possibility of compensatory mechanisms that would lead to an underestimation of the importance of FLRTs in synapse development.

In a collaborative effort of two labs we then unraveled the molecular determinants of homophilic FLRT-FLRT and heterophilic FLRT-Unc5 interactions and designed mutant

proteins to specifically disrupt these interactions independently of each other and confirmed the specificity in cell-based assays.

I used the mutants to functionally prove the inhibition of radial migration of Unc5D positive neurons by FLRT2. Furthermore, I showed that overexpression of FLRTs in radially migrating neurons drastically inhibits their migration and this effect is independent of Unc5s but requires both extracellular homophilic interaction and the intracellular domain of FLRTs. Using a conditional knock-out approach I was not able to detect a loss of function effect of FLRT3 on cortical radial migration.

Several open questions remain to be followed up in this part of the project: Is the inhibitory effect of FLRT overexpression cell autonomous or non-cell autonomous due to released ectodomains? Which pathways does the intracellular domain of FLRTs influence? What is the fate of FLRT overexpressing cells at later stages of development? Is the lack of phenotype upon loss of FLRT3 due to coexpression and compensation by FLRT1? All these questions are experimentally traceable with the tools available and will provide further insight into the functional roles of FLRTs in cell adhesion and repulsion. Furthermore they will help gain more knowledge about the intracellular signaling functions of FLRTs.

In a more broad sense, the functional FLRT mutants we established and characterized here will also allow the investigation of FLRT functions in different tissues and model systems and can be transferred to other FLRT-interacting proteins that might be described in the future.

4. Materials and Methods

4.1. Materials

4.1.1. Chemicals, reagents and kits

All chemicals and reagents were purchased from Fluka, GE Healthcare, Invitrogen, Merck, Sigma, Serva, Roche, Roth and VWR, unless stated otherwise in the methods section. Water used for buffers, solutions and reactions mixes was filtered using a Milli-Q-Water System (Millipore) and autoclaved afterwards. Taq-DNA polymerase was purchased from New England Biolabs. Plasmid preparations were done using the QIAGEN QIAprep Spin Miniprep kit or the Macherey-Nagel NucleoBond® Xtra Maxi kit.

4.1.2. Buffers for biochemistry and stainings

PBS (phosphate-buffered saline), pH 7.3

137 mM NaCl

2.7 mM KCl

4.3 mM Na₂HPO₄·7H₂O

1.4 mM KH₂PO₄

Lysis buffer for Western blotting

50 mM Tris, pH 7.4

150 mM NaCl

2mM EDTA

1% TritonX-100 (vol/vol)

Protease inhibitor (Roche)

Lysis buffer for synaptic fractionation

4 mM HEPES, pH 7.4

320 mM Sucrose

Protease inhibitor (Roche)

Lysis buffer for PSD fraction

50 mM HEPES, pH 7.4

2 mM EDTA

Protease inhibitor (Roche)

6x Protein loading buffer (reducing)

300 mM Tris-HCl, pH 6.8

600 mM Dithiothreitol (DTT)

12% SDS

0.6% BromoPhenolBlue

60% Glycerol

Tris buffered saline - Tween (TBS-T)

20 mM Tris, pH 7.5

120 mM NaCl

0.1% Tween20

X-Gal wash buffer

0.1 M Sodium phosphate buffer, pH 7.3

2 mM MgCl₂

0.25 mM Deoxycholic acid

0.02 % NP-40

X-Gal staining solution

X-Gal wash buffer containing

5 mM Potassium ferrocyanide

5 mM Potassium ferricyanide

1 mg/ml X-Gal (Fermentas)

Blocking solution for staining of tissue sections

PBS

5% serum

0.2% BSA

0.2% Lysine

0.2% Glycine

EM fixative

2 mM CaCl₂

4 mM MgSO₄

100 mM Na cacodylate

2% PFA

2.5% Glutaraldehyde

4.1.3. Media for tissue culture

0.05 M Borate Buffer, pH 8.5

50 mM Boric acid

12.5 mM Sodium tetraborate (borax)

Medium for cell lines

DMEM (Gibco)

4.5 g/l D-Glucose

1% L-Glutamine

10% FBS (HyClone)

Dissection medium

HBSS (Gibco)
1% Penicillin-Streptomycin (Invitrogen)
7 mM HEPES
2 mM L-Glutamine (PAA)

Astrocyte medium

Minimal essential medium (Gibco)
0.6% D-Glucose
1% Penicillin-Streptomycin (Invitrogen)
10% horse serum (Gibco)

Neuronal plating medium

Minimal essential medium (Gibco)
0.6% D-Glucose
1% Penicillin-Streptomycin (Invitrogen)
10% horse serum (Gibco)

Neuronal maintenance medium

Neurobasal medium (Gibco)
1x B27 supplement (Invitrogen)
2mM L-Glutamine (PAA)
1% Penicillin-Streptomycin (Invitrogen)
5 μ M AraC

4.1.4. Oligonucleotides for genotyping

All oligonucleotides were synthesized by Eurofins MWG/Operon and purified by HPSF.

FLRT1^{WT}

FLRT1-WT-For 5' CAGCGAGATGGATGAGTGCTTTGA^{3'}

FLRT1-WT-Rev 5' GCCAGCATTCTGTTCTGGTTGA^{3'}

FLRT1⁻

FLRT1-KO-F 5' TAGAGGATCAGCTTGGGCTGCAGGTCGAGG^{3'}

FLRT1-R 5' TGAGATCCACAGCGAACAGCAGGCATTAGC^{3'}

FLRT3⁻, FLRT3^{lacZ}

FLRT3-F 5' GCTTATACTACAAGGGTCTCATGTGAACGC^{3'}

FLRT3-R-1 5' CCGGTACTAAGAAAGACAACCTCCATCCTGG^{3'}

FLRT3-R-2 5' GGCTGCAGGAATTCGATATCAAGCTTATCG^{3'}

FLRT3^{lx}

FLRT3-lx-F 5' GATATTTGCCAAAGGAGACAGAAAATACTGGC^{3'}

FLRT3-lx-R 5' CTGGGTTCAATTGCTGTCTACCAACAAGCAC^{3'}

FLRT3^{lx} (recombined)

FLRT3-lx-F 5' GATATTTGCCAAAGGAGACAGAAAATACTGGC^{3'}

FLRT3-REC-R 5' GTTCTAATTCCATCAGAAGCTGACTGATCC^{3'}

*NestinCre*Cre1 5'GCCTGCATTACCGGTCGATGCAACGA^{3'}Cre2 5'GTGGCAGATGGCGCGGCAACACCATT^{3'}**4.1.5. Plasmids**4.1.5.1. Constructs used for coculture and synapse assays

| Insert | Backbone | Tag | Reference |
|-------------------------|-----------------|------------|------------------|
| mouse FLRT1 | pcDNA3.1 | Flag | S. Yamagishi |
| mouse FLRT2 | pcDNA3.1 | Flag | S.Yamagishi |
| mouse FLRT3 | pcDNA3.1 | Flag | J. Egea |
| mouse Neurexin1 β | pCMV5 | GFP | P. Scheiffele |
| mouse Neuroligin1 | pEGFP-N1 | GFP | P. Scheiffele |
| Cre recombinase | pCAG-IRES-GFP | GFP | Addgene |

4.1.5.2. Mutant FLRT and Unc5 constructs

Full length constructs of mouse FLRT2 (Uniprot Q8BLU) and FLRT3 (Uniprot Q8BGT1), mouse Unc5B (Uniprot Q8K1S3) and rat Unc5D (Uniprot F1LW30) were cloned into the Age1-Kpn1 or EcoR1-Kpn1 cloning site of vectors from the pHLSec family (Aricescu et al., 2006). Full length FLRT2, FLRT3, Unc5B and Unc5D were inserted into a pHLSec vector that codes for a C-terminal mVenus and a polyhistidine tag (Seiradake et al., 2010).

Hemagglutinin epitope (HA) tags are included at the N-terminus of transmembrane constructs, following the vector secretion signal sequence.

For expression *in vivo*, FLRT and Unc5 constructs with the pHLSec vector signal sequence and HA tag were subcloned into a pCAGIG vector coding for a C-terminal internal ribosome entry site (IRES) and GFP (Cancedda et al., 2007). Point mutants to insert N-glycosylation sites were generated using standard polymerase chain reaction techniques. The mutations inserted into the different constructs are listed below. Complete sequences and vector maps of the constructs are available upon request.

| Construct | Binding specificity | Mutations |
|---------------------|-----------------------------|---|
| FLRT2 | Homophilic and heterophilic | |
| FLRT2 ^{UF} | Homophilic only | H170N |
| FLRT2 ^{FF} | Heterophilic only | R186N, D188T |
| FLRT3 | Homophilic and heterophilic | |
| FLRT3 ^{UF} | Homophilic only | H165N |
| FLRT3 ^{FF} | Heterophilic only | R181N, D183T |
| FLRT3 ^{ΔC} | Homophilic and heterophilic | Deletion of entire intracellular domain |
| Unc5B | FLRT binding | |
| Unc5B ^{UF} | No FLRT binding | W85N, S87T |
| Unc5D | FLRT binding | |
| Unc5D ^{UF} | No FLRT binding | W89N, H91T |

4.1.6. Primary antibodies

| Antigen | Species | Supplier | Dilution | Application |
|----------------------|----------------|------------------|------------------------|--------------------|
| β -Actin | mouse | Sigma-Aldrich | 1:10000 | WB |
| β -III-Tubulin | mouse | Covance | 1:10000 | WB |
| Ctip2 | rat | Abcam | 1:500, 1:500 1:1000 | IF, IHC WB |
| Cux1 | rabbit | Santa Cruz | 1:100 | IHC |
| Flag tag | rabbit | Sigma | 1:1000 | IF |
| FLRT1 | goat | R&D Systems | 1:1000 | WB |
| FLRT2 | goat | R&D Systems | 1:1000 | WB |
| FLRT3 | goat | R&D Systems | 1:1000 | WB |
| Gephyrin | mouse | Synaptic Systems | 1:250 | IF |
| GFP | chicken | Abcam | 1:2000 | IF |
| HA tag | mouse | Roche | 1:400, | IF, WB |
| Map2 | chicken | Millipore | 1:2000 | IF |
| Munc13-1 | rabbit | Synaptic Systems | 1:1000 | WB |
| NeuN | mouse | Millipore | 1:1000 | IF |
| Prox1 | rabbit | Covance | 1:1000 | WB |
| PSD95 | mouse | Abcam | 1:200, 1:1000 | IF, WB |
| Snap25 | mouse | Synaptic Systems | 1:1000 | WB |
| Synapsin1 | rabbit | Abcam | 1:500, 1:1000 | IF, WB |
| Synaptophysin | mouse | Synaptic Systems | 1:10000 | WB |

4.1.7. Secondary antibodies

All secondary antibodies were purchased from Jackson ImmunoResearch. For Western blots, HRP coupled secondary antibodies and for immunostainings, fluorescently labelled secondary antibodies were used. Antibodies were diluted 1:5000 for Western blotting, 1:1000 for staining of cells and 1:400 for staining of sections.

4.1.8. Mouse lines

The *FLRT1*⁻, *FLRT3*⁻, *FLRT3*^{lacZ} and *FLRT3*^{lx} mouse lines were generated and validated by Satoru Yamagishi and Joaquim Egea (Yamagishi et al., 2011; Egea et al., 2008). The *NesCre* line was described previously (Tronche et al., 1999).

All experiments were performed on mice kept in a mixed Sv129 x C57BL/6 background.

4.2. Methods

4.2.1. Mouse genotyping

Mice were genotyped by PCR. For genotyping, a 1-2 mm long piece of the tail tip of each mouse was cut and boiled three times for 15 min at 95°C in 50 µl of 50 mM NaOH with vigorous vortexing inbetween. The solution was neutralized afterwards by 10 µl of 1.5 M Tris-HCl, pH 8.8. 2 µl of the tail lysate were used as a template in PCRs, which were carried out with 50 pmol of each specific primer, 5 µl 10x PCR buffer (New England Biolabs), 0.4 µl dNTP-mix (25 mM each, Fermentas) and 0.5 µl Taq polymerase (New England Biolabs) in a total reaction volume of 50 µl. 30 µl of the PCR reaction were separated on 1.5% agarose gels containing ethidium bromide and analyzed under UV light. Primers used for genotyping are described in section 4.1.4.

4.2.2. Preparation of glass coverslips

For imaging experiments of cell lines, 13 mm glass coverslips (VWR) were sterilized by overnight incubation at 180°C. Coverslips were then used directly without further treatment or coating.

For cultures of primary neurons, 18 mm glass coverslips (Fisher Scientific) were treated with 65% nitric acid under gentle agitation overnight. Afterwards, coverslips were washed for 24 h with distilled water with frequent changes of the water. At the end,

coverslips were washed 5 times with 100% EtOH and then dried completely. To sterilize the coverslips, they were incubated overnight at 180°C.

One day before preparation of neurons, paraffin dots were put on the coverslips (Kaech and Banker, 2006) and coverslips were coated with 1 mg/ml of poly-D-Lysine in borate buffer overnight in the incubator.

Before seeding of the neurons, coverslips were washed three times with distilled water and then covered with astrocyte medium without completely drying.

4.2.3. Tissue culture

4.2.3.1. Cell lines

HEK293T and COS7 cells were cultured in Falcon dishes according to ATCC's (American Type Culture Collection) recommendations concerning splitting ratios and media requirements.

4.2.3.2. Primary neurons and astrocytes

Mouse hippocampal neurons were cultured essentially according to Kaech and Banker (Kaech and Banker, 2006). Briefly, astrocytes were prepared from P1 rats according to the protocol and cultured in 75 cm² flasks until they almost reached confluency. Cells were then harvested using trypsin and frozen at -80°C in cryoprotection medium at a

density of 2×10^6 cells/ml or seeded directly into 6 cm dishes in astrocyte medium for neuronal coculture.

Neurons were cocultured once the astrocytes reached 60-70% confluency. Two days prior to neuronal coculture, the astrocyte medium was replaced by neuronal maintenance medium for preconditioning of the medium. Neurons were prepared from E17.5 embryos from either WT C57BL/6 mice or from Sv129 x C57BL/6 knockout mouse strains according to the protocol. For knockout cultures, breedings were performed in a way so knockout and control embryos could be obtained from the same litter. At the day of the experiment, embryos were removed from the uterus and a piece of tail was cut for genotyping by PCR. Embryos were stored in dissection medium on ice at 4°C in the meantime. Neurons were then seeded at a density of 125,000 cells per 6 cm dish on 18 mm poly-D-Lysine coated glass coverslips in astrocyte medium and allowed to attach for 3-4 h at 37°C in a humidified 95% air / 5% CO₂ atmosphere. After cell attachment, coverslips were flipped into 6 cm dishes containing astrocytes and further incubated at 37°C in a humidified 95% air / 5% CO₂ atmosphere. After 3-4 days AraC was added at a final concentration of 5 μM to prevent contamination of the neuronal culture with glial cells. Half of the neuronal maintenance medium was replaced with fresh medium containing AraC once a week.

4.2.3.3. Transfections

Cell lines were transfected using Fugene™ reagent (Promega) according to the manufacturers instructions. Briefly, cells were transfected at a confluency of 50-70%. On the day of transfection, Fugene™ was added to OptiMEM not containing serum or antibiotics. After 5 min incubation at RT, DNA was added and the transfection mix was incubated at RT for 15 to 30 min and then added directly to the cells. Cells were left in the incubator for 24 h to 48 h for protein expression depending on the assay. A Fugene:DNA ratio of 3:1 was used for all experiments. 0.5 to 1 µg of total DNA was used to transfect one well of a 6 well plate.

Neurons were transfected before plating using the mouse hippocampal neuron program (program O-005) on an Amaxa Nucleofector™ (Lonza) and the mouse neuron nucleofector kit from Lonza.

1×10^6 cells were resuspended in 100 µl transfection buffer, mixed with 3 µg of DNA, transferred into an electroporation cuvette and electroporated immediately. After electroporation, 400 µl of warm glial medium were added and 250,000 cells were seeded onto coverslips in a 6 cm dish.

4.2.4. Biochemistry

4.2.4.1. Western blots from cell lysates

For analysis of protein expression, HEK293 cells were transfected using Fugene™. After 2 days of expression, medium was aspirated and cells were washed twice with ice cold PBS. Lysis buffer was then added and cells were collected by scraping them off the plate. Samples were triturated 10 times with a syringe and a needle and then incubated for 15 min on ice and spun at 1000 x g for 15 min at 4°C. Supernatants were then collected and pellets were discarded. Protein content was measured using the BioRad BCA kit and samples were diluted to reach equal protein concentration. Samples were then mixed with 6 x SDS-PAGE loading buffer and boiled for 10 min at 95°C. Afterwards, samples were either frozen at -20°C for storage or immediately loaded onto SDS-PAGE gels for protein separation. 10 to 20 µg of total protein per sample were loaded on the gel. Proteins were then blotted onto PVDF membranes for 45 – 90 min at 100 mA per gel depending on the size of the proteins. Membranes were blocked with TBS-T/5% milk for 1 h at RT and then incubated with primary antibodies for 1 h at RT or overnight at 4°C. After that, blots were washed at least 3 times for 5 min with TBS-T/2.5% milk and then incubated for 1 h at RT with HRP coupled secondary antibodies (1:5000 in TBS-T/2.5% milk). Blots were then washed again 3 times with TBS-T/2.5% milk and then developed using a chemiluminescent HRP substrate and X-ray films.

4.2.4.2. Western blots from tissue lysates

Tissue samples were collected and homogenized in lysis buffer using a motorized dounce homogenizer (10 strokes at full speed) on ice. Samples were then incubated for 15 min on ice and then either subjected to a fractionation protocol or spun for 10 min at 1000 x g. Supernatants were collected and subjected to SDS-PAGE and Western blotting as described for cell culture samples. 10 to 20 µg of total protein per sample were used for analysis.

4.2.4.3. Synaptic fractionation

Synaptic fractionation of brain samples was done according to a previously published protocol (Pérez-Otaño et al., 2006). Briefly, after dissection, samples were homogenized in cold lysis buffer using 10 strokes with a motor driven dounce homogenizer. The homogenate was spun at 1,000 x g for 15 min at 4°C, and the resulting supernatant (S1) was spun at 10,000 x g for 15 min to yield the crude synaptosomal pellet (P2). The supernatant (S2) was centrifuged at 100,000 x g for 15 min to separate the cytosolic fraction (S2') from the light membrane pellet (LM). The crude synaptosomal pellet (P2) was resuspended in lysis buffer and centrifuged at 10,000 x g for 15 min at 4°C to yield the washed crude synaptosomal pellet (P2'). Nine volumes of ice cold H₂O plus protease inhibitors were added to lyse P2' membranes, and the osmolarity was rapidly readjusted by adding 1 M HEPES, pH 7.4 to a final concentration of 4 mM HEPES. Membranes were then mixed constantly at 4°C for 30 min to ensure complete lysis. The lysate was spun at 25,000 x g for 20 min to yield the lysed synaptosomal membrane fraction (P3) and

synaptic vesicles in the supernatant. The P3 pellet was resuspended and layered on a discontinuous sucrose gradient containing 1.2 M, 1 M and 0.8 M sucrose. The gradient was centrifuged at 150,000 x g for 2 h at 4°C, and upon completion, material at the 1.2 M and 1 M interface was recovered, diluted to 0.32 M sucrose and spun at 150,000 x g for 30 min to yield the synaptic plasma membrane fraction (SPM). The SPM pellet was resuspended in 3-5 ml of ice-cold 50 mM HEPES pH 7.4, 2 mM EDTA, plus protease inhibitors. To obtain the PSD-1 pellet, 0.5 % Triton X-100 was added to the SPM fraction and the solubilized membranes were centrifuged at 32,000 x g for 20 min. The resulting supernatant constitutes the SPM-TX soluble fraction (presynapse). Samples were then subjected to Western blot analysis.

4.2.4.4. Hippocampus microdissection

Hippocampi from P20/21 mice were dissected out on ice and cut into 1 mm sections using a tissue chopper. The sections were then further dissected into CA1, CA3 and DG regions using fine dissection knives under a dissection microscope. The distribution of cell bodies of pyramidal neurons was used as landmarks to distinguish CA1 and CA3. CA1 and DG were torn apart along the hippocampal fissure. All tissue pieces from one region of both hippocampi from one brain were pooled and treated as one sample. Samples were then lysed and subjected to Western blot analysis.

4.2.5. X-Gal staining

FLRT3^{lacZ} mice were transcardially perfused with PBS to wash out the blood and with 4% PFA in PBS to fix the brains. Brains were then dissected out and postfixed over night at 4°C. Fixed brains were embedded in 4% low melting temperature agarose and cut on a vibratome. Sections were washed twice with X-Gal wash buffer and then incubated with X-Gal staining solution at 37°C in the dark until clear staining was visible. Sections were again washed twice with X-Gal wash buffer and then mounted onto glass slides using mowiol.

For staining of neurons from *FLRT3^{lacZ}* mouse embryos, cells were fixed with 4% PFA in PBS and washed twice with X-Gal wash buffer. Coverslips were then incubated with X-Gal staining solution for 2 h at 37°C in the dark. Afterwards, cells were permeabilized, blocked and subjected to antibody stainings. Samples were then mounted on glass slides using ProLong™ Gold antifade reagent (Invitrogen) and imaged on a fluorescent microscope (Olympus).

4.2.6. Immunostainings

4.2.6.1. Cell lines

Medium was aspirated from cells and coverslips were washed once with PBS. Then cells were fixed for 10 min at RT with 4% PFA and washed twice with PBS afterwards. Cells were then washed for 10 min with PBS/50 mM NH₄Cl to quench PFA autofluorescence and then permeabilized for 10 min with PBS/0.1% TritonX-100. After blocking for 1 h at

RT with PBS/10% FBS cells were incubated with primary antibodies in PBS/3% BSA for 2 h at RT or overnight at 4°C, respectively. Samples were then washed 5 times with PBS and incubated with secondary antibodies diluted 1:1000 in PBS/3% BSA for 1 h at RT. Afterwards, cells were washed 5 times with PBS, counterstained with DAPI (1 µg/ml) for 10 min at RT and then mounted on glass slides using ProLong™ Gold antifade reagent (Invitrogen).

For surface stainings, cells were blocked using PBS/10% FBS and stained with primary and secondary antibody before permeabilization. Cells were then washed 5 times and subjected to the aforementioned staining protocol.

4.2.6.2. Primary neurons

Neurons were fixed for 3 min at RT using 4% PFA containing 4% Sucrose (wt/vol) preheated to 37°C. Afterwards, cells were washed twice with RT PBS and then stained following the protocol for cell lines.

4.2.6.3. Tissue sections

Vibratome sections were stained in 24 well plates using net inserts for easy transfer of the sections.

Sections were washed twice with PBS/50 mM NH₄Cl for 10 min at RT and then permeabilized with PBS/0.5% TritonX-100 for 30 min to 2 h at RT depending on the thickness of the sections. Afterwards, sections were blocked for 2 h at RT with blocking

buffer (see materials section). Sections were then washed for 1 h at RT with PBS/0.5% TritonX-100 and incubated with primary antibodies in PBS/2% BSA/0.3% TritonX-100 overnight at 4°C. The next day, sections were washed 3 times for 30 min with PBS and then incubated with fluorescently labelled secondary antibodies (1:400) in PBS/3% serum/0.3% TritonX-100 for 2 h at RT. After three 30 min washes with PBS, sections were counterstained with DAPI (1 µg/ml) for 10 min at RT and then mounted on glass slides (Thermo Scientific) using mowiol.

4.2.7. HEK Neuron coculture assay

HEK neuron coculture assays to assess the synaptogenic potential of FLRTs were essentially performed as previously described (Biederer and Scheiffele, 2007) with minor modifications. Briefly, HEK cells were transfected with plasmids coding for the proteins of interest and collected after 24 h using 5 mM EDTA. Cells were then counted and diluted in Neurobasal/B27 medium containing 5 µM AraC. 30,000 cells per well were seeded onto neurons on coverslips in 24 well plates. Neurons were DIV8 to assess presynaptic differentiation and DIV10 to assess postsynaptic differentiation respectively. After two days in culture, cells were fixed with 4% PFA for 5 min at RT and stained for FLAG to visualize expressing HEK cells and Map2 to visualize dendrites of neurons. Furthermore, coverslips were stained for Synapsin1, Gephyrin or PSD95 to mark sites of synaptic differentiation. Coverslips were mounted on glass slides using DAKO mounting medium.

4.2.8. Synapse quantification on primary neurons

For quantification of synapse density in primary neurons, cells were cultured for 21 days in sandwich culture on top of rat astrocytes (see 4.2.3.2). Neurons were then fixed for 3 min at RT with 4% PFA and stained for Ctip2, Synapsin1 and PSD95.

At least 20 cells per condition were imaged on a Leica SP2 confocal microscope in each experiment. Image stacks spanning the neuron from top to bottom were taken at 1 μ m steps using a 63 x oil immersion objective using similar settings for laser power, gain and offset throughout each experiment. For analysis of synapse density, image stacks were collapsed using maximum projection and the PSD95 and Synapsin1 channels were merged in ImageJ. The main neuron in each image was manually isolated from the image to clear the quantification from synaptic structures on other neurites passing through the image. Number of Synapsin1-positive, PSD95-positive and colocalized puncta was determined using the puncta analyzer plugin for ImageJ 1.26 (written by Bary Wark) according to the published protocol (Ippolito and Eroglu, 2010). Overall length of neurites of every neuron was measured with the NeuronJ 1.4.2 plugin for ImageJ (written by Erik Meijering) based on the background fluorescence of the Synapsin1 staining or GFP fluorescence in experiments involving transfections. Number of puncta per 10 μ m neurite length was calculated for each neuron and averaged for each experiment. Results represent average \pm SEM of 3 independent experiments. Imaging and quantification was done blindly to experimental condition.

4.2.9. Electron microscopic analysis of synapses

For ultrastructural analysis of synapse density in the hippocampus, mice were anesthetized with 5% chloral hydrate in 0.9% saline. When no reflexes were detectable anymore, mice were transcardially perfused with 15 ml of PBS to wash out the blood and then with 15 ml of EM fixative. Brains were dissected out and postfixed in EM fixative over night at 4°C. Brains were then embedded in gelatin albumin and 200 µm sections were cut on a vibratome. Tissue blocks of roughly 2 mm x 2 mm size were cut from the stratum radiatum of CA1 and CA3 and the middle molecular layer of the dentate gyrus using fine dissection scalpels. Thin sectioning, ultrathin sectioning, osmium tetroxide staining and imaging were done by the EM core facility of the MPI Neurobiology according to standard procedures. Two samples from each region per mouse were used for analysis (one from each hippocampus). 15 ultrathin sections per sample were imaged at 25,000 x magnification. Synapses were then counted manually in ImageJ. Any structure that had two closely aligned membranes and a clearly stained PSD was considered a synapse. Number of synapses was counted for each image, normalized to area and averaged per mouse. Results are given as average \pm SEM of four mice for each genotype. Counting of synapses was done blindly to genotype.

4.2.10. Cell surface binding assay

COS7 cells were grown on glass coverslips, transfected using Fugene™ reagent and incubated for 24 h for protein expression.

Purified ectodomains of the protein of interest fused to human Fc were preclustered in PBS^{-/-} using a Cy3 coupled anti-human Fc antibody for 1 h at RT in the dark. Then the preclustered proteins were added to the transfected cells at a final concentration of 100 nM in OptiMEM and incubated for 30 min at RT in the dark. Afterwards, the supernatant was aspirated and the cells were washed once with room temperature PBS and fixed with 4% PFA for 10 min at RT.

Coverslips were stained with DAPI (1 µg/ml) for 10 min at RT and then mounted on glass slides using ProLongTM Gold antifade reagent (Invitrogen).

4.2.11. HEK293 cell aggregation assay

For aggregation assays, HEK293 cells were transfected with pCAG-IRES-GFP or pCAG-FLRT-IRES-GFP constructs and collected after one day with 5 mM EDTA to preserve surface proteins. 170,000 cells per well in 500 µl medium were then incubated for 6 days in BSA coated 24 well plates under constant orbital shaking (120 rpm) at 37°C in a humidified 95% air / 5% CO₂ atmosphere. After aggregation, samples were fixed by adding one volume of 8% PFA directly into the medium. GFP-positive clusters were imaged with a fluorescent microscope and brightfield images were taken to visualize the entire aggregates. For quantification, the GFP channel was thresholded manually and cluster size was measured using ImageJ. Results were averaged for every condition and expressed as percent of GFP control.

Culture plates were coated with 2% BSA in PBS for at least 2 h at 37°C and then washed 3 times with PBS before the experiment.

4.2.12. *In utero* electroporation

In utero electroporations were essentially performed as described previously (Tabata and Nakajima, 2001; Saito and Nakatsuji, 2001). Briefly, timed pregnant female mice were anesthetized using Isoflourane. When no reflexes were detectable anymore, the uterus was exposed and 1 μ l of TE buffer containing 2 μ g of DNA and 0.02% FastGreen was injected into the lateral ventricle of one hemisphere of each embryos brain using a Picospritzer III (Intracel). Glass capillaries for injection (1.5x0.86x80 mm, Science Products) were pulled on a micropipette puller (Sutter Instruments, settings: 680°C, pull = 30, velocity = 125, time = 210) and the tips were broken manually. Then, five 50 ms current pulses were applied at 30 volts at 1 second intervals with the positively charged electrode placed on the injected side using an ECM830 electroporator (Harvard Apparatus). After electroporation, the peritoneal wall and the skin were sewed and the mice were allowed to wake up and recover for 30 min on a heating pad. After 3 days, mice were sacrificed, brains dissected from the embryos and fixed overnight in 4% PFA at 4°C.

After fixation, brains were embedded in 4% low melting temperature agarose and 100 μ m sections were cut on a vibratome (Leica Microsystems) and stained with DAPI (1 μ g/ml) for 10 min at RT. Sections were then mounted on glass slides (Thermo Scientific) using mowiol and imaged on a Leica SP2 confocal laser scanning microscope with a 20 x oil immersion objective.

Stacks of 4 images were taken from the top of each section at a step size of 4 μ m. 3-4 adjacent sections within the somatosensory cortex were imaged and analyzed per embryo. For analysis, stacks were collapsed using maximum projection in ImageJ.

Regions of interest (ROIs) of the VZ/SVZ, IZ and CP were defined based on the DAPI staining and transferred onto the GFP image. The GFP image was thresholded manually and the distribution of GFP-positive pixels in each ROI was measured with ImageJ. Percentage of GFP-positive pixels in each ROI was then calculated and averaged over all sections from one embryo. For some experiments, the cortical plate was divided into three equally sized bins and the distribution of GFP-positive pixels between the bins was calculated. At least four embryos per condition from at least two independent electroporations were analyzed in each experiment. Quantification was done blindly to experimental condition.

4.2.13. Statistical analyses

Statistical significance was determined using unpaired, two-tailed Student's T-test or one way ANOVA with Bonferroni post test in Microsoft Excel or GraphPad Prism if not mentioned otherwise in the figure legend. Results were considered statistically significant when the p-value was lower than 0.05. All values in the text and in the figure legends indicate mean \pm standard error of the mean (SEM).

5. References

- Alvarez, V.A., D.A. Ridenour, and B.L. Sabatini. 2006. Retraction of synapses and dendritic spines induced by off-target effects of RNA interference. *J. Neurosci.* 26:7820–5. doi:10.1523/JNEUROSCI.1957-06.2006.
- Anderson, S. 1999. Differential Origins of Neocortical Projection and Local Circuit Neurons: Role of Dlx Genes in Neocortical Interneuronogenesis. *Cereb. Cortex.* 9:646–654. doi:10.1093/cercor/9.6.646.
- Anderson, S., O. Marin, C. Horn, K. Jennings, and J. Rubenstein. 2001. Distinct cortical migrations from the medial and lateral ganglionic eminences. *Development.* 128:353–363.
- Ang, E.S.B.C., J., T.F. Haydar, V. Gluncic, and P. Rakic. 2003. Four-Dimensional Migratory Coordinates of GABAergic Interneurons in the Developing Mouse Cortex. *J. Neurosci.* 23:5805–5815.
- Angevine, J.B., and R.L. Sidman. 1961. Autoradiographic Study of Cell Migration during Histogenesis of Cerebral Cortex in the Mouse. *Nature.* 192:766–768. doi:10.1038/192766b0.
- Anthony, T.E., C. Klein, G. Fishell, and N. Heintz. 2004. Radial Glia Serve as Neuronal Progenitors in All Regions of the Central Nervous System. *Neuron.* 41:881–890. doi:10.1016/S0896-6273(04)00140-0.
- Anton, E., J.A. Kreidberg, and P. Rakic. 1999. Distinct Functions of $\alpha 3$ and αV Integrin Receptors in Neuronal Migration and Laminal Organization of the Cerebral Cortex. *Neuron.* 22:277–289. doi:10.1016/S0896-6273(00)81089-2.
- Aricescu, A.R., W. Lu, and E.Y. Jones. 2006. A time- and cost-efficient system for high-level protein production in mammalian cells. *Acta Crystallogr. D. Biol. Crystallogr.* 62:1243–50. doi:10.1107/S09074444906029799.
- Ayala, R., T. Shu, and L.-H. Tsai. 2007. Trekking across the brain: the journey of neuronal migration. *Cell.* 128:29–43. doi:10.1016/j.cell.2006.12.021.
- Azzarelli, R., E. Pacary, R. Garg, P. Garcez, D. van den Berg, P. Riou, A.J. Ridley, R.H. Friedel, M. Parsons, and F. Guillemot. 2014. An antagonistic interaction between PlexinB2 and Rnd3 controls RhoA activity and cortical neuron migration. *Nat. Commun.* 5:3405. doi:10.1038/ncomms4405.
- Bai, J., R.L. Ramos, J.B. Ackman, A.M. Thomas, R. V Lee, and J.J. LoTurco. 2003. RNAi reveals doublecortin is required for radial migration in rat neocortex. *Nat. Neurosci.* 6:1277–83. doi:10.1038/nn1153.

- Banker, G.A., and W.M. Cowan. 1977. Rat hippocampal neurons in dispersed cell culture. *Brain Res.* 126:397–425. doi:10.1016/0006-8993(77)90594-7.
- Battye, R., A. Stevens, and J. Jacobs. 1999. Axon repulsion from the midline of the *Drosophila* CNS requires slit function. *Development.* 126:2475–2481.
- Bayer, S.A., and J. Altman. 1991. Neocortical development. Raven Press, New York.
- Bella, J., K.L. Hindle, P.A. McEwan, and S.C. Lovell. 2008. The leucine-rich repeat structure. *Cell. Mol. Life Sci.* 65:2307–33. doi:10.1007/s00018-008-8019-0.
- Bermingham, J.R., H. Shearin, J. Pennington, J. O’Moore, M. Jaegle, S. Driegen, A. van Zon, A. Darbas, E. Ozkaynak, E.J. Ryu, J. Milbrandt, and D. Meijer. 2006. The claw paw mutation reveals a role for Lgi4 in peripheral nerve development. *Nat. Neurosci.* 9:76–84. doi:10.1038/nn1598.
- Biederer, T., Y. Sara, M. Mozhayeva, D. Atasoy, X. Liu, E.T. Kavalali, and T.C. Südhof. 2002. SynCAM, a synaptic adhesion molecule that drives synapse assembly. *Science.* 297:1525–31. doi:10.1126/science.1072356.
- Biederer, T., and P. Scheiffele. 2007. Mixed-culture assays for analyzing neuronal synapse formation. *Nat. Protoc.* 2:670–6. doi:10.1038/nprot.2007.92.
- Björklund, A.K., D. Ekman, and A. Elofsson. 2006. Expansion of protein domain repeats. *PLoS Comput. Biol.* 2:e114. doi:10.1371/journal.pcbi.0020114.
- Blundell, J., C.A. Blaiss, M.R. Etherton, F. Espinosa, K. Tabuchi, C. Walz, M.F. Bolliger, T.C. Südhof, and C.M. Powell. 2010. Neuroligin-1 deletion results in impaired spatial memory and increased repetitive behavior. *J. Neurosci.* 30:2115–29. doi:10.1523/JNEUROSCI.4517-09.2010.
- Borrell, V., and M. Götz. 2014. Role of radial glial cells in cerebral cortex folding. *Curr. Opin. Neurobiol.* 27C:39–46. doi:10.1016/j.conb.2014.02.007.
- Borrell, V., and I. Reillo. 2012. Emerging roles of neural stem cells in cerebral cortex development and evolution. *Dev. Neurobiol.* 72:955–71. doi:10.1002/dneu.22013.
- Böttcher, R.T., N. Pollet, H. Delius, and C. Niehrs. 2004. The transmembrane protein XFLRT3 forms a complex with FGF receptors and promotes FGF signalling. *Nat. Cell Biol.* 6:38–44. doi:10.1038/ncb1082.
- Brose, K., K.S. Bland, K.H. Wang, D. Arnott, W. Henzel, C.S. Goodman, M. Tessier-Lavigne, and T. Kidd. 1999. Slit Proteins Bind Robo Receptors and Have an Evolutionarily Conserved Role in Repulsive Axon Guidance. *Cell.* 96:795–806. doi:10.1016/S0092-8674(00)80590-5.

- Brunstrom, J.E., M.R. Gray-Swain, P.A. Osborne, and A.L. Pearlman. 1997. Neuronal Heterotopias in the Developing Cerebral Cortex Produced by Neurotrophin-4. *Neuron*. 18:505–517. doi:10.1016/S0896-6273(00)81250-7.
- Cancedda, L., H. Fiumelli, K. Chen, and M. Poo. 2007. Excitatory GABA action is essential for morphological maturation of cortical neurons in vivo. *J. Neurosci.* 27:5224–35. doi:10.1523/JNEUROSCI.5169-06.2007.
- Cappello, S., M.J. Gray, C. Badouel, S. Lange, M. Einsiedler, M. Srour, D. Chitayat, F.F. Hamdan, Z.A. Jenkins, T. Morgan, N. Preitner, T. Uster, J. Thomas, P. Shannon, V. Morrison, N. Di Donato, L. Van Maldergem, T. Neuhann, R. Newbury-Ecob, M. Swinkells, P. Terhal, L.C. Wilson, P.J.G. Zwijnenburg, A.J. Sutherland-Smith, M.A. Black, D. Markie, J.L. Michaud, M.A. Simpson, S. Mansour, H. McNeill, M. Götz, and S.P. Robertson. 2013. Mutations in genes encoding the cadherin receptor-ligand pair DCHS1 and FAT4 disrupt cerebral cortical development. *Nat. Genet.* 45:1300–8. doi:10.1038/ng.2765.
- Casarosa, S., C. Fode, and F. Guillemot. 1999. Mash1 regulates neurogenesis in the ventral telencephalon. *Development*. 126:525–534.
- Caviness, V.S., and T. Takahashi. 1995. Proliferative events in the cerebral ventricular zone. *Brain Dev.* 17:159–163. doi:10.1016/0387-7604(95)00029-B.
- Chardin, P. 2006. Function and regulation of Rnd proteins. *Nat. Rev. Mol. Cell Biol.* 7:54–62. doi:10.1038/nrm1788.
- Chen, X., E. Koh, M. Yoder, and B.M. Gumbiner. 2009. A protocadherin-cadherin-FLRT3 complex controls cell adhesion and morphogenesis. *PLoS One*. 4:e8411. doi:10.1371/journal.pone.0008411.
- Chenn, A., and S.K. McConnell. 1995. Cleavage orientation and the asymmetric inheritance of notch1 immunoreactivity in mammalian neurogenesis. *Cell*. 82:631–641. doi:10.1016/0092-8674(95)90035-7.
- Chih, B., H. Engelman, and P. Scheiffele. 2005. Control of excitatory and inhibitory synapse formation by neuroligins. *Science*. 307:1324–8. doi:10.1126/science.1107470.
- Cho, G.-S., S.-C. Choi, and J.-K. Han. 2013. BMP signal attenuates FGF pathway in anteroposterior neural patterning. *Biochem. Biophys. Res. Commun.* 434:509–15. doi:10.1016/j.bbrc.2013.03.105.
- Chothia, C., and E.Y. Jones. 1997. The molecular structure of cell adhesion molecules. *Annu. Rev. Biochem.* 66:823–62. doi:10.1146/annurev.biochem.66.1.823.
- Coles, C.H., Y. Shen, A.P. Tenney, C. Siebold, G.C. Sutton, W. Lu, J.T. Gallagher, E.Y. Jones, J.G. Flanagan, and A.R. Aricescu. 2011. Proteoglycan-specific molecular switch for

- RPTP σ clustering and neuronal extension. *Science*. 332:484–8. doi:10.1126/science.1200840.
- Conover, J.C., F. Doetsch, J.M. Garcia-Verdugo, N.W. Gale, G.D. Yancopoulos, and A. Alvarez-Buylla. 2000. Disruption of Eph/ephrin signaling affects migration and proliferation in the adult subventricular zone. *Nat. Neurosci.* 3:1091–7. doi:10.1038/80606.
- Cremer, H., R. Lange, A. Christoph, M. Plomann, G. Vopper, J. Roes, R. Brown, S. Baldwin, P. Kraemer, and S. Scheff. 1994. Inactivation of the N-CAM gene in mice results in size reduction of the olfactory bulb and deficits in spatial learning. *Nature*. 367:455–9. doi:10.1038/367455a0.
- Dehay, C., and H. Kennedy. 2007. Cell-cycle control and cortical development. *Nat. Rev. Neurosci.* 8:438–50. doi:10.1038/nrn2097.
- Delloye-Bourgeois, C., J. Fitamant, A. Paradisi, D. Cappellen, S. Douc-Rasy, M.-A. Raquin, D. Stupack, A. Nakagawara, R. Rousseau, V. Combaret, A. Puisieux, D. Valteau-Couanet, J. Bénard, A. Bernet, and P. Mehlen. 2009. Netrin-1 acts as a survival factor for aggressive neuroblastoma. *J. Exp. Med.* 206:833–47. doi:10.1084/jem.20082299.
- Dhavan, R., and L.H. Tsai. 2001. A decade of CDK5. *Nat. Rev. Mol. Cell Biol.* 2:749–59. doi:10.1038/35096019.
- Dick, O., S. tom Dieck, W.D. Altmann, J. Ammermüller, R. Weiler, C.C. Garner, E.D. Gundelfinger, and J.H. Brandstätter. 2003. The Presynaptic Active Zone Protein Bassoon Is Essential for Photoreceptor Ribbon Synapse Formation in the Retina. *Neuron*. 37:775–786. doi:10.1016/S0896-6273(03)00086-2.
- Dimidschstein, J., L. Passante, A. Dufour, J. van den Aamele, L. Tiberi, T. Hrechdakian, R. Adams, R. Klein, D.C. Lie, Y. Jossin, and P. Vanderhaeghen. 2013. Ephrin-B1 controls the columnar distribution of cortical pyramidal neurons by restricting their tangential migration. *Neuron*. 79:1123–35. doi:10.1016/j.neuron.2013.07.015.
- Dulabon, L. 2000. Reelin Binds alpha3beta1 Integrin and Inhibits Neuronal Migration. *Neuron*. 27:33–44. doi:10.1016/S0896-6273(00)00007-6.
- Echeverri, C.J., P.A. Beachy, B. Baum, M. Boutros, F. Buchholz, S.K. Chanda, J. Downward, J. Ellenberg, A.G. Fraser, N. Hacohen, W.C. Hahn, A.L. Jackson, A. Kiger, P.S. Linsley, L. Lum, Y. Ma, B. Mathey-Prévôt, D.E. Root, D.M. Sabatini, J. Taipale, N. Perrimon, and R. Bernards. 2006. Minimizing the risk of reporting false positives in large-scale RNAi screens. *Nat. Methods*. 3:777–9. doi:10.1038/nmeth1006-777.
- Edmondson, J.C. 1988. Astrotactin: a novel neuronal cell surface antigen that mediates neuron-astroglial interactions in cerebellar microcultures. *J. Cell Biol.* 106:505–517. doi:10.1083/jcb.106.2.505.

- Egea, J., C. Erlacher, E. Montanez, I. Burtscher, S. Yamagishi, M. Hess, F. Hampel, R. Sanchez, M.T. Rodriguez-Manzaneque, M.R. Bösl, R. Fässler, H. Lickert, and R. Klein. 2008. Genetic ablation of FLRT3 reveals a novel morphogenetic function for the anterior visceral endoderm in suppressing mesoderm differentiation. *Genes Dev.* 22:3349–62. doi:10.1101/gad.486708.
- Elias, G.M., L. Funke, V. Stein, S.G. Grant, D.S. Bredt, and R.A. Nicoll. 2006. Synapse-specific and developmentally regulated targeting of AMPA receptors by a family of MAGUK scaffolding proteins. *Neuron.* 52:307–20. doi:10.1016/j.neuron.2006.09.012.
- Elias, L.A.B., D.D. Wang, and A.R. Kriegstein. 2007. Gap junction adhesion is necessary for radial migration in the neocortex. *Nature.* 448:901–7. doi:10.1038/nature06063.
- Feng, G., R.H. Mellor, M. Bernstein, C. Keller-Peck, Q.T. Nguyen, M. Wallace, J.M. Nerbonne, J.W. Lichtman, and J.R. Sanes. 2000. Imaging Neuronal Subsets in Transgenic Mice Expressing Multiple Spectral Variants of GFP. *Neuron.* 28:41–51. doi:10.1016/S0896-6273(00)00084-2.
- Fietz, S.A., I. Kelava, J. Vogt, M. Wilsch-Bräuninger, D. Stenzel, J.L. Fish, D. Corbeil, A. Riehn, W. Distler, R. Nitsch, and W.B. Huttner. 2010. OSVZ progenitors of human and ferret neocortex are epithelial-like and expand by integrin signaling. *Nat. Neurosci.* 13:690–9. doi:10.1038/nn.2553.
- Fitzjohn, S.M., A.J. Doherty, and G.L. Collingridge. 2006. Promiscuous interactions between AMPA-Rs and MAGUKs. *Neuron.* 52:222–4. doi:10.1016/j.neuron.2006.10.002.
- Flintoff, K.A., Y. Arudchelvan, and S.-G. Gong. 2014. FLRT2 interacts with fibronectin in the ATDC5 chondroprogenitor cells. *J. Cell. Physiol.* 229:1538–47. doi:10.1002/jcp.24597.
- Fox, J.W., E.D. Lamperti, Y.Z. Ekşioğlu, S.E. Hong, Y. Feng, D.A. Graham, I.E. Scheffer, W.B. Dobyns, B.A. Hirsch, R.A. Radtke, S.F. Berkovic, P.R. Huttenlocher, and C.A. Walsh. 1998. Mutations in filamin 1 Prevent Migration of Cerebral Cortical Neurons in Human Periventricular Heterotopia. *Neuron.* 21:1315–1325. doi:10.1016/S0896-6273(00)80651-0.
- Franco, S.J., I. Martinez-Garay, C. Gil-Sanz, S.R. Harkins-Perry, and U. Müller. 2011. Reelin Regulates Cadherin Function via Dab1/Rap1 to Control Neuronal Migration and Lamination in the Neocortex. *Neuron.* 69:482–497.
- Fukata, Y., H. Adesnik, T. Iwanaga, D.S. Bredt, R.A. Nicoll, and M. Fukata. 2006. Epilepsy-related ligand/receptor complex LGI1 and ADAM22 regulate synaptic transmission. *Science.* 313:1792–5. doi:10.1126/science.1129947.
- Fukata, Y., K.L. Lovero, T. Iwanaga, A. Watanabe, N. Yokoi, K. Tabuchi, R. Shigemoto, R.A. Nicoll, and M. Fukata. 2010. Disruption of LGI1-linked synaptic complex causes

- abnormal synaptic transmission and epilepsy. *Proc. Natl. Acad. Sci. U. S. A.* 107:3799–804. doi:10.1073/pnas.0914537107.
- Gelman, D.M., and O. Marín. 2010. Generation of interneuron diversity in the mouse cerebral cortex. *Eur. J. Neurosci.* 31:2136–41. doi:10.1111/j.1460-9568.2010.07267.x.
- Giagtzoglou, N., C. V Ly, and H.J. Bellen. 2009. Cell adhesion, the backbone of the synapse: “vertebrate” and “invertebrate” perspectives. *Cold Spring Harb. Perspect. Biol.* 1:a003079. doi:10.1101/cshperspect.a003079.
- Gibson, J.R., K.M. Huber, and T.C. Südhof. 2009. Neuroligin-2 deletion selectively decreases inhibitory synaptic transmission originating from fast-spiking but not from somatostatin-positive interneurons. *J. Neurosci.* 29:13883–97. doi:10.1523/JNEUROSCI.2457-09.2009.
- Götz, M., and W.B. Huttner. 2005. The cell biology of neurogenesis. *Nat. Rev. Mol. Cell Biol.* 6:777–88. doi:10.1038/nrm1739.
- Graf, E.R., X. Zhang, S.-X. Jin, M.W. Linhoff, and A.M. Craig. 2004. Neurexins induce differentiation of GABA and glutamate postsynaptic specializations via neuroligins. *Cell.* 119:1013–26. doi:10.1016/j.cell.2004.11.035.
- Gregory, W., J. Edmondson, M. Hatten, and C. Mason. 1988. Cytology and neuron-glia apposition of migrating cerebellar granule cells in vitro. *J. Neurosci.* 8:1728–1738.
- Guasch, R.M., P. Scambler, G.E. Jones, and A.J. Ridley. 1998. RhoE Regulates Actin Cytoskeleton Organization and Cell Migration. *Mol. Cell. Biol.* 18:4761–4771.
- Haines, B.P., L.M. Wheldon, D. Summerbell, J.K. Heath, and P.W.J. Rigby. 2006. Regulated expression of FLRT genes implies a functional role in the regulation of FGF signalling during mouse development. *Dev. Biol.* 297:14–25. doi:10.1016/j.ydbio.2006.04.004.
- Hampel, F. 2012. Functional analysis of FLRT proteins in nervous system development.
- Hansen, D. V, J.H. Lui, P.R.L. Parker, and A.R. Kriegstein. 2010. Neurogenic radial glia in the outer subventricular zone of human neocortex. *Nature.* 464:554–561. doi:10.1038/nature08845.
- Heath, R.J.W., J.M. Leong, B. Visegrády, L.M. Machesky, and R.J. Xavier. 2011. Bacterial and host determinants of MAL activation upon EPEC infection: the roles of Tir, ABRA, and FLRT3. *PLoS Pathog.* 7:e1001332. doi:10.1371/journal.ppat.1001332.
- Heng, J.I.-T., L. Nguyen, D.S. Castro, C. Zimmer, H. Wildner, O. Armant, D. Skowronska-Krawczyk, F. Bedogni, J.-M. Matter, R. Hevner, and F. Guillemot. 2008. Neurogenin 2 controls cortical neuron migration through regulation of Rnd2. *Nature.* 455:114–8. doi:10.1038/nature07198.

- Hippenmeyer, S., Y.H. Youn, H.M. Moon, K. Miyamichi, H. Zong, A. Wynshaw-Boris, and L. Luo. 2010. Genetic mosaic dissection of *Lis1* and *Ndel1* in neuronal migration. *Neuron*. 68:695–709. doi:10.1016/j.neuron.2010.09.027.
- Hong, W., H. Zhu, C.J. Potter, G. Barsh, M. Kurusu, K. Zinn, and L. Luo. 2009. Leucine-rich repeat transmembrane proteins instruct discrete dendrite targeting in an olfactory map. *Nat. Neurosci.* 12:1542–50. doi:10.1038/nn.2442.
- Horton, S., A. Meredith, J.A. Richardson, and J.E. Johnson. 1999. Correct coordination of neuronal differentiation events in ventral forebrain requires the bHLH factor MASH1. *Mol. Cell. Neurosci.* 14:355–69. doi:10.1006/mcne.1999.0791.
- Hu, H., H. Tomasiewicz, T. Magnuson, and U. Rutishauser. 1996. The Role of Polysialic Acid in Migration of Olfactory Bulb Interneuron Precursors in the Subventricular Zone. *Neuron*. 16:735–743. doi:10.1016/S0896-6273(00)80094-X.
- Ippolito, D.M., and C. Eroglu. 2010. Quantifying synapses: an immunocytochemistry-based assay to quantify synapse number. *J. Vis. Exp.* e2270. doi:10.3791/2270.
- Islam, M., J. Gor, S.J. Perkins, Y. Ishikawa, H.P. Bachinger, and E. Hohenester. 2013. The Concave Face of Decorin Mediates Reversible Dimerization and Collagen Binding. *J. Biol. Chem.* 288:35526–35533. doi:10.1074/jbc.M113.504530.
- Jiménez, D., L.M. López-Mascaraque, F. Valverde, and J.A. De Carlos. 2002. Tangential migration in neocortical development. *Dev. Biol.* 244:155–69. doi:10.1006/dbio.2002.0586.
- Jossin, Y., and J.A. Cooper. 2011. Reelin, Rap1 and N-cadherin orient the migration of multipolar neurons in the developing neocortex. *Nat. Neurosci.* 14:697–703. doi:10.1038/nn.2816.
- Kaech, S., and G. Banker. 2006. Culturing hippocampal neurons. *Nat. Protoc.* 1:2406–15. doi:10.1038/nprot.2006.356.
- Kajava, A.V. 1998. Structural diversity of leucine-rich repeat proteins. *J. Mol. Biol.* 277:519–527. doi:10.1006/jmbi.1998.1643.
- Karaulanov, E., R.T. Böttcher, P. Stannek, W. Wu, M. Rau, S. Ogata, K.W.Y. Cho, and C. Niehrs. 2009. *Unc5B* interacts with *FLRT3* and *Rnd1* to modulate cell adhesion in *Xenopus* embryos. *PLoS One*. 4:e5742. doi:10.1371/journal.pone.0005742.
- Karaulanov, E.E., R.T. Böttcher, and C. Niehrs. 2006. A role for fibronectin-leucine-rich transmembrane cell-surface proteins in homotypic cell adhesion. *EMBO Rep.* 7:283–90. doi:10.1038/sj.embor.7400614.
- Karayannis, T., E. Au, J.C. Patel, I. Kruglikov, S. Markx, R. Delorme, D. Héron, D. Salomon, J. Glessner, S. Restituto, A. Gordon, L. Rodriguez-Murillo, N.C. Roy, J.A. Gogos, B. Rudy, M.E. Rice, M. Karayiorgou, H. Hakonarson, B. Keren, G. Huguet, T. Bourgeron,

- C. Hoeffler, R.W. Tsien, E. Peles, and G. Fishell. 2014. Cntnap4 differentially contributes to GABAergic and dopaminergic synaptic transmission. *Nature*. 511:236–240. doi:10.1038/nature13248.
- Kawauchi, T., K. Sekine, M. Shikanai, K. Chihama, K. Tomita, K. Kubo, K. Nakajima, Y. Nabeshima, and M. Hoshino. 2010. Rab GTPases-Dependent Endocytic Pathways Regulate Neuronal Migration and Maturation through N-Cadherin Trafficking. *Neuron*. 67:588–602.
- Kim, J., S.-Y. Jung, Y.K. Lee, S. Park, J.-S. Choi, C.J. Lee, H.-S. Kim, Y.-B. Choi, P. Scheiffele, C.H. Bailey, E.R. Kandel, and J.-H. Kim. 2008. Neuroligin-1 is required for normal expression of LTP and associative fear memory in the amygdala of adult animals. *Proc. Natl. Acad. Sci. U. S. A.* 105:9087–92. doi:10.1073/pnas.0803448105.
- Kim, S., A. Burette, H.S. Chung, S.-K. Kwon, J. Woo, H.W. Lee, K. Kim, H. Kim, R.J. Weinberg, and E. Kim. 2006. NGL family PSD-95-interacting adhesion molecules regulate excitatory synapse formation. *Nat. Neurosci.* 9:1294–301. doi:10.1038/nn1763.
- Klein, R., and A. Kania. 2014. Ephrin signalling in the developing nervous system. *Curr. Opin. Neurobiol.* 27:16–24. doi:10.1016/j.conb.2014.02.006.
- Ko, J., M. V Fuccillo, R.C. Malenka, and T.C. Südhof. 2009. LRRTM2 functions as a neurexin ligand in promoting excitatory synapse formation. *Neuron*. 64:791–8. doi:10.1016/j.neuron.2009.12.012.
- Ko, J., S. Kim, H.S. Chung, K. Kim, K. Han, H. Kim, H. Jun, B.-K. Kaang, and E. Kim. 2006. SALM synaptic cell adhesion-like molecules regulate the differentiation of excitatory synapses. *Neuron*. 50:233–45. doi:10.1016/j.neuron.2006.04.005.
- Kobe, B. 2001. The leucine-rich repeat as a protein recognition motif. *Curr. Opin. Struct. Biol.* 11:725–732. doi:10.1016/S0959-440X(01)00266-4.
- Kobe, B., and J. Deisenhofer. 1993. Crystal structure of porcine ribonuclease inhibitor, a protein with leucine-rich repeats. *Nature*. 366:751–756. doi:10.1038/366751a0.
- Kobe, B., and J. Deisenhofer. 1994. The leucine-rich repeat: a versatile binding motif. *Trends Biochem. Sci.* 19:415–421. doi:10.1016/0968-0004(94)90090-6.
- Kobe, B., and J. Deisenhofer. 1995. Proteins with leucine-rich repeats. *Curr. Opin. Struct. Biol.* 5:409–416. doi:10.1016/0959-440X(95)80105-7.
- Krause, M., E.W. Dent, J.E. Bear, J.J. Loureiro, and F.B. Gertler. 2003. Ena/VASP proteins: regulators of the actin cytoskeleton and cell migration. *Annu. Rev. Cell Dev. Biol.* 19:541–64. doi:10.1146/annurev.cellbio.19.050103.103356.

- Kurusu, M., A. Cording, M. Taniguchi, K. Menon, E. Suzuki, and K. Zinn. 2008. A screen of cell-surface molecules identifies leucine-rich repeat proteins as key mediators of synaptic target selection. *Neuron*. 59:972–85. doi:10.1016/j.neuron.2008.07.037.
- Kwon, H.-B., Y. Kozorovitskiy, W.-J. Oh, R.T. Peixoto, N. Akhtar, J.L. Saulnier, C. Gu, and B.L. Sabatini. 2012. Neuroligin-1-dependent competition regulates cortical synaptogenesis and synapse number. *Nat. Neurosci.* 15:1667–1674. doi:10.1038/nn.3256.
- Lacy, S.E., C.G. Bönnemann, E.A. Buzney, and L.M. Kunkel. 1999. Identification of FLRT1, FLRT2, and FLRT3: a novel family of transmembrane leucine-rich repeat proteins. *Genomics*. 62:417–26. doi:10.1006/geno.1999.6033.
- Lee, X., Z. Yang, Z. Shao, S.S. Rosenberg, M. Levesque, R.B. Pepinsky, M. Qiu, R.H. Miller, J.R. Chan, and S. Mi. 2007. NGF regulates the expression of axonal LINGO-1 to inhibit oligodendrocyte differentiation and myelination. *J. Neurosci.* 27:220–5. doi:10.1523/JNEUROSCI.4175-06.2007.
- Lein, E.S., M.J. Hawrylycz, N. Ao, M. Ayres, A. Bensinger, A. Bernard, A.F. Boe, M.S. Boguski, K.S. Brockway, E.J. Byrnes, L. Chen, L. Chen, T.-M. Chen, M.C. Chin, J. Chong, B.E. Crook, A. Czaplinska, C.N. Dang, S. Datta, N.R. Dee, A.L. Desaki, T. Desta, E. Diep, T.A. Dolbeare, M.J. Donelan, H.-W. Dong, J.G. Dougherty, B.J. Duncan, A.J. Ebbert, G. Eichele, L.K. Estin, C. Faber, B.A. Facer, R. Fields, S.R. Fischer, T.P. Fliiss, C. Frensley, S.N. Gates, K.J. Glattfelder, K.R. Halverson, M.R. Hart, J.G. Hohmann, M.P. Howell, D.P. Jeung, R.A. Johnson, P.T. Karr, R. Kawal, J.M. Kidney, R.H. Knapik, C.L. Kuan, J.H. Lake, A.R. Laramée, K.D. Larsen, C. Lau, T.A. Lemon, A.J. Liang, Y. Liu, L.T. Luong, J. Michaels, J.J. Morgan, R.J. Morgan, M.T. Mortrud, N.F. Mosqueda, L.L. Ng, R. Ng, G.J. Orta, C.C. Overly, T.H. Pak, S.E. Parry, S.D. Pathak, O.C. Pearson, R.B. Puchalski, Z.L. Riley, H.R. Rockett, S.A. Rowland, J.J. Royall, M.J. Ruiz, N.R. Sarno, K. Schaffnit, N. V Shapovalova, T. Sivasay, C.R. Slaughterbeck, S.C. Smith, K.A. Smith, B.I. Smith, A.J. Sodt, N.N. Stewart, K.-R. Stumpf, S.M. Sunkin, M. Sutram, A. Tam, C.D. Teemer, C. Thaller, C.L. Thompson, L.R. Varnam, A. Visel, R.M. Whitlock, P.E. Wohnoutka, et al. 2007. Genome-wide atlas of gene expression in the adult mouse brain. *Nature*. 445:168–76. doi:10.1038/nature05453.
- Letinic, K., R. Zoncu, and P. Rakic. 2002. Origin of GABAergic neurons in the human neocortex. *Nature*. 417:645–9. doi:10.1038/nature00779.
- Leyva-Díaz, E., D. del Toro, M.J. Menal, S. Cambray, R. Susín, M. Tessier-Lavigne, R. Klein, J. Egea, and G. López-Bendito. 2014. FLRT3 is a Robo1-interacting protein that determines Netrin-1 attraction in developing axons. *Curr. Biol.* 24:494–508. doi:10.1016/j.cub.2014.01.042.
- Li, Y., H. Lu, P. Cheng, S. Ge, H. Xu, S.-H. Shi, and Y. Dan. 2012. Clonally related visual cortical neurons show similar stimulus feature selectivity. *Nature*. 486:118–21. doi:10.1038/nature11110.

- Linhoff, M.W., J. Laurén, R.M. Cassidy, F.A. Dobie, H. Takahashi, H.B. Nygaard, M.S. Airaksinen, S.M. Strittmatter, and A.M. Craig. 2009. An unbiased expression screen for synaptogenic proteins identifies the LRRTM protein family as synaptic organizers. *Neuron*. 61:734–49. doi:10.1016/j.neuron.2009.01.017.
- Llambi, F., F. Causeret, E. Bloch-Gallego, and P. Mehlen. 2001. Netrin-1 acts as a survival factor via its receptors UNC5H and DCC. *EMBO J*. 20:2715–22. doi:10.1093/emboj/20.11.2715.
- López-Bendito, G., and Z. Molnár. 2003. Thalamocortical development: how are we going to get there? *Nat. Rev. Neurosci*. 4:276–89. doi:10.1038/nrn1075.
- LoTurco, J.J., and J. Bai. 2006. The multipolar stage and disruptions in neuronal migration. *Trends Neurosci*. 29:407–13. doi:10.1016/j.tins.2006.05.006.
- Luo, L. 2000. Rho GTPases in neuronal morphogenesis. *Nat. Rev. Neurosci*. 1:173–80. doi:10.1038/35044547.
- Madigan, J., B. Bodemann, D. Brady, B. Dewar, P. Keller, M. Leitges, M. Philips, A. Ridley, C. Der, and A. Cox. 2009. Regulation of Rnd3 localization and function by protein kinase Calpha-mediated phosphorylation.
- Mah, W., J. Ko, J. Nam, K. Han, W.S. Chung, and E. Kim. 2010. Selected SALM (synaptic adhesion-like molecule) family proteins regulate synapse formation. *J. Neurosci*. 30:5559–68. doi:10.1523/JNEUROSCI.4839-09.2010.
- Malatesta, P., M.A. Hack, E. Hartfuss, H. Kettenmann, W. Klinkert, F. Kirchhoff, and M. Götz. 2003. Neuronal or Glial Progeny Regional Differences in Radial Glia Fate. *Neuron*. 37:751–764. doi:10.1016/S0896-6273(03)00116-8.
- Maretto, S., P.-S. Müller, A.R. Aricescu, K.W.Y. Cho, E.K. Bikoff, and E.J. Robertson. 2008. Ventral closure, headfold fusion and definitive endoderm migration defects in mouse embryos lacking the fibronectin leucine-rich transmembrane protein FLRT3. *Dev. Biol*. 318:184–93. doi:10.1016/j.ydbio.2008.03.021.
- Martin, S., C. Söllner, V. Charoensawan, B. Adryan, B. Thisse, C. Thisse, S. Teichmann, and G.J. Wright. 2010. Construction of a large extracellular protein interaction network and its resolution by spatiotemporal expression profiling. *Mol. Cell. Proteomics*. 9:2654–65. doi:10.1074/mcp.M110.004119.
- Mi, S., X. Lee, Z. Shao, G. Thill, B. Ji, J. Relton, M. Levesque, N. Allaire, S. Perrin, B. Sands, T. Crowell, R.L. Cate, J.M. McCoy, and R.B. Pepinsky. 2004. LINGO-1 is a component of the Nogo-66 receptor/p75 signaling complex. *Nat. Neurosci*. 7:221–8. doi:10.1038/nn1188.
- Mi, S., R.H. Miller, X. Lee, M.L. Scott, S. Shulag-Morskaya, Z. Shao, J. Chang, G. Thill, M. Levesque, M. Zhang, C. Hession, D. Sah, B. Trapp, Z. He, V. Jung, J.M. McCoy, and

- R.B. Pepinsky. 2005. LINGO-1 negatively regulates myelination by oligodendrocytes. *Nat. Neurosci.* 8:745–51. doi:10.1038/nn1460.
- Mishra, A., B. Knerr, S. Paixão, E.R. Kramer, and R. Klein. 2008. The protein dendrite arborization and synapse maturation 1 (Dasm-1) is dispensable for dendrite arborization. *Mol. Cell. Biol.* 28:2782–91. doi:10.1128/MCB.02102-07.
- Miyata, T., A. Kawaguchi, H. Okano, and M. Ogawa. 2001. Asymmetric Inheritance of Radial Glial Fibers by Cortical Neurons. *Neuron.* 31:727–741. doi:10.1016/S0896-6273(01)00420-2.
- Miyata, T., A. Kawaguchi, K. Saito, M. Kawano, T. Muto, and M. Ogawa. 2004. Asymmetric production of surface-dividing and non-surface-dividing cortical progenitor cells. *Development.* 131:3133–45. doi:10.1242/dev.01173.
- Miyoshi, G., and G. Fishell. 2012. Dynamic FoxG1 expression coordinates the integration of multipolar pyramidal neuron precursors into the cortical plate. *Neuron.* 74:1045–58. doi:10.1016/j.neuron.2012.04.025.
- Molyneaux, B.J., P. Arlotta, J.R.L. Menezes, and J.D. Macklis. 2007. Neuronal subtype specification in the cerebral cortex. *Nat. Rev. Neurosci.* 8:427–37. doi:10.1038/nrn2151.
- Müller, P.-S., R. Schulz, S. Maretto, I. Costello, S. Srinivas, E. Bikoff, and E. Robertson. 2011. The fibronectin leucine-rich repeat transmembrane protein Flrt2 is required in the epicardium to promote heart morphogenesis. *Development.* 138:1297–308. doi:10.1242/dev.059386.
- Nadarajah, B., J.E. Brunstrom, J. Grutzendler, R.O. Wong, and A.L. Pearlman. 2001. Two modes of radial migration in early development of the cerebral cortex. *Nat. Neurosci.* 4:143–50. doi:10.1038/83967.
- Nagano, T., S. Morikubo, and M. Sato. 2004. Filamin A and FILIP (Filamin A-Interacting Protein) regulate cell polarity and motility in neocortical subventricular and intermediate zones during radial migration. *J. Neurosci.* 24:9648–57. doi:10.1523/JNEUROSCI.2363-04.2004.
- Nieto, M., E.S. Monuki, H. Tang, J. Imitola, N. Haubst, S.J. Khoury, J. Cunningham, M. Gotz, and C.A. Walsh. 2004. Expression of Cux-1 and Cux-2 in the subventricular zone and upper layers II-IV of the cerebral cortex. *J. Comp. Neurol.* 479:168–80. doi:10.1002/cne.20322.
- Nobes, C.D. 1998. A New Member of the Rho Family, Rnd1, Promotes Disassembly of Actin Filament Structures and Loss of Cell Adhesion. *J. Cell Biol.* 141:187–197. doi:10.1083/jcb.141.1.187.

- Noctor, S.C., V. Martínez-Cerdeño, L. Ivic, and A.R. Kriegstein. 2004. Cortical neurons arise in symmetric and asymmetric division zones and migrate through specific phases. *Nat. Neurosci.* 7:136–44. doi:10.1038/nn1172.
- Nuriya, M., and R.L. Huganir. 2006. Regulation of AMPA receptor trafficking by N-cadherin. *J. Neurochem.* 97:652–61. doi:10.1111/j.1471-4159.2006.03740.x.
- O'Brien, R., D. Xu, R. Petralia, O. Steward, R. Huganir, and P. Worley. 1999. Synaptic Clustering of AMPA Receptors by the Extracellular Immediate-Early Gene Product Narp. *Neuron.* 23:309–323. doi:10.1016/S0896-6273(00)80782-5.
- O'Rourke, N., D. Sullivan, C. Kaznowski, A. Jacobs, and S. McConnell. 1995. Tangential migration of neurons in the developing cerebral cortex. *Development.* 121:2165–2176.
- O'Sullivan, M.L., J. de Wit, J.N. Savas, D. Comoletti, S. Otto-Hitt, J.R. Yates, and A. Ghosh. 2012. FLRT Proteins Are Endogenous Latrophilin Ligands and Regulate Excitatory Synapse Development. *Neuron.* 73:903–910. doi:10.1016/j.neuron.2012.01.018.
- O'Sullivan, M.L., F. Martini, S. von Daake, D. Comoletti, and A. Ghosh. 2014. LPHN3, a presynaptic adhesion-GPCR implicated in ADHD, regulates the strength of neocortical layer 2/3 synaptic input to layer 5. *Neural Dev.* 9:7. doi:10.1186/1749-8104-9-7.
- Ogata, S., J. Morokuma, T. Hayata, G. Kolle, C. Niehrs, N. Ueno, and K.W.Y. Cho. 2007. TGF-beta signaling-mediated morphogenesis: modulation of cell adhesion via cadherin endocytosis. *Genes Dev.* 21:1817–31. doi:10.1101/gad.1541807.
- Ohtsuki, G., M. Nishiyama, T. Yoshida, T. Murakami, M. Histed, C. Lois, and K. Ohki. 2012. Similarity of visual selectivity among clonally related neurons in visual cortex. *Neuron.* 75:65–72. doi:10.1016/j.neuron.2012.05.023.
- Oinuma, I., Y. Ishikawa, H. Katoh, and M. Negishi. 2004. The Semaphorin 4D receptor Plexin-B1 is a GTPase activating protein for R-Ras. *Science.* 305:862–5. doi:10.1126/science.1097545.
- Ozkaynak, E., G. Abello, M. Jaegle, L. van Berge, D. Hamer, L. Kegel, S. Driegen, K. Sagane, J.R. Bermingham, and D. Meijer. 2010. Adam22 is a major neuronal receptor for Lgi4-mediated Schwann cell signaling. *J. Neurosci.* 30:3857–64. doi:10.1523/JNEUROSCI.6287-09.2010.
- Pacary, E., J. Heng, R. Azzarelli, P. Riou, D. Castro, M. Lebel-Potter, C. Parras, D.M. Bell, A.J. Ridley, M. Parsons, and F. Guillemot. 2011a. Proneural Transcription Factors Regulate Different Steps of Cortical Neuron Migration through Rnd-Mediated Inhibition of RhoA Signaling. *Neuron.* 69:1069–1084.
- Pacary, E., J. Heng, R. Azzarelli, P. Riou, D. Castro, M. Lebel-Potter, C. Parras, D.M. Bell, A.J. Ridley, M. Parsons, and F. Guillemot. 2011b. Proneural transcription factors

- regulate different steps of cortical neuron migration through Rnd-mediated inhibition of RhoA signaling. *Neuron*. 69:1069–84. doi:10.1016/j.neuron.2011.02.018.
- Passafaro, M., T. Nakagawa, C. Sala, and M. Sheng. 2003. Induction of dendritic spines by an extracellular domain of AMPA receptor subunit GluR2. *Nature*. 424:677–81. doi:10.1038/nature01781.
- Pasterkamp, R.J. 2012. Getting neural circuits into shape with semaphorins. *Nat. Rev. Neurosci.* 13:605–18. doi:10.1038/nrn3302.
- Pérez-Otaño, I., R. Luján, S.J. Tavalin, M. Plomann, J. Modregger, X.-B. Liu, E.G. Jones, S.F. Heinemann, D.C. Lo, and M.D. Ehlers. 2006. Endocytosis and synaptic removal of NR3A-containing NMDA receptors by PACSIN1/syndapin1. *Nat. Neurosci.* 9:611–21. doi:10.1038/nn1680.
- Pinto Lord, M.C., and V.S. Caviness. 1979. Determinants of cell shape and orientation: a comparative Golgi analysis of cell-axon interrelationships in the developing neocortex of normal and reeler mice. *J. Comp. Neurol.* 187:49–69. doi:10.1002/cne.901870104.
- Poulopoulos, A., G. Aramuni, G. Meyer, T. Soykan, M. Hoon, T. Papadopoulos, M. Zhang, I. Paarmann, C. Fuchs, K. Harvey, P. Jedlicka, S.W. Schwarzacher, H. Betz, R.J. Harvey, N. Brose, W. Zhang, and F. Varoqueaux. 2009. Neuroligin 2 drives postsynaptic assembly at perisomatic inhibitory synapses through gephyrin and collybistin. *Neuron*. 63:628–42. doi:10.1016/j.neuron.2009.08.023.
- Rakic, P. 1971. Neuron-glia relationship during granule cell migration in developing cerebellar cortex. A Golgi and electronmicroscopic study in Macacus Rhesus. *J. Comp. Neurol.* 141:283–312. doi:10.1002/cne.901410303.
- Rakic, P. 1972. Mode of cell migration to the superficial layers of fetal monkey neocortex. *J. Comp. Neurol.* 145:61–83. doi:10.1002/cne.901450105.
- Rakic, P. 1974. Neurons in Rhesus Monkey Visual Cortex: Systematic Relation between Time of Origin and Eventual Disposition. *Science (80-)*. 183:425–427. doi:10.1126/science.183.4123.425.
- Rakic, P. 1988. Specification of cerebral cortical areas. *Science (80-)*. 241:170–176. doi:10.1126/science.3291116.
- Rakic, P. 2007. The radial edifice of cortical architecture: from neuronal silhouettes to genetic engineering. *Brain Res. Rev.* 55:204–19. doi:10.1016/j.brainresrev.2007.02.010.
- Reillo, I., C. de Juan Romero, M.Á. García-Cabezas, and V. Borrell. 2011. A role for intermediate radial glia in the tangential expansion of the mammalian cerebral cortex. *Cereb. Cortex*. 21:1674–94. doi:10.1093/cercor/bhq238.

- Riento, K., N. Totty, P. Villalonga, R. Garg, R. Guasch, and A.J. Ridley. 2005. RhoE function is regulated by ROCK I-mediated phosphorylation. *EMBO J.* 24:1170–80. doi:10.1038/sj.emboj.7600612.
- Ringstedt, T., S. Linnarsson, J. Wagner, U. Lendahl, Z. Kokaia, E. Arenas, P. Ernfors, and C.F. Ibáñez. 1998. BDNF Regulates Reelin Expression and Cajal-Retzius Cell Development in the Cerebral Cortex. *Neuron.* 21:305–315. doi:10.1016/S0896-6273(00)80540-1.
- Rivas, R., and M. Hatten. 1995. Motility and cytoskeletal organization of migrating cerebellar granule neurons. *J. Neurosci.* 15:981–989.
- Robinson, M., M.C. Parsons Perez, L. Tébar, J. Palmer, A. Patel, D. Marks, A. Sheasby, C. De Felipe, R. Coffin, F.J. Livesey, and S.P. Hunt. 2004. FLRT3 is expressed in sensory neurons after peripheral nerve injury and regulates neurite outgrowth. *Mol. Cell. Neurosci.* 27:202–14. doi:10.1016/j.mcn.2004.06.008.
- Rubio-Garrido, P., F. Pérez-de-Manzo, C. Porrero, M.J. Galazo, and F. Clascá. 2009. Thalamic input to distal apical dendrites in neocortical layer 1 is massive and highly convergent. *Cereb. Cortex.* 19:2380–95. doi:10.1093/cercor/bhn259.
- Saglietti, L., C. Dequidt, K. Kamieniarz, M.-C. Rousset, P. Valnegri, O. Thoumine, F. Beretta, L. Fagni, D. Choquet, C. Sala, M. Sheng, and M. Passafaro. 2007. Extracellular interactions between GluR2 and N-cadherin in spine regulation. *Neuron.* 54:461–77. doi:10.1016/j.neuron.2007.04.012.
- Saito, T., and N. Nakatsuji. 2001. Efficient gene transfer into the embryonic mouse brain using in vivo electroporation. *Dev. Biol.* 240:237–46. doi:10.1006/dbio.2001.0439.
- Sara, Y., T. Biederer, D. Atasoy, A. Chubykin, M.G. Mozhayeva, T.C. Südhof, and E.T. Kavalali. 2005. Selective capability of SynCAM and neuroligin for functional synapse assembly. *J. Neurosci.* 25:260–70. doi:10.1523/JNEUROSCI.3165-04.2005.
- Scheiffele, P. 2003. Cell-cell signaling during synapse formation in the CNS. *Annu. Rev. Neurosci.* 26:485–508. doi:10.1146/annurev.neuro.26.043002.094940.
- Scheiffele, P., J. Fan, J. Choih, R. Fetter, and T. Serafini. 2000. Neuroligin Expressed in Nonneuronal Cells Triggers Presynaptic Development in Contacting Axons. *Cell.* 101:657–669. doi:10.1016/S0092-8674(00)80877-6.
- Schlessinger, A.R., W.M. Cowan, and D.I. Gottlieb. 1975. An autoradiographic study of the time of origin and the pattern of granule cell migration in the dentate gyrus of the rat. *J. Comp. Neurol.* 159:149–75. doi:10.1002/cne.901590202.
- Schoch, S., P.E. Castillo, T. Jo, K. Mukherjee, M. Geppert, Y. Wang, F. Schmitz, R.C. Malenka, and T.C. Südhof. 2002. RIM1alpha forms a protein scaffold for regulating neurotransmitter release at the active zone. *Nature.* 415:321–6. doi:10.1038/415321a.

- Schulte, U., J.-O. Thumfart, N. Klöcker, C.A. Sailer, W. Bildl, M. Biniossek, D. Dehn, T. Deller, S. Eble, K. Abbass, T. Wangler, H.-G. Knaus, and B. Fakler. 2006. The epilepsy-linked Lgi1 protein assembles into presynaptic Kv1 channels and inhibits inactivation by Kvbeta1. *Neuron*. 49:697–706. doi:10.1016/j.neuron.2006.01.033.
- Scott, P.G., P.A. McEwan, C.M. Dodd, E.M. Bergmann, P.N. Bishop, and J. Bella. 2004. Crystal structure of the dimeric protein core of decorin, the archetypal small leucine-rich repeat proteoglycan. *Proc. Natl. Acad. Sci. U. S. A.* 101:15633–8. doi:10.1073/pnas.0402976101.
- Seeger, M., G. Tear, D. Ferres-Marco, and C.S. Goodman. 1993. Mutations affecting growth cone guidance in drosophila: Genes necessary for guidance toward or away from the midline. *Neuron*. 10:409–426. doi:10.1016/0896-6273(93)90330-T.
- Seiradake, E., C.H. Coles, P. V Perestenko, K. Harlos, R.A.J. McIlhinney, A.R. Aricescu, and E.Y. Jones. 2011. Structural basis for cell surface patterning through NetrinG-NGL interactions. *EMBO J.* 30:4479–88. doi:10.1038/emboj.2011.346.
- Seiradake, E., K. Harlos, G. Sutton, A.R. Aricescu, and E.Y. Jones. 2010. An extracellular steric seeding mechanism for Eph-ephrin signaling platform assembly. *Nat. Struct. Mol. Biol.* 17:398–402. doi:10.1038/nsmb.1782.
- Shen, K., and P. Scheiffele. 2010. Genetics and cell biology of building specific synaptic connectivity. *Annu. Rev. Neurosci.* 33:473–507. doi:10.1146/annurev.neuro.051508.135302.
- Sheng, M., and C. Sala. 2001. PDZ domains and the organization of supramolecular complexes. *Annu. Rev. Neurosci.* 24:1–29. doi:10.1146/annurev.neuro.24.1.1.
- Shieh, J.C., B.T. Schaar, K. Srinivasan, F.M. Brodsky, and S.K. McConnell. 2011. Endocytosis regulates cell soma translocation and the distribution of adhesion proteins in migrating neurons. *PLoS One*. 6:e17802. doi:10.1371/journal.pone.0017802.
- Shikanai, M., K. Nakajima, and T. Kawauchi. 2011. N-cadherin regulates radial glial fiber-dependent migration of cortical locomoting neurons. *Commun. Integr. Biol.* 4:326–30. doi:10.4161/cib.4.3.14886.
- Shinza-Kameda, M., E. Takasu, K. Sakurai, S. Hayashi, and A. Nose. 2006. Regulation of layer-specific targeting by reciprocal expression of a cell adhesion molecule, capricious. *Neuron*. 49:205–13. doi:10.1016/j.neuron.2005.11.013.
- Shishido, E. 1998. Drosophila Synapse Formation: Regulation by Transmembrane Protein with Leu-Rich Repeats, CAPRICIOUS. *Science (80-)*. 280:2118–2121. doi:10.1126/science.280.5372.2118.
- Sia, G.-M., J.-C. Béïque, G. Rumbaugh, R. Cho, P.F. Worley, and R.L. Huganir. 2007. Interaction of the N-terminal domain of the AMPA receptor GluR4 subunit with the

- neuronal pentraxin NP1 mediates GluR4 synaptic recruitment. *Neuron*. 55:87–102. doi:10.1016/j.neuron.2007.06.020.
- Siddiqui, T.J., and A.M. Craig. 2011. Synaptic organizing complexes. *Curr. Opin. Neurobiol.* 21:132–43. doi:10.1016/j.conb.2010.08.016.
- Siddiqui, T.J., R. Pancaroglu, Y. Kang, A. Rooyakkers, and A.M. Craig. 2010. LRRTMs and neuroligins bind neurexins with a differential code to cooperate in glutamate synapse development. *J. Neurosci.* 30:7495–506. doi:10.1523/JNEUROSCI.0470-10.2010.
- Silva, J.-P., and Y.A. Ushkaryov. 2010. The latrophilins, “split-personality” receptors. *Adv. Exp. Med. Biol.* 706:59–75.
- Smart, I.H. 1973. Proliferative characteristics of the ependymal layer during the early development of the mouse neocortex: a pilot study based on recording the number, location and plane of cleavage of mitotic figures. *J. Anat.* 116:67–91.
- Smart, I.H.M. 2002. Unique Morphological Features of the Proliferative Zones and Postmitotic Compartments of the Neural Epithelium Giving Rise to Striate and Extrastriate Cortex in the Monkey. *Cereb. Cortex.* 12:37–53. doi:10.1093/cercor/12.1.37.
- Solecki, D.J. 2012. Sticky situations: recent advances in control of cell adhesion during neuronal migration. *Curr. Opin. Neurobiol.* 22:791–8. doi:10.1016/j.conb.2012.04.010.
- Söllner, C., and G.J. Wright. 2009. A cell surface interaction network of neural leucine-rich repeat receptors. *Genome Biol.* 10:R99. doi:10.1186/gb-2009-10-9-r99.
- Sperry, R.W. 1963. CHEMOAFFINITY IN THE ORDERLY GROWTH OF NERVE FIBER PATTERNS AND CONNECTIONS. *Proc. Natl. Acad. Sci. U. S. A.* 50:703–10.
- Stipursky, J., T.C.L. de S.E. Spohr, V.O. Sousa, and F.C.A. Gomes. 2012. Neuron-astroglial interactions in cell-fate commitment and maturation in the central nervous system. *Neurochem. Res.* 37:2402–18. doi:10.1007/s11064-012-0798-x.
- Tabata, H., and K. Nakajima. 2001. Efficient in utero gene transfer system to the developing mouse brain using electroporation: visualization of neuronal migration in the developing cortex. *Neuroscience.* 103:865–872. doi:10.1016/S0306-4522(01)00016-1.
- Tabata, H., and K. Nakajima. 2003. Multipolar Migration: The Third Mode of Radial Neuronal Migration in the Developing Cerebral Cortex. *J. Neurosci.* 23:9996–10001.
- Takemoto, M., Y. Hattori, H. Zhao, H. Sato, A. Tamada, S. Sasaki, K. Nakajima, and N. Yamamoto. 2011. Laminar and areal expression of unc5d and its role in cortical cell survival. *Cereb. Cortex.* 21:1925–34. doi:10.1093/cercor/bhq265.

- Tan, S.S., and S. Breen. 1993. Radial mosaicism and tangential cell dispersion both contribute to mouse neocortical development. *Nature*. 362:638–40. doi:10.1038/362638a0.
- Tanabe, K., I. Bonilla, J.A. Winkles, and S.M. Strittmatter. 2003. Fibroblast Growth Factor-Inducible-14 Is Induced in Axotomized Neurons and Promotes Neurite Outgrowth. *J. Neurosci.* 23:9675–9686.
- Tanaka, D., Y. Nakaya, Y. Yanagawa, K. Obata, and F. Murakami. 2003. Multimodal tangential migration of neocortical GABAergic neurons independent of GPI-anchored proteins. *Development*. 130:5803–13. doi:10.1242/dev.00825.
- Tanikawa, C., K. Matsuda, S. Fukuda, Y. Nakamura, and H. Arakawa. 2003. p53RDL1 regulates p53-dependent apoptosis. *Nat. Cell Biol.* 5:216–23. doi:10.1038/ncb943.
- Tomás, A.R., A.C. Certal, and J. Rodríguez-León. 2011. FLRT3 as a key player on chick limb development. *Dev. Biol.* 355:324–33. doi:10.1016/j.ydbio.2011.04.031.
- Torii, M., K. Hashimoto-Torii, P. Levitt, and P. Rakic. 2009. Integration of neuronal clones in the radial cortical columns by EphA and ephrin-A signalling. *Nature*. 461:524–8. doi:10.1038/nature08362.
- Tronche, F., C. Kellendonk, O. Kretz, P. Gass, K. Anlag, P.C. Orban, R. Bock, R. Klein, and G. Schütz. 1999. Disruption of the glucocorticoid receptor gene in the nervous system results in reduced anxiety. *Nat. Genet.* 23:99–103. doi:10.1038/12703.
- Tsai, J.-W., Y. Chen, A.R. Kriegstein, and R.B. Vallee. 2005. LIS1 RNA interference blocks neural stem cell division, morphogenesis, and motility at multiple stages. *J. Cell Biol.* 170:935–45. doi:10.1083/jcb.200505166.
- Tsuji, L., T. Yamashita, T. Kubo, T. Madura, H. Tanaka, K. Hosokawa, and M. Tohyama. 2004. FLRT3, a cell surface molecule containing LRR repeats and a FNIII domain, promotes neurite outgrowth. *Biochem. Biophys. Res. Commun.* 313:1086–91.
- Umemori, H., and J.R. Sanes. 2008. Signal regulatory proteins (SIRPS) are secreted presynaptic organizing molecules. *J. Biol. Chem.* 283:34053–61. doi:10.1074/jbc.M805729200.
- Varoqueaux, F., G. Aramuni, R.L. Rawson, R. Mohrmann, M. Missler, K. Gottmann, W. Zhang, T.C. Südhof, and N. Brose. 2006. Neuroligins determine synapse maturation and function. *Neuron*. 51:741–54. doi:10.1016/j.neuron.2006.09.003.
- Wei, K., Y. Xu, H. Tse, M.F. Manolson, and S.-G. Gong. 2011. Mouse FLRT 2 Interacts with the Extracellular and Intracellular Regions of FGFR2. *J. Dent. Res.* doi:10.1177/0022034511415272.
- Wheldon, L.M., B.P. Haines, R. Rajappa, I. Mason, P.W. Rigby, and J.K. Heath. 2010. Critical role of FLRT1 phosphorylation in the interdependent regulation of FLRT1

- function and FGF receptor signalling. *PLoS One*. 5:e10264. doi:10.1371/journal.pone.0010264.
- Whitford, K.L., V. Marillat, E. Stein, C.S. Goodman, M. Tessier-Lavigne, A. Chédotal, and A. Ghosh. 2002. Regulation of Cortical Dendrite Development by Slit-Robo Interactions. *Neuron*. 33:47–61. doi:10.1016/S0896-6273(01)00566-9.
- Wichterle, H., D.H. Turnbull, S. Nery, G. Fishell, and A. Alvarez-Buylla. 2001. In utero fate mapping reveals distinct migratory pathways and fates of neurons born in the mammalian basal forebrain. *Development*. 128:3759–3771.
- Williams, M.E., P. Strickland, K. Watanabe, and L. Hinck. 2003. UNC5H1 induces apoptosis via its juxtamembrane region through an interaction with NRAGE. *J. Biol. Chem*. 278:17483–90. doi:10.1074/jbc.M300415200.
- Wilson, P.M., R.H. Fryer, Y. Fang, and M.E. Hatten. 2010. Astn2, a novel member of the astrotactin gene family, regulates the trafficking of ASTN1 during glial-guided neuronal migration. *J. Neurosci*. 30:8529–40. doi:10.1523/JNEUROSCI.0032-10.2010.
- De Wit, J., W. Hong, L. Luo, and A. Ghosh. 2011. Role of leucine-rich repeat proteins in the development and function of neural circuits. *Annu. Rev. Cell Dev. Biol*. 27:697–729. doi:10.1146/annurev-cellbio-092910-154111.
- De Wit, J., M.L. O’Sullivan, J.N. Savas, G. Condomitti, M.C. Caccese, K.M. Vennekens, J.R. Yates, and A. Ghosh. 2013. Unbiased Discovery of Glypican as a Receptor for LRRTM4 in Regulating Excitatory Synapse Development. *Neuron*. null. doi:10.1016/j.neuron.2013.06.049.
- De Wit, J., E. Sylwestrak, M.L. O’Sullivan, S. Otto, K. Tiglio, J.N. Savas, J.R. Yates, D. Comoletti, P. Taylor, and A. Ghosh. 2009. LRRTM2 interacts with Neurexin1 and regulates excitatory synapse formation. *Neuron*. 64:799–806. doi:10.1016/j.neuron.2009.12.019.
- Woo, J., S.-K. Kwon, S. Choi, S. Kim, J.-R. Lee, A.W. Dunah, M. Sheng, and E. Kim. 2009. Trans-synaptic adhesion between NGL-3 and LAR regulates the formation of excitatory synapses. *Nat. Neurosci*. 12:428–37. doi:10.1038/nn.2279.
- Yamagata, M., J.R. Sanes, and J.A. Weiner. 2003. Synaptic adhesion molecules. *Curr. Opin. Cell Biol*. 15:621–632. doi:10.1016/S0955-0674(03)00107-8.
- Yamagishi, S., F. Hampel, K. Hata, D. Del Toro, M. Schwark, E. Kvachnina, M. Bastmeyer, T. Yamashita, V. Tarabykin, R. Klein, and J. Egea. 2011. FLRT2 and FLRT3 act as repulsive guidance cues for Unc5-positive neurons. *EMBO J*. doi:10.1038/emboj.2011.189.

- Yu, Y.-C., R.S. Bultje, X. Wang, and S.-H. Shi. 2009. Specific synapses develop preferentially among sister excitatory neurons in the neocortex. *Nature*. 458:501–4. doi:10.1038/nature07722.
- Zanata, S.M., I. Hovatta, B. Rohm, and A.W. Puschel. 2002. Antagonistic Effects of Rnd1 and RhoD GTPases Regulate Receptor Activity in Semaphorin 3A-Induced Cytoskeletal Collapse. *J. Neurosci.* 22:471–477.
- Zhou, Y.-D., S. Lee, Z. Jin, M. Wright, S.E.P. Smith, and M.P. Anderson. 2009. Arrested maturation of excitatory synapses in autosomal dominant lateral temporal lobe epilepsy. *Nat. Med.* 15:1208–14. doi:10.1038/nm.2019.
- Zimmerman, L., U. Lendahl, M. Cunningham, R. McKay, B. Parr, B. Gavin, J. Mann, G. Vassileva, and A. McMahon. 1994. Independent regulatory elements in the nestin gene direct transgene expression to neural stem cells or muscle precursors. *Neuron*. 12:11–24. doi:10.1016/0896-6273(94)90148-1.
- Zipursky, S.L., W.M. Wojtowicz, and D. Hattori. 2006. Got diversity? Wiring the fly brain with Dscam. *Trends Biochem. Sci.* 31:581–8. doi:10.1016/j.tibs.2006.08.003.

6. Appendix

List of Figures

| | |
|--|----|
| Fig. 1 Inside-out development of the cerebral cortex | 4 |
| Fig. 2 Generation of cortical projection neurons in the VZ and SVZ | 5 |
| Fig. 3 Migration paths of interneurons and pyramidal neurons | 7 |
| Fig. 4 Synapse formation occurs in three main steps | 16 |
| Fig. 5 Domain structure of FLRT family members | 23 |
| Fig. 6 FLRTs are localized to Synapses <i>in vivo</i> | 30 |
| Fig. 7 FLRTs expressed in HEK293 cells do not induce excitatory postsynaptic differentiation in neurons | 32 |
| Fig. 8 FLRTs expressed in HEK293 cells do not induce inhibitory postsynaptic differentiation in neurons | 34 |
| Fig. 9 FLRTs expressed in HEK293 cells do not induce presynaptic differentiation in neurons | 35 |
| Fig. 10 Distribution of Ctip2-positive cells in hippocampus | 38 |
| Fig. 11 Example of synapse quantification in primary neurons | 39 |
| Fig. 12 Genetic knock-out of FLRT1 does not change synapse number in primary hippocampal neurons | 40 |
| Fig. 13 Distribution of FLRT3-positive cells in hippocampus and primary culture | 42 |
| Fig. 14 Conditional genetic knock-out of FLRT3 does not change synapse number in primary hippocampal neurons | 43 |
| Fig. 15 Sparse knock-out of FLRT3 does not change synapse number in primary hippocampal neurons | 45 |
| Fig. 16 Overexpression of FLRT3 does not change synapse number in primary hippocampal neurons | 47 |
| Fig. 17 Validation of hippocampal microdissection | 48 |
| Fig. 18 Analysis of synaptic proteins in microdissected hippocampus | 50 |
| Fig. 19 Ultrastructural quantification of synapses in the hippocampus | 52 |
| Fig. 20 Summary of structural data | 54 |

| | |
|---|-----------|
| Fig. 21 Overview of FLRT and Unc5D binding mutant constructs | 56 |
| Fig. 22 Surface staining of mVenus constructs | 57 |
| Fig. 23 Validation of FLRT2 binding mutants | 58 |
| Fig. 24 Validation of FLRT3 binding mutants | 59 |
| Fig. 25 Validation of the Unc5D binding mutant | 61 |
| Fig. 26 Validation of homophilic binding of FLRT mutants | 62 |
| Fig. 27 Expression analysis of pCAG-IRES-EGFP constructs by Western blotting | 63 |
| Fig. 28 Surface expression of pCAG-IRES-EGFP constructs | 64 |
| Fig. 29 Inhibition of migration by Unc5D is partially mediated by FLRTs | 66 |
| Fig. 30 Loss of FLRT3 does not influence radial migration of neurons | 69 |
| Fig. 31 Ectopic expression of FLRT2 or FLRT3 interferes with radial migration independently of Unc5s | 72 |
| Fig. 32 Homophilic binding of FLRTs is involved in inhibiting radial migration | 74 |
| Fig. 33 The FLRT3 intracellular domain is involved in regulating migration in the cortex | 75 |
| Fig. 34 Overexpression of FLRT3 does not change cell fate | 77 |

List of Abbreviations

| | |
|------|--|
| A | Ampere |
| aa | Amino acid |
| AMPA | α -amino-3-hydroxy-5-methyl-4-isoxazolepropionic acid |
| AraC | Cytosine arabinoside |
| BDNF | Brain derived neurotrophic factor |
| BMP | Bone morphogenetic protein |
| bRGC | Basal radial glia cell |
| BSA | Bovine serum albumine |
| CA | Cornu ammonis |
| CAM | Cell adhesion molecule |
| CNS | Central nervous system |
| CP | Cortical plate |
| DAPI | 4',6-diamidino-2-phenylindole |
| DCC | Deleted in colorectal cancer |
| DG | Dentate gyrus |
| DIV | Days in vitro |
| DNA | Desoxyribonucleic acid |
| DTT | Dithiothreitol |
| E | Embryonic day |
| ECM | Extracellular matrix |
| EDTA | Ethylenediaminetetraacetic acid |
| EHEC | Enterohemorrhagic <i>E. coli</i> |
| EM | Electron microscope |
| EPEC | Enteropathogenic <i>E. coli</i> |

Appendix

| | |
|-------|---|
| ERK | Extracellular signal regulated kinase |
| FBS | Fetal bovine serum |
| FGF | Fibroblast growth factor |
| FGFR | Fibroblast growth factor receptor |
| FLRT | Fibronectin-leucine-rich-repeat transmembrane protein |
| FN | Fibronectin |
| GABA | γ -aminobutyric acid |
| GE | Ganglionic eminence |
| GFP | Green fluorescent protein |
| GTP | Guanosine-5'-triphosphate |
| h | Hour |
| HA | Hemagglutinin |
| HBSS | Hanks balanced salt solution |
| HEK | Human embryonic kidney |
| HEPES | 4-(2-hydroxyethyl)-1-piperazineethanesulfonic acid |
| HRP | Horseradish peroxidase |
| Ig | Immunoglobulin |
| ISVZ | Inner subventricular zone |
| IUE | <i>In utero</i> electroporation |
| KO | Knock-out |
| Kv | Voltage gated potassium channel |
| LGE | Lateral ganglionic eminence |
| LRR | Leucine-rich repeat |
| LRRTM | Leucine-rich repeat transmembrane protein |
| m | milli |
| Map2 | Microtubule associated protein 2 |

| | |
|--------------------|--|
| MAPK | Mitogen activated protein kinase |
| MGE | Medial ganglionic eminence |
| ML | Molecular layer |
| MZ | Marginal zone |
| n | Nano |
| NCAM | Neuronal cell adhesion molecule |
| NeuN | Neuronal nuclei |
| NGL-3 | Netrin-G ligand 3 |
| NMDA | N-methyl-D-aspartic acid |
| NT-4 | Neurotrophin 4 |
| OSVZ | Outer subventricular zone |
| p | Pico |
| P | Postnatal day |
| PAGE | Polyacrylamide gel electrophoresis |
| PBS | Phosphate buffered saline |
| PBS ^{+/+} | PBS containing calcium chloride and magnesium chloride |
| PBS ^{-/-} | PBS not containing calcium chloride and magnesium chloride |
| PCR | Polymerase chain reaction |
| PFA | Paraformaldehyde |
| PNS | Peripheral nervous system |
| PP | Preplate |
| PSD | Postsynaptic density |
| PVDF | Polyvinylidene difluoride |
| RGC | Radial glia cell |
| RNA | Ribonucleic acid |
| RNAi | RNA interference |

Appendix

| | |
|--------------|--|
| ROI | Region of interest |
| rpm | Rounds per minute |
| RT | Room temperature |
| s | Second |
| SALM | Synaptic adhesion like molecule |
| SDS | Sodium dodecyl sulfate |
| SEM | Standard error of the mean |
| shRNA | Short hairpin RNA |
| siRNA | Short interfering RNA |
| SPM | Synaptic plasma membrane |
| SRF | Serum response factor |
| SVZ | Subventricular zone |
| SynCAM1 | Synaptic cell adhesion molecule 1 |
| TGF | Transforming growth factor |
| TrkB | Tropomyosin related kinase B |
| TSP | Thrombospondin |
| Unc5 | Uncoordinated 5 |
| UV | Ultraviolet |
| VZ | Ventricular zone |
| WM | White matter |
| X-Gal | 5-bromo-4-chloro-3-indolyl- β -D-galactopyranoside |
| μ | micro |
| $^{\circ}$ C | Degree celsius |

Acknowledgements

Zu allererst möchte ich meinen Eltern für ihre Unterstützung in allen Lebenslagen danken! Sie waren immer für mich da und standen mit Rat und Tat bereit, wann immer es nötig war. Dabei haben sie mir aber nie gute Ratschläge aufgedrängt oder mich bevormundet. So hatte ich immer die Möglichkeit meine Fähigkeiten und Interessen zu entfalten und weiterzuentwickeln. Andernfalls wäre ich nie bei dieser Danksagung angekommen. Vielen Dank für alles!

Mein ganz besonderer Dank gilt auch Christine für's Zuhören, all die aufbauenden Worte und das gute Zureden während der letzten fünfeinhalb Jahre aber auch die vielen Einschnitte die sie in Kauf genommen hat um mich zu unterstützen. Vielen Dank auch für die fachliche Hilfe und die Unterstützung durch alles um was ich mich nicht kümmern musste, weil „jemand, man und einer“ es schon erledigt hatten! Ich liebe dich!

I would like to thank my supervisor Ruediger Klein for his patience, constant support and guidance throughout the course of my PhD and for the opportunity to work in a great, international atmosphere. There was always enough drive to keep me going but never too much pressure to demotivate me.

Thanks a lot to Daniel del Toro Ruiz for sharing his project and of course for all the help he was willing to offer whenever needed, be it weekends or late evenings! Thanks for discussing ideas, for great guidance, for giving input, for sharing protocols in Catalan, and for answering all my questions in great detail.

Thanks to Elena Seiradake for a great and very successful collaboration, good discussions and for providing an incredible array of mutant constructs that allowed me to lots of cool experiments.

Thanks to the MPI EM core facility, Marianne Braun and Ursula Weber, for providing awesome support cutting, staining and imaging my samples and thus pushing the project forward while I was dealing with other problems.

Thanks to the members of my thesis committee, Stephan Kröger and Volker Scheuss for good discussions and great suggestions during the TAC meetings, helping to drive the project to the right direction.

Thanks a lot to all the former and present members of the Klein department for scientific and nonscientific discussions, Christmas parties, Happy Hours, Wiesn visits, coffee breaks and support and help in all situations whenever needed. Special thanks to Pontus for fun conferences and late night behavior marathons, to Graziana for taking lots of embarrassing pictures, to Sonia for occasional complaining, to Tom and Louise for

coffee breaks, introducing me to a variety of cool movies and for figuring out what the fox says, to Jorg for some poetry and to Aarathi for dealing with my silliness for not killing me at some point.

Thanks a lot also to Isabella, Cora and Anne for coffee and lunch breaks, discussions about life *per se*, distractions from painful and failed experiments and alcohol-induced short working days.

Furthermore I would like to thank all the people I met during my time at the MPI that helped whenever possible and made the past five and a half years such an incredible experience, and the PhD community for great retreats and creating a very nice atmosphere to work and spend time in.

Big thanks to Tom, Dani and Elena for critically reading this thesis and useful comments.

Curriculum Vitae

Daniel Matthias Nagel

Born 02.01.1984 in Berlin

Education

- 2014 **PhD**, Graduate School of Systemic Neurosciences, Ludwig-Maximilians University, Munich, Germany
- 2009 – 2014 **PhD thesis**, laboratory of Prof. Rüdiger Klein, Department Molecules – Signalling – Development, Max-Planck Institute of Neurobiology, Martinsried, Germany
- **Analysis of adhesive and repulsive functions of FLRT proteins in central nervous system development**
- 2008 **Diploma** (equivalent to Masters), University of Constance, Germany
- 2007 – 2008 **Master's thesis**, laboratory of Prof. Marcel Leist, Doerenkamp-Zbinden chair of Alternative *in vitro* Methods, University of Constance, Germany
- **Evaluation of a human dopaminergic cell line as *in vitro* model for Parkinson's disease**
- 2003 – 2008 **Student** of Biology, University of Constance, Germany, emphasize on: cell biology and molecular biology
- 2003 **High School Graduation** (Abitur), Constance, Germany
- 1994 – 2003 High School, Alexander-von-Humboldt Gymnasium, Constance, Germany
-

Publications

FLRT structure: balancing repulsion and cell adhesion in cortical and vascular development.

Seiradake E, del Toro D, **Nagel D**, Cop F, Härtl R, Ruff T, Seyit-Bremer G, Harlos K, Border EC, Acker-Palmer A, Jones EY, Klein R (2014)

Neuron, in press

Development of a new photochromic ion channel blocker via azologization of fomocaine.

Schoenberger M, Damijonaitis A, Zhang Z, **Nagel D**, Trauner D (2014)

ACS Chem Neurosci 5, 514-518

Requirement of a dopaminergic neuronal phenotype for toxicity of low concentrations of 1-methyl-4-phenylpyridinium to human cells.

Schildknecht S, Pörtl D, **Nagel DM**, Matt F, Scholz D, Lotharius J, Schmieg N, Salvo-Vargas A, Leist M (2009)

Toxicol Appl Pharmacol 241, 23-35

Permissions

Figures 1 and 2

Neuronal subtype specification in the cerebral cortex

Bradley J. Molyneaux, Paola Arlotta, Joao R. L. Menezes & Jeffrey D. Macklis

Nature Reviews Neuroscience 8, 427-437; doi:10.1038/nrn2151

License number: 3475970357774

Eidesstattliche Versicherung/Affidavit

Hiermit versichere ich an Eides statt, dass ich die vorliegende Dissertation „**Analysis of adhesive and repulsive functions of FLRT proteins in central nervous system development**“ selbstständig angefertigt habe, mich außer der angegebenen keiner weiteren Hilfsmittel bedient und alle Erkenntnisse, die aus dem Schrifttum ganz oder annähernd übernommen sind, als solche kenntlich gemacht und nach ihrer Herkunft unter Bezeichnung der Fundstelle einzeln nachgewiesen habe.

I hereby confirm that the dissertation „ **Analysis of adhesive and repulsive functions of FLRT proteins in central nervous system development** “ is the result of my own work and that I have only used sources or materials listed and specified in the dissertation.

München, den /Munich, Date

Unterschrift/ Signature

List of author contributions

Daniel Nagel generated all data and prepared all figures if not stated otherwise.

Dr. Daniel del Toro Ruiz generated the data for Fig. 6 and Fig. 13 A.

Dr. Elena Seiradake generated all the structural data and the graphics in Fig. 20 A, B, C and cloned the mutant FLRT and Unc5 constructs.

Dr. Gönül Seyit-Bremer generated the data for Fig. 26.

Marianne Braun and Ursula Weber performed thin sectioning, staining and imaging for the electron microscopy experiments in Fig. 19.

Signature of lab head:

Signature of student: